CELLULAR AND BIOCHEMICAL REGULATION OF CDC25A PHOSPHATASE BY NITROSATIVE STRESS

by

Robert J. Tomko Jr.

B.S., Lebanon Valley College, 2002

Submitted to the Graduate Faculty of

the School of Medicine in partial fulfillment

of the requirements for the degree of

Doctor of Philosophy

University of Pittsburgh

2008

UNIVERSITY OF PITTSBURGH

School of Medicine

This dissertation was presented

by

Robert J. Tomko Jr.

It was defended on

April 24th, 2008

and approved by

Chairperson: Donald B. DeFranco, Ph.D., Professor, Department of Pharmacology and Chemical Biology

Valerian E. Kagan, Ph.D., Professor, Department of Environmental and Occupational Health

Bruce R. Pitt, Ph.D., Professor, Department of Environmental and Occupational Health

Billy W. Day, Ph.D., Professor, Department of Pharmaceutical Sciences

Dissertation Advisor: John S. Lazo, Ph.D., Allegheny Foundation Professor, Department of Pharmacology and Chemical Biology

CELLULAR AND BIOCHEMICAL REGULATION OF CDC25A PHOSPHATASE BY NITROSATIVE STRESS

Robert J. Tomko Jr., Ph.D.

University of Pittsburgh, 2008

Numerous reports correlate nitric oxide (•NO) production with stalled S-phase progression, but the molecular mechanism(s) of cell cycle arrest remains elusive. Paradoxically numerous human tumors are exposed to vast quantities of nitric oxide and its reactive byproducts *in situ*, yet they continue to grow and proliferate. The dual-specificity phosphatase Cdc25A promotes cell cycle progression by dephosphorylating and activating cyclin-dependent kinases. Deregulation of Cdc25A is characteristic of human tumors, accelerates the cell cycle, and confers resistance to apoptosis, highlighting the importance of stringent Cdc25A control. Biochemical and structural analyses of Cdc25A indicate the potential for inhibition by *S*-nitrosation of the catalytic cysteine, providing a linkage between •NO and cytostatic signaling. Thus, the overall hypothesis examined in this dissertation was that Cdc25A is a target and transducer of signaling by •NO and •NO-derived reactive species. The specific aims were to: 1) probe the susceptibility of Cdc25A to enzymatic regulation by •NO-derived reactive species; 2) examine regulation of Cdc25A protein in nitrosatively challenged cells; and 3) determine whether Cdc25A activity was limiting for S-phase progression in nitrosatively-challenged tumor cells. My studies identified novel mechanisms controlling Cdc25A abundance and activity. *S*-Nitrosothiols rapidly *S*-nitrosated and inactivated Cdc25A *in vitro*, and Cdc25A activity was restored by reductants. Generation of nitrosative stress in cells either by iNOS-derived •NO or

the cell-permeable *S*-nitrosating agent *S*-nitrosocysteine ethyl ester (SNCEE) caused translational inhibition of Cdc25A via hyperphosphorylation and inhibition of the eukaryotic translational regulator eIF2α. Although iNOS-derived •NO and SNCEE inhibited DNA synthesis coincident with Cdc25A loss, restoration of Cdc25A activity in nitrosatively-challenged cells did not alter DNA synthesis inhibition, distinguishing nitrosative inhibition of DNA synthesis from the canonical intra-S-phase checkpoint. SNCEE decoupled Cdc25A from ASK-1 and sensitized cells to chemotherapeutic-induced apoptosis, suggesting that Cdc25A suppression by nitrosative stress may lower the apoptotic threshold in nitrosatively-challenged cells by priming ASK-1 for activation. In summary, these studies describe novel regulation of Cdc25A translation and activity, and a model wherein selective inhibition of Cdc25A phosphatase-dependent and independent activities can occur under nitrosative stress, and implicate Cdc25A as a regulator of apoptotic threshold following nitrosative insult via priming of ASK-1.

TABLE OF CONTENTS

LIST OF TABLES

LIST OF FIGURES

PREFACE

When life gives you lemons, make lemonade, and then throw it in the face of the person who gave you the lemons until they give you the oranges you originally asked for.

--Phil Hartman's character Bill McNeal from *News Radio*

All the effort you are making will ultimately pay off.

--Fortune from a Fuel & Fuddle fortune cookie

This thesis is dedicated to my parents, who taught me "don't" and "shouldn't" but never "can't."

ACKNOWLEDGEMENT

I would first and foremost like to thank Dr. John S. Lazo for his guidance, friendship, and support through my graduate studies. From John I learned my most valuable skills for the road ahead: how to think without inhibition, and the ability to put a positive spin on the seemingly most negative results. His frequent pep-talks (intentional or not) were many times my impetus to push forward with the resolve and velocity I have mustered. Any success I achieve will be a reflection of him.

I'm also grateful to the members of the Lazo laboratory past and present, especially Pallavi Bansal and Alexander P. Ducruet, who were kind enough to answer a billion dumb questions when I began my research, and who served as my role models of graduate study. I am also thankful to the younger Lazo laboratory graduate students Pierre E. Queiroz de Oliveira, Carolyn A. Kitchens, and Yan Wang for the opportunity to guide them as best I can as a senior graduate student, for by teaching one truly learns. Maybe most importantly I thank John Skoko and CC Corey whom as lab managers have withstood a million of my near explosions and emergencies yet were always willing to donate their time and efforts to ease my load.

I would like to thank my committee members Drs. Don DeFranco, Valerian Kagan, Bruce Pitt, and Billy Day for their intellectual support, thoughtful suggestions and constructive criticisms that have helped to shape this dissertation.

I am indebted to Paul Robbins for providing adenoviruses, Detcho Stoyanovsky for use of his nitric oxide analyzer and helpful discussions, Bert Vogelstein for cell lines, and to David Morgan, Steven Grant, Tom Roberts, and Peter Houghton for plasmids. I'd also like to thank Bruce Freeman for numerous helpful discussions toward the end of my thesis.

I am also grateful to the Department of Pharmacology and Chemical Biology, especially Sharon Webb, Rhonda Toth, Jennifer Wong, Patricia Smith, Jim Kaczynski, Jeanette McDew, and Linda Sorch for administrative support. I am also indebted to Cindy Duffy and Jennifer Walker from the INTBP Grad Office for administrative and emotional support over the years. I would also like to thank all of my friends from college and from Pittsburgh, particularly Mike Freeman, Dan Constantinescu, and Mike Turner, and especially my friends from home for their undying support and encouragement over the years, even though I was (am) rarely around.

I would like to thank my parents, Robert J. Tomko and Nancy Tomko for repeatedly sacrificing their time, knowledge, and resources to propel me forward in life as best they could, for their unconditional love and support, and for nodding along when I'd explain to them what I do (Mom). I must thank my brothers, Matthew S. Tomko, and Michael A. Tomko, for unwittingly reminding me about what's most important in life when I needed focus the most.

Lastly my sincerest gratitude to Antonia A. Nemec, who stood by me proudly during the best times, and during my biggest defeats, drove me home from the bar without complaint or question no matter how "spirited" I was. Most importantly, whenever I was truly down, or thinking of giving up, she always had the courage and the peace of mind to smack me and tell me to suck it up.

ABBREVIATIONS

3-NT	3-Nitrotyrosine
APC/C	Anaphase-promoting complex/Cyclosome
ASK-1	Apoptosis signal-regulating kinase-1
ATM	Ataxia telangiectasia-mutated
ATP	Adenosine triphosphate
ATR	ATM- and Rad3-related
β-ME	β-Mercaptoethanol
β-TrCP	β-Transducin repeat-containing protein
BSA	Bovine serum albumin
CAK	Cdk-activating kinase
CDDP	*cis*-Diaminodichloroplatinum (cisplatin)
Cdk	Cyclin-dependent kinase
CdkI	Cyclin-dependent kinase inhibitor
CEE	Cysteine ethyl ester hydrochloride
cGMP	Cyclic guanosine monophosphate
Chk	Checkpoint kinase
CHX	Cycloheximide
DAF-2	Diaminofluorescein-2
DMSO	Dimethylsulfoxide
DTPA	Diethylene triamine pentaacetic acid
DTT	Dithiothreitol
eIF2α	Eukaryotic initiation factor 2α
eNOS	Endothelial nitric oxide synthase
GAPDH	Glyceraldehyde-3-phosphate dehydrogenase
GSH	Reduced glutathione
GSSG	Glutathione disulfide
GST	Glutathione *S*-transferase
HA	Influenza virus hemaglutinin epitope
HRI	Heme-regulated inhibitor
IAC	Iodoacetamide
iNOS	Inducible nitric oxide synthase
IR	Ionizing radiation
LMM	Low molecular mass
L-NMMA	N^G-monomethyl-*L*-arginine monoacetate
MALDI	Matrix-assisted laser desorption-ionization
MAPKAPK-2	Mitogen-activated protein kinase-activated protein kinase-2

MEF	Mouse embryonic fibroblast
Mn-SOD	Manganese-superoxide dismutase
MS	Mass spectrometry
MOI	Multiplicity of infection
NADPH	Reduced nicotinamide adenine dinucleotide phosphate
$NADP^+$	Oxidized nicotinamide adenine dinucleotide phosphate
nNOS	Neuronal nitric oxide synthase
•NO	Nitric oxide
NO^+	Nitrosonium ion
NO^-/HNO	Nitroxyl anion
NOS	Nitric oxide synthase
•OH	Hydroxyl radical
OMFP	*O*-Methylfluorescein phosphate
PBS	Phosphate-buffered saline
PDI	Protein disulfide isomerase
PERK	PKR-like endoplasmic reticulum kinase
PP1	Protein serine/threonine phosphatase 1
PTM	Post-translational modification
PTP1B	Protein tyrosine phosphatase 1B
Rb	Retinoblastoma
RDS	Radioresistant DNA synthesis
Redox	Reduction/oxidation
RIPA	Radioimmunoprecipitation assay
RNNO	*N*-Nitrosamine
RNS	•NO-derived reactive species
ROS	Reactive oxygen species
RPA	Replication protein A
RR	Ribonucleotide reductase
RS•	Thiyl radical
RSNO	*S*-Nitrosothiol
SCF	Skp1/Cul1/F-box protein complex
SDS	Sodium dodecyl sulfate
sGC	Soluble guanylate cyclase
SNCEE	*S*-Nitrosocysteine ethyl ester
TOF	Time of flight
TBS-T	Tris-buffered saline, 0.01% Tween-20
Trx	Thioredoxin
UV	Ultraviolet

1.0 INTRODUCTION

1.1 GENERAL INTRODUCTION: CANCER AND CELL DIVISION

In 2008, it is estimated that more than 1.4 million United States citizens will be diagnosed with cancer,[1] more than the populations of 11 of the 50 states.[2] Cancer is the second largest killer in the U.S. (over 560,000 deaths predicted for 2008) and causes 1 in 4 total deaths, with more than 1500 deaths per day.[3] This high incidence of disease strains families, medical resources, the healthcare system, as well as the economy. Thus the impetus to eradicate cancer is clear.

Before malignancies can be effectively controlled, it is necessary to understand the molecular mechanisms by which cancer evolves. The origins of cancer reside in DNA; accumulation of mutations in the cellular genome due to normal and aberrant cellular processes and environmental exposures eventually override normal cell signaling to promote malignancy. Although the term cancer envelops many physical manifestations with diverse origins, all cancerous cells display at least one common phenotype: uncontrolled or aberrant proliferation. Cancer is by nature a hyperproliferative disease; cancer cells undergo cell division either in the absence of growth signals or in the presence of anti-growth signals. Although much progress has

---

[1] American Cancer Society: 2008 Facts and Figures (http://www.cancer.org/downloads/STT/2008CAFFfinalsecured.pdf)

[2] United States Census Bureau: Annual population estimates 2000 to 2007 (http://www.census.gov)

[3] American Cancer Society: 2008 Facts and Figures (http://www.cancer.org/downloads/STT/2008CAFFfinalsecured.pdf)

been made in the understanding of cancer biology, the origins and targets of antigrowth signaling are not fully elucidated, and the effects of aberrant protein expression and activity on antigrowth signaling remain to be explored. Thus, the purpose of the work described herein is to provide novel insight into the mechanisms by which antigrowth signals elicit their effects, and to examine potential mechanisms by which insensitivity to these signals is acquired.

1.2 THE MAMMALIAN CELL DIVISION CYCLE

The evolutionary survival of an organism is dependent upon successful transmission of its genetic makeup from one generation to the next. The primary mechanism by which genetic material is passed down is by replication and segregation of this material in the form of chromosomes equally to the daughter cells originating from the dividing parent cell. For successful cell division, the cell must therefore generate an exact copy of its genome, and then divide those copies between the daughter cells. This is the function of the mammalian cell cycle. The mammalian cell cycle is divided into four principle phases, G_1, S, G_2, and M. In G_1, a newly divided cell accumulates energy and nutrients and senses its surroundings to commit to cell division, and readies DNA replication complexes at various sites around the genome. During S, the genome is replicated, as are cellular components such as centrosomes that are necessary for division. G_2 provides time to sense and correct any errors in DNA replication not repaired during S, and to prepare for mitosis. Finally, in M-phase, the cell segregates its components, and physically cleaves into two daughter cells identical in makeup to each other and to the parent cell.

1.3 THE CYCLIN-DEPENDENT KINASES AS THE DRIVERS OF THE CELL CYCLE

The precise timing of cell cycle events is critical to allow proper chromosomal duplication and segregation before cytokinesis, and failure to control these processes induces DNA damage and inheritance of mutations. To ensure strict control of cell cycle progression, there are a number of redundant yet independent mechanisms controlling the activity of positive cell cycle regulators. Many of these mechanisms target the cyclin-dependent kinase (Cdk) family. The Cdks are serine-threonine kinases conserved throughout eukaryotes that act to phosphorylate cell cycle phase-specific proteins to promote movement through specific cell cycle phases. The Cdk family consists of 11 currently known members, each of which requires binding of a cyclin partner for activity, with the exception of Cdk5, which is activated by binding of non-cyclin proteins. Cdks harbor a number of cellular roles, including protein activation, regulation of transcription, RNA splicing, regulation of neuronal development, apoptotic signaling, centrosome duplication, but were originally identified for their role in cell cycle progression.

Cdks 1, 2, 4, 6 and 7 are considered cell cycle-regulating Cdks, and each functions differentially to promote cell division. Cdk4 and/or 6 provide the initial stimulus of cell cycle progression in response to extracellular nutrient-sensing, whereas Cdk2 provides the driving force through the G_1-S transition, S-phase and early G_2. Cdk1 (called Cdc2 in yeast) promotes progression through late G_2 and mitosis, and its destruction is a prerequisite for cytokinesis. Cdk7 is also known as Cdk-activating kinase (CAK) and is required for full activation of other Cdk complexes as described below.

Cdk activity is regulated by phosphorylation and protein-protein interactions. These regulatory events can be activating or inhibitory. The first step in Cdk regulation is mediated

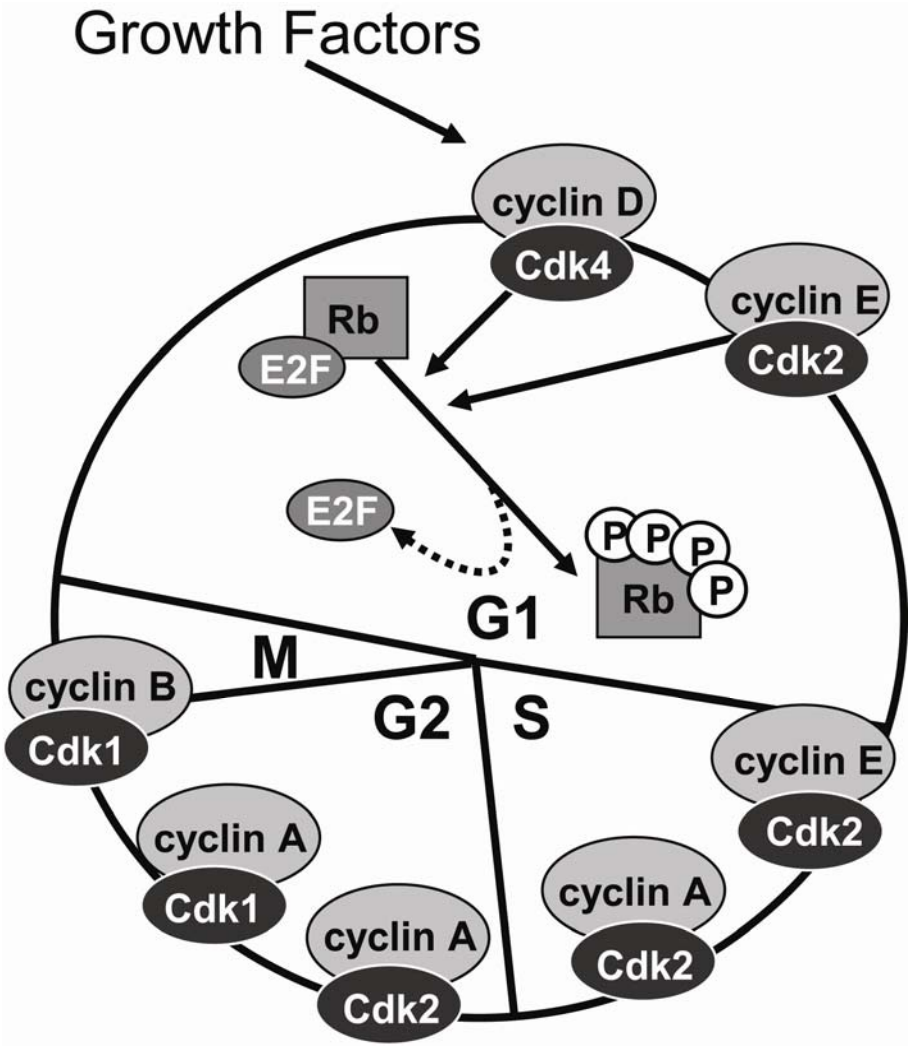

Figure 1. Regulation of the mammalian cell cycle by Cdks.

The mammalian cell cycle is composed of four phases, G_1, S, G_2, and M phase. The approximate duration of each phase relative to the time required for a total cell cycle is depicted by the size of the pie fraction of the circle. The Cdks display distinct, but overlapping temporal activities and substrate specificities. Mitogens provide the initial stimulus for cell cycle progression by promoting the production of Cyclin D, which subsequently binds and activates Cdk4, which in turn phosphorylates and dissociates Rb from E2F, allowing transcription of cyclin E and genes required for DNA synthesis.

through activating (cyclins) and inhibitory (Cdk inhibitors, CdkIs) protein-protein interactions. Cdks readily bind cyclins in the absence of CdkIs, which prime them for further stimulatory processes. Binding of CdkIs to Cdks or Cdk/cyclin complexes can either sequester Cdks from cyclins or inhibit their activity. CdkIs are divided into two groups, based on sequence homology and binding specificity. The Cip/Kip family, which encompasses the $p21^{CIP}$ and $p27^{KIP}$ inhibitors, bind to E-type and D-type Cdk/cyclin complexes and inactivate them (1). The second group of CdkIs is known as the INK4 family, and encompasses p15, p16, p18 and p19-type CdkIs (1). These CdkIs bind only to Cdk4 or Cdk6 and not to Cdk/cyclin complexes (1). Thus the initial step in Cdk activation requires proper and specific binding to its cognate cyclins, and removal of any CdkIs by preoteasomal degradation or pre-association (in the case of INK4 family CdkIs) of Cdks with other Cdk-binding proteins (1, 2).

Activation of Cdk kinase activity after cyclin binding is achieved through a number of sequence-specific phosphorylation and dephosphorylation steps, initiated by binding of the cyclin cofactor (Figure 2). Cyclin binding partially activates Cdk activity and makes it a substrate for inhibitory phosphorylations at Thr14 and Tyr15 (human Cdk1 nomenclature) by the Wee1 and Myt1 kinases (3-6). Phosphorylation at these residues promotes activating phosphorylation at Cdk1-Thr161 (Thr160 in Cdk2) by the Cdk-activating kinase, although the Thr161-phosphorylated complexes are still inactive; the inhibitory phosphorylations at Thr14 and Tyr15 must first be removed (7). Phosphorylation of Thr161 by the Cdk-activating kinase is inhibited by association of both the INK4 and Cip/Kip family proteins with Cdks, adding a further regulatory role for protein-protein interaction in Cdk activation (8). The final step promoting full Cdk activation is removal of the inhibitory Thr14 and Tyr15 phosphates by the Cdc25 dual-specificity phosphatases.

1.3.1 The Cdc25 family of dual-specificity phosphatases

The Cdc25 phosphatase was first identified in the fission yeast *Saccharomyces pombe* as the 25th gene discovered that regulated the cell division cycle (9). Mutation of the Cdc25^{+} gene resulted in overly large yeast cells, characteristic of failure to undergo mitosis (9). Conversely, introduction of extra copies of the Cdc25^{+} gene caused mitotic initiation at reduced cell size similar to the Wee^{+} phenotype, so named because yeast lacking Wee^{+} divided before full cell size had been achieved (10-12). Indeed, mutation of both Cdc25 and Wee genes resulted in normal mitoses, suggesting opposing roles for these proteins (9). This phenotypic antagonism of Cdc25^{+} loss to the Wee^{+} gene provided some of the evidence that later identified Cdc25^{+} as a phosphatase, as Wee^{+} encoded a protein kinase (13). Clues to the function of Cdc25 were originally derived from genetic studies in yeast that determined mutation of Cdc25^{+} could complement a Cdc2 (the yeast homolog of human Cdk1) mutant that was unable to drive mitosis (14, 15) and that Cdc25 mutation attenuated Cdc2 kinase activity (16). Notably, Cdc25 expression was found to peak at mitosis, consistent with a role in mitotic induction (15). Arguably the most important evidence that Cdc25 was a phosphatase, however, came from studies of p34^{Cdc2} showing that dephosporylation of p34$^{Cdc2\text{-}Tyr15}$ is required for mitotic initiation (17). A Tyr15Phe mutation in p34^{Cdc2} that ablates phosphorylation but resembles tyrosine bypasses the requirement for functional Cdc25, suggesting a role for Cdc25 in dephosphorylating this residue. Early reports suggested that Cdc25^{+} encodes a protein that regulates the phosphatase activity of another protein, thus controlling p34^{Cdc2} phosphorylation and activity as Cdc25^{+} does not bear significant sequence homology to traditional tyrosine phosphatases (18); in 1991 however, four independent groups reported in rapid succession that the Cdc25 gene products from different organisms (*Homo sapiens*, *Drosophila*, *Xenopus*) each harbors

phosphatase activity directed toward $p34^{Cdc2}$ (19-22). These studies in different organisms highlighted the cross-species conservation of the eukaryotic cell cycle machinery, and brought Cdc25 to the spotlight in cell cycle regulation.

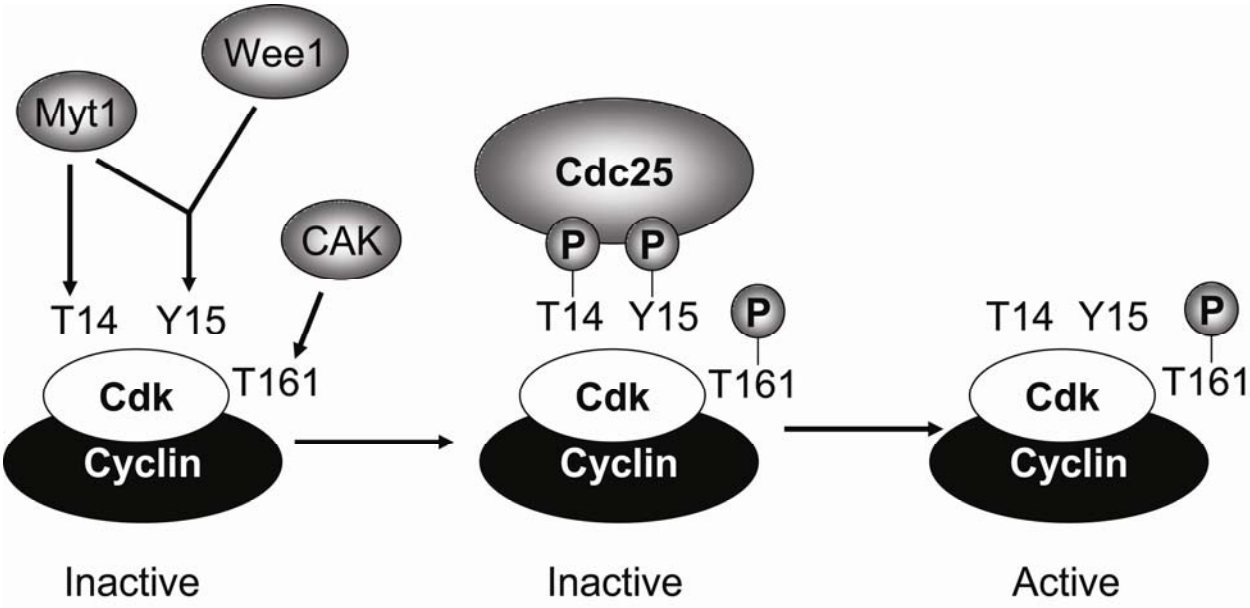

Figure 2. Activation of the Cdks is a multi-step process.

Activation of Cdks is tightly controlled by activating (T161) and inhibitory (T14, Y15) phosphorylation, and protein-protein interactions with cyclins.

1.3.2 The human Cdc25 phosphatases

Since the initial studies in yeast were performed, three isoforms of Cdc25 have been identified in humans: Cdc25A, B and C (23, 24). Cdc25C was originally discovered using a degenerate primer PCR approach based on the yeast $Cdc25^{+}$ gene (23), whereas Cdc25A and Cdc25B were identified using the same approach based on the human Cdc25C gene sequence (24). All three isoforms complement the temperature-sensitive $Cdc25^{+}$ mutants in yeast, and thus were considered human Cdc25s on the basis of their homology and activity (23, 24). Each human Cdc25 isoform is encoded by a distinct gene, located on a different chromosome: Cdc25A maps

to 3p21, Cdc25B to 20p13, and Cdc25C to 5q31 (25-27). It remains unclear how and why humans (and mammals) evolved three isoforms. Notably, each gene can also generate mRNA splice variants (two for Cdc25A, three for Cdc25B, and five for Cdc25C), further increasing the complexity of Cdc25 activities *in vivo* (28, 29). The determinants and patterns of expression of the splice variants' protein products, however, remains unexamined.

The three human Cdc25 isoforms share sequence homology both with the Cdc25s from other species as well as with each other, although this homology is limited to the C-terminal portion of the protein. Thus, the human Cdc25 proteins are generally structurally divided into two primary domains (Figure 3), the N-terminal domain, which shares little (if any) sequence homology among isoforms and the C-terminal domain, which houses the catalytic activity of the protein and has greater than 40% identity among the human isoforms (24). The conserved protein sequence LIGD marks the end of the N-terminal domain and the beginning of the catalytic domain (30).

The N-terminal region of the human Cdc25s is a regulatory domain not necessary for catalytic activity; rather, deletion of the N-terminus is reported to stimulate activity in *in vitro* phosphatase assays towards the small molecule substrate *O*-methylfluorescein phosphate (OMFP) (30). The N-terminus of each Cdc25 isoform harbors a nuclear localization sequence (NLS) and at least one nuclear export sequence (NES), and reports describe nuclear-cytoplasmic shuttling for each (31-34). In addition to the NES and NLS, there exist numerous phosphorylation sites in the N-terminus of each Cdc25 isoform. The effects of these post-translational modifications discovered to date fall into three categories: regulation of localization; regulation of protein stability; and regulation of phosphatase activity. The former is discussed here; the latter two will be discussed below.

Each Cdc25 N-terminus contains consensus sequences for mode I-type binding sites for 14-3-3 proteins (35-38). The 14-3-3 family of proteins comprises phosphoserine and phosphothreonine-binding proteins that act as regulators of signaling proteins by interacting with and altering their activities or intracellular locations (36). Indeed, all three Cdc25 isoforms interact with 14-3-3 proteins in cells, primarily in response to cellular stress or DNA damage (35, 37, 39). Some reports suggest however that binding of 14-3-3 isoforms to Cdc25B may be independent of phosphorylation, although the possibility that more than one 14-3-3 binding site exists on Cdc25B has not been ruled out (38, 39).

Current knowledge of the N-terminal domain of the Cdc25s is derived almost entirely from mutagenesis, biochemical regulation of phosphorylation and primary protein sequence information, as no crystal structure of the regulatory domain exists for any human Cdc25. The C-terminal catalytic domain however has been crystallized at better than 2.5 Å resolution for both Cdc25A and Cdc25B (40-42). Topologically, the Cdc25 catalytic domain is a distinct class most similar to the sulfur transfer protein rhodanese, and does not harbor significant overall homology to any other phosphatases, including other dual-specificity phosphatases (40, 42). Superimposition of the two structures indicates near identical folding in all conserved regions with the only significant degeneration occurring in the extreme C-termini (40). Whereas the Cdc25B C-terminal tail (residues 530+) folds back upon itself, perhaps to aid in substrate binding, the Cdc25A tail (residues 488+) is directed away from the active site, leaving it largely exposed (40, 42).

The active site of the enzymes is relatively shallow with no auxiliary loops extending over the active site, which distinguishes it from that of other tyrosine phosphatases (40, 42). This presumably is to facilitate access of the enzyme to the less obtrusive phosphoserine and

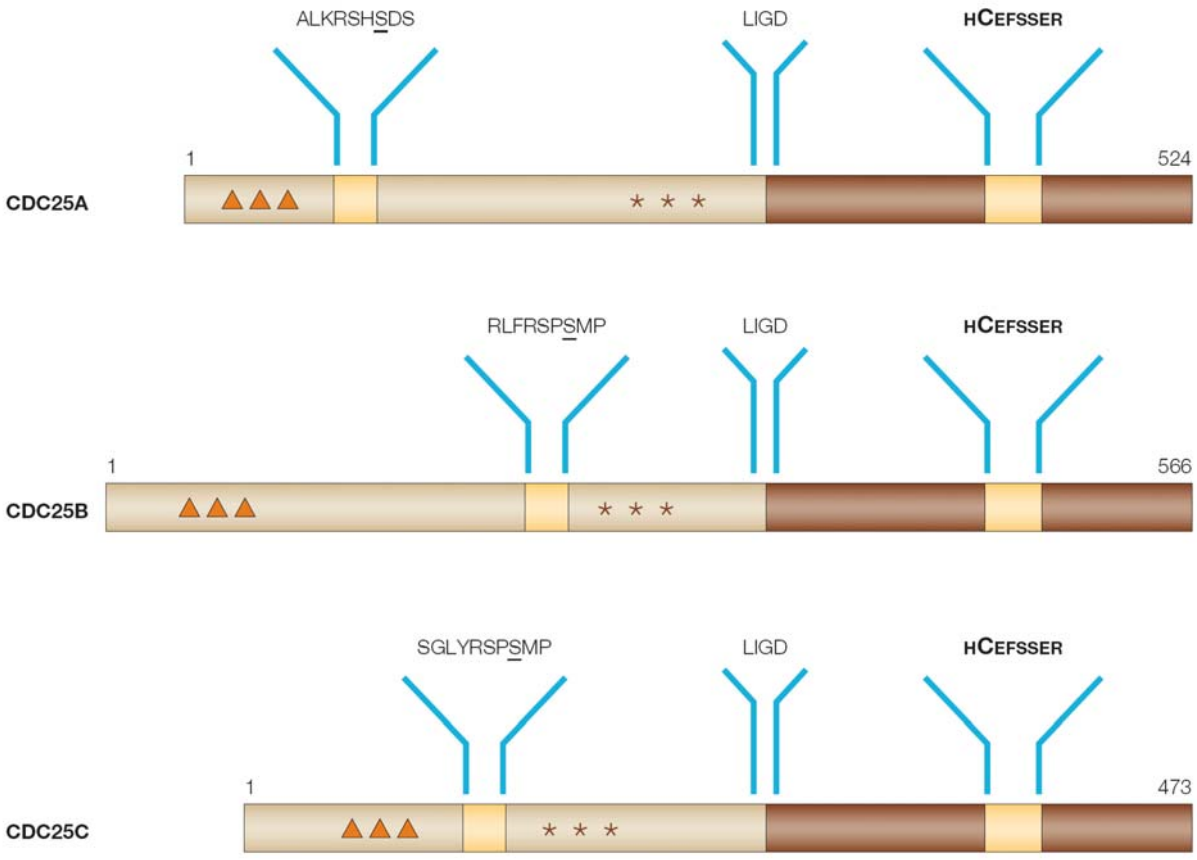

Figure 3. Structural comparison of the three human Cdc25 isoforms.

The human Cdc25 phosphatases are encoded by distinct genes, yet show sequence and structural similarity. The proteins are comprised of an amino-terminal regulatory domain (beige) and a carboxy-terminal catalytic domain (brown), the beginning of which is marked by the protein sequence L-I-G-D. The regulatory domain of each contains at least one verified NLS (triangles) and one verified NES (asterisks), as well as 14-3-3 binding sites separating the NLS and NES (the underlined serine residue is the phosphoserine in the 14-3-3 binding motif). The highly conserved tyrosine phosphatase motif HCX_5R (where X is any amino acid) is displayed in bold, with the catalytic cysteine in larger type. The full-length splice variant is depicted for each isoform. Modified from (30).

phosphothreonine residues. Both structures demonstrate an active site organization nearly identical to that found in other tyrosine phosphatases with the absolutely conserved canonical HCX_5R catalytic motif (where X is any amino acid) organized in a loop between a β-strand and an α-helix. Curiously, the crystal structure of Cdc25A failed to bind sulfate in its active site, whereas the Cdc25B structure readily bound both tungstate and sulfate (40, 42). Whether this is purely an artifact or of biochemical significance remains unknown.

The catalytic mechanism of Cdc25 phosphatase has been studied in great detail by the laboratory of Johannes Rudolph. The catalytic mechanism of the Cdc25s is enzymatically shared with other dual-specificity and tyrosine phosphatases, but Cdc25 preferentially dephosphorylates a monoanionic phosphate group as opposed to the bisanionic groups favored by other phosphatases (43). The phosphosubstrate is bound so that the charge of the phosphate is borne by the amide backbones and the positively charged arginine sidechain of the HCX_5R motif (43). The enzyme dephosphorylates the substrate using a two-step mechanism characteristic of tyrosine phosphatases (Figure 4) in which the first step is nucleophilic attack of the phosphorus atom of the phosphate moiety by the catalytic thiolate, forming a covalent phosphocysteine intermediate. The second step is hydrolysis of this phosphocysteine intermediate to release organic phosphate and regenerate the catalytic thiolate. The rate constants have been determined such that phosphate is removed from Thr14 before Tyr15 (43). Aside from the catalytic cysteine, a catalytic acid is required to protonate the tyrosyl, threonyl or seryl oxygen, making it a good leaving group. No residue to fulfill this role has been identified on Cdc25B, and it is postulated that the residue may reside on the Cdk2/cyclin A substrate because no acidic amino acid residue is perched appropriately in the Cdc25B crystal structure and pH dependence of

Cdc25B activity consistent with protonation of the substrate leaving group is observed toward Cdk2/cyclin A but not toward artificial substrates (44).

1.3.3 Regulation of the cell cycle by the Cdc25s

1.3.3.1 Basal activities

Regulation of the mammalian cell cycle requires the cumulative efforts of all three phosphatases, although their expression and activities are cell cycle phase-dependent (Figure 5). Initiation of the mammalian cell cycle occurs in response to mitogen-stimulated expression of cyclin D, which activates Cdk4 complexes. There is limited evidence for a role of the Cdc25s in regulating Cdk4 activity, although tyrosine dephosphorylation of $Cdk4^{Tyr17}$ is a prerequisite for Cdk4 activation, and that this residue becomes phosphorylated in response to genotoxic stress (45). $Cdk4^{Tyr17}$ dephosphorylation appears to be mediated by Cdc25A, as microinjection with Cdc25A antibodies prevents accumulation of rat fibroblasts in mitosis 22 hours after synchronization and expression of a $Cdk4^{Tyr17Phe}$ mutant that cannot be phosphorylated bypassed this requirement for Cdc25A (45). Also, incubation of immunoprecipitated Cdk4 or Cdk6 with recombinant Cdc25A results in an increase in Cdk4/6 kinase activity toward Rb *in vitro* (46), suggesting that dephosphorylation of Cdk4/6 may be required for their activity towards Rb in cells.

Cdc25A acts as the main regulator of the G_1-S transition by dephosphorylating and activating Cdk2/cyclin E complexes (46). Cdc25A can dephosphorylate Cdk2/cyclin E and Cdk2/cyclin A both *in vitro* and *in vivo* (46). Several reports have described shortening of G_1 in response to Cdc25A overexpression, and accelerated G_1-S transition induced by Cdc25A correlates with increased activity of cyclin E- and cyclin A-associated kinase activity (46, 47).

Indeed, microinjection of Cdc25A antibodies into cells blocked entry into S-phase (48, 49) consistent with a requirement for Cdc25A in the G_1-S transition. Upon activation of Cdk2/cyclin E, a positive feedback loop is initiated in which Cdk2/cyclin E phosphorylates Cdc25A, increasing its activity until the cell is irreversibly commited to DNA synthesis (48). It should be noted that the specific site(s) of phosphorylation by Cdk2 complexes remains unknown, as does the identity of the phosphatase(s) that remove the phosphorylation(s), should such a phosphatase exist.

Initially, S-phase was thought to be controlled solely by Cdc25A, as Cdc25B and Cdc25C had been reported to control dephosphorylation of Cdk1/cyclin B, and Cdc25A dephosphorylated the S-phase Cdk/cyclin complexes. However, later reports illustrated potential roles for these phosphatases in S-phase progression as well. Cdc25B dephosphorylates phospho-Thr14 and phospho-Tyr15 on Cdk2/cyclin E and Cdk2/cyclin A complexes (50, 51). In HeLa cells, Cdc25B levels accumulate in S-phase and antisense oligonucleotides toward Cdc25B cause S-phase delay (52). It remains unclear however whether this represents a cell-type specific effect, because microinjection of antisense Cdc25B oligonucleotides into Fs68 fibroblasts or Cdc25B antibodies into Hs68 cells failed to suppress DNA synthesis (51, 53). Similarly, some reports have indicated that Cdc25C is required for S-phase progression, as Cdc25C antisense oligonucleotides prevented DNA synthesis in Fs68 fibroblasts, and reintroduction of Cdc25C by microinjection restored it (53), while other reports indicated that microinjection of Cdc25C antibodies into cells failed to elicit any effect (48, 51). These biochemical experiments are supported by the observations that Cdc25B and/or C knockout mice (described below) display no obvious S-phase defect (54-56).

Regulation of G_2 and M events by the Cdc25s is complex, requiring the cumulative but distinct temporal and spatial efforts of all three phosphatases. Cdc25A and B appear to be primarily responsible for movement through G_2, as overexpression of either these phosphatases in S or G_2 cells triggers mitotic initiation whereas Cdc25C overexpression alone does not (57, 58). In agreement, cells with reduced Cdc25A or B levels are delayed in G_2/M progression (59). The current model of Cdc25-dependent mitotic initiation requires activation of differentially located Cdk1/cyclin B by different phosphatases. Cdk1/cyclin B accumulates in the cytoplasm during interphase although Cdk1 is distributed throughout both the cytoplasm and the nucleus (60, 61). Prior to mitosis, Cdk1/cyclin B accumulates at the centrosome, where the initial activation of this complex occurs (60-62). Cdc25B activity peaks before that of Cdc25C (51), and is responsible for initial Cdk1/cyclin B activation at the centrosome (59). Activation of centrosomal Cdk1/cyclin B initiates a positive feedback loop in which phosphorylation of Cdc25A and Cdc25C by Cdk1/cyclin B stimulates their activities and, in the case of Cdc25A, stabilizes the normally labile protein (57, 63). These phosphatases in turn promote full activation of nuclear and cytoplasmic Cdk1/cyclin B, initiating mitosis (57). This model is supported by evidence that Cdk1/cyclin B phosphorylates Cdc25A and Cdc25C and that mutation of these phosphorylation sites prevents mitotic Cdc25A stabilization (57, 63). In agreement with a function for all three Cdc25 isoforms in mitosis, depletion of Cdc25A with siRNA decreases Cdk1/cyclin B activation and inhibits progression into mitosis (57), while microinjection of antibodies against Cdc25C or expression of a catalytically inactive Cdc25C mutant inhibits mitotic entry in HeLa cells (64, 65). Similarly, Cdc25B suppression by siRNA in HeLa cells delays mitotic entry (59). Also, microinjection of pre-metaphase Hs68 cells with Cdc25B antibodies inhibits cell division, and injection with GST-Cdc25B reinstates cytokinesis (51).

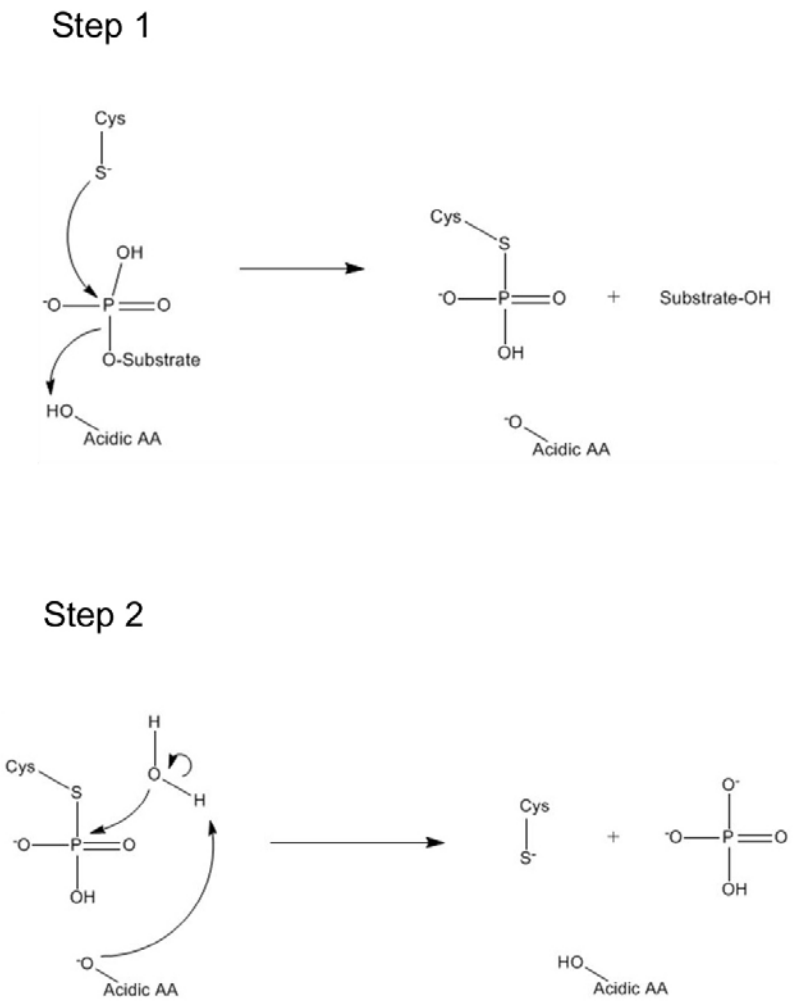

Figure 4. Catalytic mechanism of Cdc25.

The Cdc25 phosphatases dephosphorylate their substrates using a two-step mechanism that is conserved among tyrosine phosphatases. In the first step, the catalytic thiolate (Cys-S^-) attacks the nucleophilic phosphorous atom of the phosphosubstrate, generating a covalent bond. Protonation of the tyrosyl, threonyl, or seryl oxygen by the catalytic acid (Acidic AA) generates a good leaving group, and the substrate is expelled from the active site, leaving a thiophosphate intermediate. In the second step, the catalytic acid, now a base, abstracts a proton from a water molecule, promoting nucleophilic attack of the phosphorous atom, and release of organic phosphate with regeneration of the catalytic thiolate. The identity of the catalytic acid remains unknown, although some evidence suggests it may reside on the substrate (44).

Aside from regulation of Cdks in the cell cycle, there is recent evidence accumulating that the Cdc25s may have distinct roles in additional cellular processes required for cell division, although substantial data exists to support this hypothesis only for Cdc25B. Aside from initiation of Cdk1/cyclin B activation, Cdc25B is responsible for the proper formation and separation of the centrosome-linked microtubule networks. Accumulation of Cdc25B in the cytoplasm triggers mitotic microtubule nucleation at the centrosomes (64, 66) whereas treatment of HeLa cells with Cdc25 inhibitor BN82685 or with Cdc25B siRNA alters microtubule spindle assembly, resulting in lagging chromosomes, failure to localize γ-tubulin to the centrosomes and centrosomal separation delay (59, 66, 67). Cdc25B also appears to regulate centrosome duplication as overexpression of catalytically active Cdc25B results in centrosome overreplication (66). Preliminary evidence suggests Cdc25A may regulate chromatin condensation, consistent with its role of activating Cdk1/cyclin B in the nucleus, as Cdc25A siRNA increases the time between centrosome separation and DNA condensation (59). Notably, active Cdc25C is located microscopically and biochemically in the Golgi apparatus and the centrosomes, although a function for Cdc25C at these organelles has not yet been uncovered (68, 69).

1.3.3.2 The Cdc25s as regulators of cell cycle checkpoints

The human genetic code contains more than 3 billion base pairs of DNA. Faithful replication and segregation of this blueprint equally into daughter cells without generation of errors or the accumulation of damage is essentially impossible. Each cell experiences spontaneous hydrolysis of approximately 18,000 purines, 100 to 500 spontaneous cytosine deaminations and greater than 1200 methylations (both intentional and not) from endogenous sources every day at 37^{o}C (70). Generation of intracellular free radicals, exposure to ultraviolet

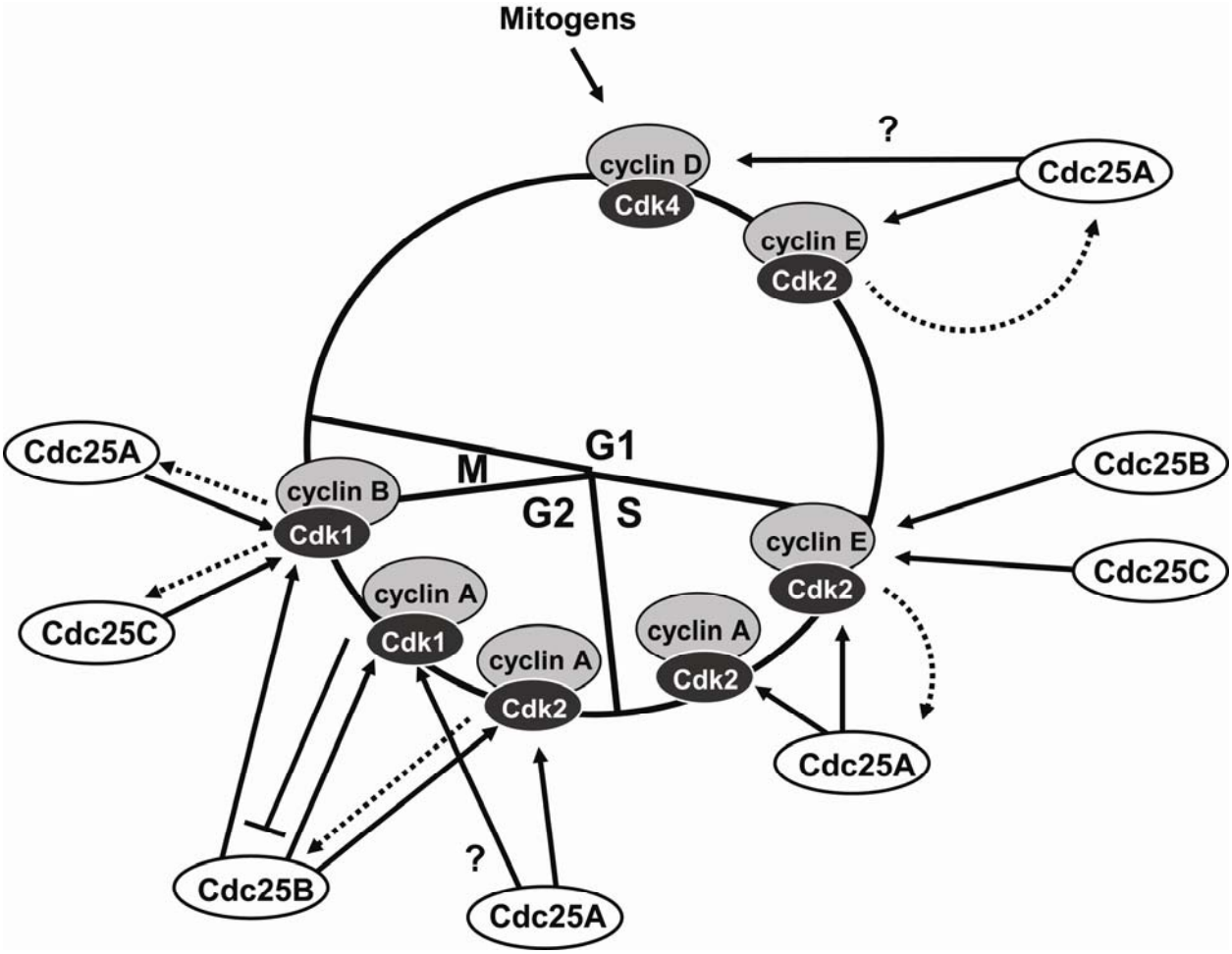

Figure 5. Regulation of Cdks and the cell cycle by the Cdc25 phosphatases.

The Cdc25 phosphatases dephosphorylate and activate Cdk/cyclin complexes in distinct but overlapping phases of the cell cycle. Cdc25A may be required for activation of Cdk4 complexes via dephosphorylation of $Cdk4^{Tyr17}$. Cdc25A is responsible for the G_1-S transition by activating Cdk2/cyclin E complexes. Recent evidence suggests that Cdc25A, B, and C combine their efforts to promote DNA synthesis in S-phase, and Cdc25A and B appear necessary for progression through G_2 up to the G_2-M transition, where the cumulative efforts of all three Cdc25 isoforms are required via distinct spatial and temporal activities for the initiation of mitosis. Question marks indicate activities that are supported by limited experimental evidence, and dotted arrows illustrate known positive feedback phosphorylations by Cdk/cyclin complexes. The T-bar from Cdk1/cyclin A to Cdc25B represents inhibitory phosphorylation that targets Cdc25B for ubiquitin-proteasomal degradation, thus limiting its activity.

and ionizing radiation, as well as numerous environmental insults such as cigarette smoke, radioactive materials and manmade chemicals also contribute to the constant assault suffered by DNA. The genome itself even encodes regions that are difficult to replicate (due to nucleotide repeats and repetitive DNA elements, and perhaps DNA inflexibility/conformation); attempts to replicate these sections or sections of damaged DNA can result in accumulation of mutations that are passed down to daughter cells upon cell divisions; thus, it is necessary to find and correct these lesions before cell division occurs.

To ease this process, cells have evolved several so-called "cell cycle checkpoints" to slow or stop cell cycle progression in cells either with damage to DNA or other physiological stresses that challenge cell division (for example, nucleotide depletion, replication fork stalling, aberrant DNA structures, failure to attach chromosomal kinetochores to the mitotic spindle), allowing time to rectify the stress(es). There exist several cell cycle checkpoints and they are named after the phase(s) of the cell cycle in which they act, namely the G_1, S-phase, G_2/M and M-phase checkpoints.

Each of these checkpoints is triggered by a cascade of protein-DNA and protein-protein interactions, and kinase activities (Figure 6). The process is initialized by the recognition of aberrant DNA, which in turn promotes binding of mediator proteins and activation of transducing checkpoint (Chk) kinases. Activation of the Chk kinases results in phosphorylation of target proteins that induce cell cycle arrest. As the Cdks are one of the major driving forces of the cell cycle, they are a target for inhibition by the checkpoints. Inhibition of the Cdks is mediated primarily by inactivation of Cdk-associated Cdc25 activity, resulting in Thr14- and Tyr15-hyperphosphorylated Cdks.

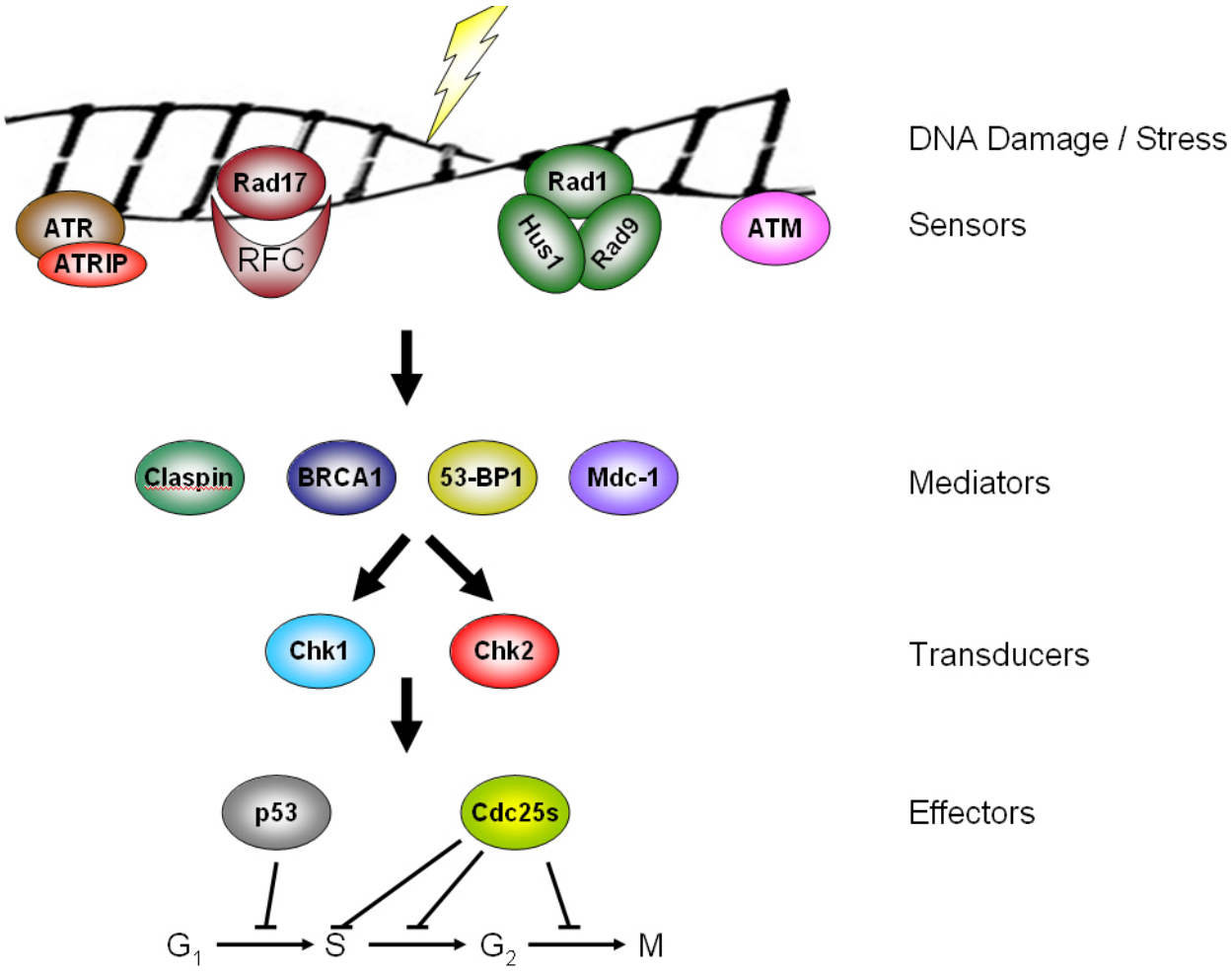

Figure 6. The DNA Damage Checkpoint Cascade.

Sensing of and response to DNA damage in the form either of DNA breaks (single- and double-stranded), mutated or mismatched bases, and replication stress (stalled or collapsed replication forks) is mediated by DNA-binding proteins that associate with mediators, promoting phosphorylation and activation of the transducer kinases Chk1 and Chk2. These kinases in turn phosphorylate target proteins, including the Cdc25s, inactivating them either by phosphorylation-dependent sequestration by 14-3-3 proteins, or by proteolytic degradation. In addition to Chk kinase-mediated inactivation of the Cdc25s, p53 can be phosphorylated and thus stabilized either by the Chk kinases or directly by the DNA damage-sensing kinases ATM and ATR. Adapted from (83).

Targeting of the Cdc25s by checkpoint initiation is biphasic, with a rapid phase (within an hour) and a sustained phase that takes several hours to initiate. Rapid inactivation of the Cdc25s following checkpoint activation is mediated by phosphorylation. Following checkpoint initiation, the Chk kinases, p38, glycogen synthase kinase 3β (GSK-3β) and MAPKAPK-2 can phosphorylate the Cdc25s at specific residues that regulate their stability and intracellular location (71-76). The mechanism by which the Cdc25s are inactivated following checkpoint initiation differs somewhat among isoforms: Cdc25A protein is rapidly degraded (71, 72, 74, 76-80) in a p53-independent fashion (72), whereas Cdc25B and Cdc25C are phosphorylated on serine (Ser) residues (Ser309 in Cdc25B (39), Ser216 for Cdc25C (35)), generating binding sites for 14-3-3, which sequesters Cdc25B and Cdc25C away from their Cdk substrates (35, 75)(Figure 7). Cdc25C protein degradation via the ubiquitin-proteasome pathway can be triggered in response to some agents, although the mechanism of targeting is poorly understood (81, 82). Sustained suppression of Cdc25 activity following checkpoint activation is mediated at the level of gene transcription. Following DNA damage, p21 binds and represses transcription from the Cdc25A promoter (84); a similar event occurs in response to hypoxia, in which p21 displaces c-Myc from the Cdc25A promoter (85).

p53 also requires a cell cycle-dependent element (CDE)/cell cycle homology region (CHR) site distal to the p53 binding site, and does not directly bind p53 (86). Inhibition through this site is independent of the p53 binding site and vice versa. Repression through the CDE/CHR site appears to be regulated by p21-dependent and p21-independent mediators (86). There are no reported transcriptional suppressors of Cdc25B following checkpoint activation. Curiously, Cdc25B protein levels are rapidly increased following checkpoint initiation via a post-transcriptional mechanism, and this appears to regulate cell cycle reentry (87, 88).

1.3.4 Cdc25A as the master regulator of cell cycle progression

Although the conventional cell cycle paradigm prescribes essential roles for each Cdc25 isoform, recent studies have questioned the necessity of Cdc25B and C in the mammalian cell cycle. Cdc25A is the only reported isoform active in G_1, implying Cdc25B and C are not necessary for early cell cycle events. Cdc25A knockout mice are not viable and fail to develop beyond the blast phase (89). In contrast, Cdc25B mice progress normally through development, and the males are completely absent of a phenotype; females are sterile due to their inability to activate maturation-promoting factor (ie, meiotic cell Cdk1/cyclin B) but otherwise normal (56). Similarly, Cdc25C-null mice are viable and apparently normal (54). Subsequently Cdc25B/C-null mice were generated from Cdc25B-null males and Cdc25C-null females, and these too display no apparent phenotype (55). This implies that Cdc25A alone is sufficient to sustain the mammalian cell cycle.

In favor of a model where Cdc25A is the primary essential regulator of cell cycle progression, $Cdc25A^{+/-}$ mouse embryonic fibroblasts (MEF) display higher levels of phospho-$Cdk1/2^{Tyr15}$ and have a shortened proliferative lifespan, although levels of Cdc25B and C are similar between $Cdc25A^{+/+}$ and $Cdc25A^{+/-}$ MEFs (89). These hemizygous MEFs also demonstrate difficulty recovering from G_2 checkpoint, suggesting either that Cdc25A activity is limiting for cell cycle reentry from checkpoint (89). Collectively, the data from knockout mouse models and heterozygous MEFs indicate that Cdc25A is indispensable for normal cell cycling, whereas Cdc25B and C are not necessary.

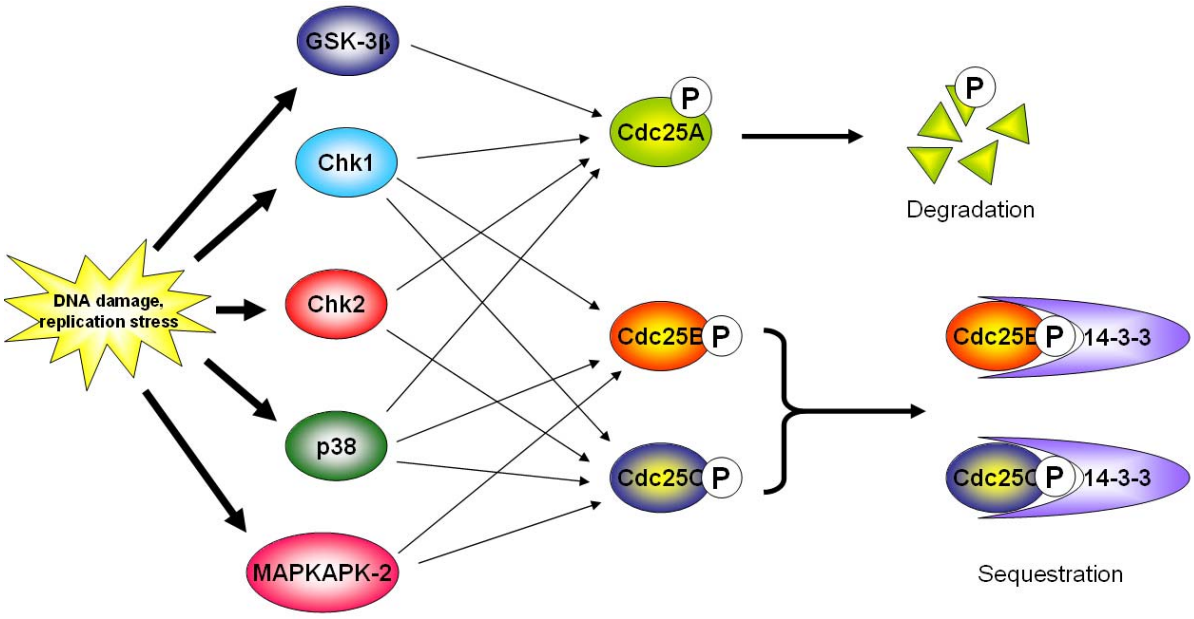

Figure 7. Regulation of the Cdc25s by checkpoint signaling.

Induction of cellular stress activates the Chk kinases and/or p38, GSK-3β, and MAPKAPK-2, which in turn phosphorylate each Cdc25 isoform on specific residues (see text for details). Phosphorylation of Cdc25A targets it for ubiquitination by the $SCF^{\beta\text{-}TrCP}$ complex and subsequent proteasomal degradation. Phosphorylation of Cdc25B and Cdc25C completes 14-3-3 binding sites, promotes 14-3-3-binding, and sequestration of the phosphatases away from their Cdk substrates. The culmination of these events is hyperphosphorylation and inactivation of Cdk complexes, slowing or stopping the cell cycle.

1.3.4.1 The role of Cdc25A in malignancy

Several hallmarks of human cancers have been described (90). Acquisition of these phenotypes is essential for the successful and continued proliferation of the cancerous cells in the host. These characteristics include a limitless replicative potential, resistance to anti-growth signals, and resistance to apoptosis (90). As an essential cell cycle regulator, aberrant control of Cdc25A has the potential to provide cells with the means to escape anti-growth signals and proliferate inappropriately. Examination of the available clinical data supports this hypothesis

(91). Cdc25A is overexpressed in numerous human cancers derived from a distinct array of cellular tissues, including esophageal, thyroid, breast, ovarian, non-small cell lung, colorectal, laryngeal, hepatocelluar, head and neck, and non-Hodgkin's lymphoma (reviewed in (91)). Indeed, in many cases, Cdc25A levels correlate with poor prognosis or particularly aggressive cancers (91).

A particularly insightful study in 2003 identified several distinct modes of Cdc25A deregulation in breast cancer cell lines (92). Although the levels of Cdc25A mRNA were largely unaltered and only slightly (two to three-fold) higher than in normal human mammary epithelial cells in the most severe cases, the protein levels of Cdc25A were as much as 49 times higher, and the phosphatase activity as much as nine times higher (92). This indicates that deregulation of basal protein levels generally occurs at a post-transcriptional level, and that protein levels and phosphatase activity are not necessarily correlated one-to-one. Notably, Cdc25A was not destroyed in response to ionizing radiation (IR) in some of these cell lines, indicating that deregulation of the checkpoint signaling machinery may also contribute to Cdc25A deregulation in breast cancer (92).

Although these studies provide correlative evidence of a role for Cdc25A in carcinogenesis, several studies have provided more direct evidence for Cdc25A deregulation contributing to tumor formation (Figure 8). Early studies showed that expression of human Cdc25A could cooperate with oncogenic Ras^{G12V} or Rb loss to transform rat fibroblasts as assayed by anchorage-independent growth in soft agar and loss of contact inhibition by focus formation assay (93). In agreement with this study, transgenic mice expressing Cdc25A and H-Ras under the control of the mouse mammary tumor virus (MMTV) promoter display a decreased tumor-free latency compared to H-ras-MMTV transgenic mice, from 20 weeks of age

to 12 weeks (94). Similarly, transgenic mice expressing Cdc25A and Erb2/*neu* under control of the MMTV promoter display no difference in the median time of tumor-free survival, but display greatly accelerated growth of breast tumors compared to MMTV-Erb2/*neu* transgenic mice alone as determined by tumor volume (94). These observations are corroborated by reciprocal studies in which Cdc25A$^{+/-}$ MEFs display resistance to transformation by H-ras in conjunction with a dominant-negative p53 compared to wild-type MEFs. Indeed, transgenic Cdc25A$^{+/-}$ mice also harboring MMTV H-ras or MMTV-*neu* display increased tumor latency. Interestingly, Induction of tumor formation by MMTV-myc is not affected by Cdc25A heterozygosity, suggesting that Cdc25A may cooperate selectively with oncogenes or tumor suppressors to induce transformation; alternatively, it may represent the fact that the *CDC25A* gene is a target for the myc oncogene, making this "two-hit" redundant.

Recent studies have also implicated Cdc25A in directly generating accumulation of DNA damage, thus contributing to genomic instability in tumor cells. Ectopic expression of Cdc25A alone is sufficient to induce expression of the DNA damage/checkpoint markers p53, γH2AX, phospho-Ser317 and phospho-Ser345 Chk1, phospho-Thr68 Chk2, and Rad17-associated phospho-serine (95). Also, breast tumors derived from MMTV-Cdc25A/*neu* mice display increased frequency of karyotypic abnormalities compared to tumors from MMTV-*neu* mice, consistent with a role for Cdc25A in the induction of genomic instability (94).

Although severe destabilization of the genome is normally a cytotoxic event, the ability of Cdc25A to induce DNA damage without inducing cell death may lie in its ability to regulate apoptosis. Reports exist citing both pro- and anti-apoptotic activities of Cdc25A (96-100), and it has even been suggested that Cdc25A intracellular localization may determine whether it elicits pro- or antiapoptotic effects (101). Most evidence that Cdc25A is pro-apoptotic is derived from

studies examining c-Myc-induced apoptosis (97, 98, 100) and is dependent upon ectopic Cdc25A expression, drawing into question their physiological relevance. It has been postulated that the role of Cdc25A in c-Myc-induced apoptosis may derive from mismatching cell cycle and growth factor signals as a result of deregulated Cdc25A (102). Those authors also observed downregulation of Cdc25A but not c-Myc during TNFα-induced apoptosis in N.1 ovarian carcinoma cells and that Cdc25A overexpression suppressed apoptosis in non-transformed rat 423 cells in response to serum withdrawal (96). Notably, these cells did not express detectable levels of c-Myc, consistent with the above hypothesis (96, 102). Irrespective of its potential role in c-Myc-regulated apoptosis, an elaborate study demonstrated inhibition of apoptosis signal-regulating kinase-1 (ASK-1) by Cdc25A in a phosphatase activity-independent manner (103). The authors identified Cdc25A in a yeast two-hybrid assay for ASK-1-interacting proteins and further studies found that Cdc25A colocalized with ASK-1 in 293 and OVCAR-8 cells and was associated with ASK-1 in reciprocal immunoprecipitates from mammalian cells. Moreover, Cdc25A overexpression diminished activation of the downstream kinases of ASK-1, and blunted apoptosis in response to oxidative stress. As ASK-1 is activated in response to a number of genotoxic stimuli (104), it is attractive to posit that Cdc25A may blunt apoptotic signaling in response to other noxious stimuli as well as to oxidative stress.

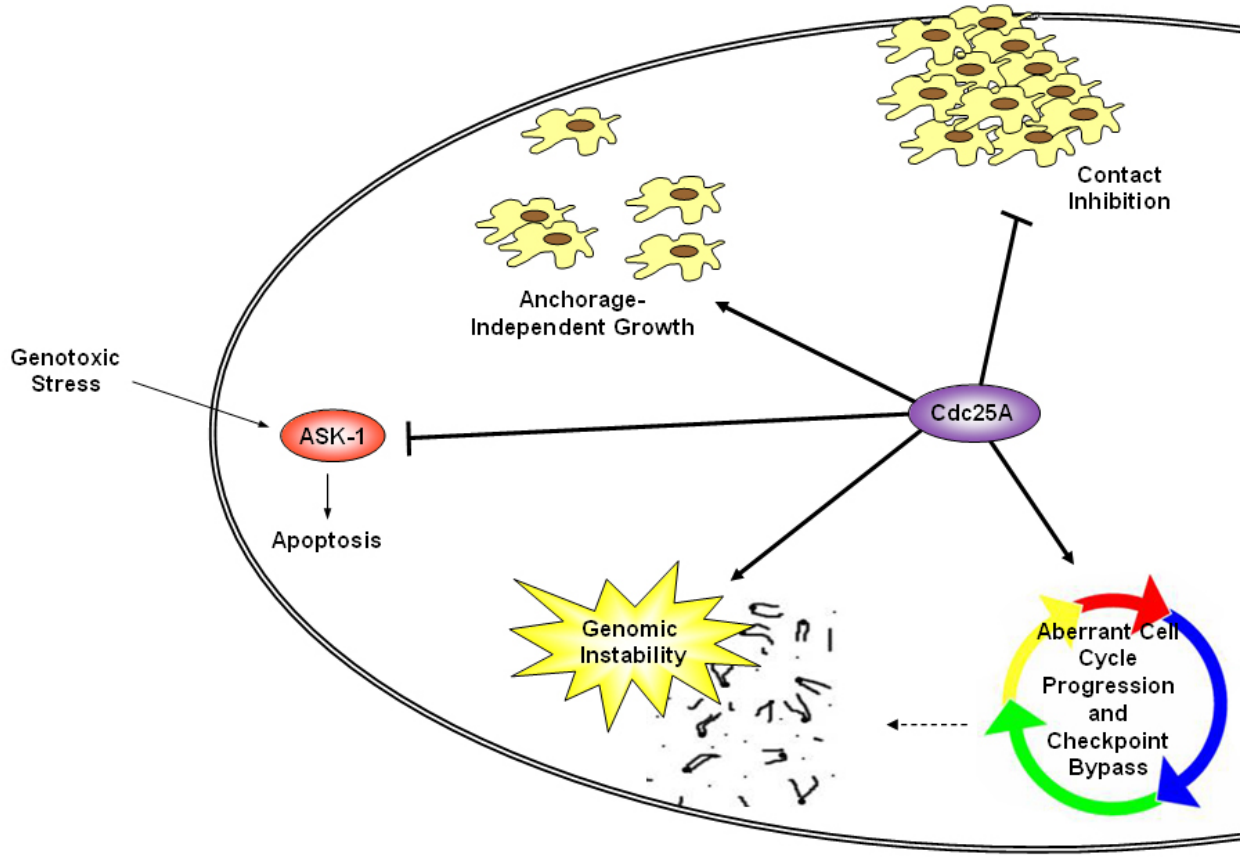

Figure 8. Cdc25A deregulation promotes tumorigenesis.

Overexpression of Cdc25A promotes many characteristics of human cancers. Early studies demonstrated that Cdc25A cooperates with H-Ras^{G12V} or Rb$^{-/-}$ in rodent fibroblasts to promote focus formation and anchorage-independent growth in soft-agar (93). This evidence is supported by studies in a MMTV-H-ras model of breast tumorigenesis in which Cdc25A$^{+/-}$ MEFs were resistant to transformation whereas overexpression of Cdc25A increased tumor incidence, size, and promoted apparent genomic instability (89, 94). Also, Cdc25A binds to and inhibits the activity of ASK-1 (103), and attenuates apoptotic induction in response to H_2O_2 and serum-deprivation (96, 103). Several studies have demonstrated that Cdc25A overexpression promotes accumulation of DNA damage and premature progression through the cell cycle both in the presence and absence of checkpoint activation (46, 57, 71, 94, 95, 105).

1.4 REGULATION OF CDC25A ACTIVITY

Stringent control over Cdc25A expression and activity are essential to allow productive cell growth under the appropriate signals without unwarranted proliferation. Deregulation of Cdc25A promotes tumorigenesis, damages DNA, and prevents apoptosis (89, 93-96, 103). These data support the observation that overexpression of Cdc25A is a hallmark of human cancers (91). Cells have thus evolved multiple mechanisms to control the levels and function of Cdc25A both on a cellular or biochemical level. The summation of these restraints allows for fine-tuning of Cdc25A activity in response to the cell environment, and prevents aberrant accumulation of Cdc25A protein or activity.

1.4.1.1 Cellular regulation

Regulation of Cdc25A is temporally and spatially complex, involving changes in the expression and intracellular localization in response to intra- and extracellular stimuli. Reports describing control of Cdc25A transcription and stability abound in the literature. Transcription of Cdc25A is controlled by numerous transcription factors eliciting both postive (c-Myc, STAT3, E2F) and negative (p53, p21, STAT3, and HIF-1α) control over the *CDC25A* promoter. Negative regulation of Cdc25A transcription by p21 and HIF-1α in response to stress has already been discussed (see Section 1.4.2.2) (84, 85). Transcription from the *CDC25A* gene first occurs in early G_1 in response to mitogen-stimulated E2F release from Rb by Cdk4 (106, 107). c-Myc is also capable of inducing transcription from the *CDC25A* gene (97), and recent studies suggest that it cooperates with STAT3 in response to mitogens to promote Cdc25A transcription (108).

Without c-Myc, STAT3 fails to regulate Cdc25A transcription, indicating that these two transcription factors likely collaborate to induce Cdc25A expression. Surprisingly, STAT3 also can negatively regulate Cdc25A transcription in response to H_2O_2 by forming a transcriptional repressor complex with Rb that binds the *CDC25A* promoter (108). Finally, p53 decreases expression from the *CDC25A* gene and this action is dependent upon p53 DNA-binding, but apparently not to the *CDC25A* promoter as chromatin immunoprecipitation experiments failed to identify p53-bound DNA fragments associated with the Cdc25A promoter (109).

The most-studied aspect of Cdc25A expression is the regulation of the Cdc25A protein half-life. The protein half-life of Cdc25A is regulated by the ubiquitin-proteasome system; two different E3 ubiquitin ligases have been identified that target Cdc25A for proteolysis, and they operate in different phases of the cell cycle. The half-life of Cdc25A in G_1, S, and G_2 cells is regulated by the Skp/Cullin/F-box (SCF) family E3 ligase Skp1/Cul1/β-transducin repeat-containing protein (β-TrCP). Proteolysis induced by $SCF^{\beta\text{-TrCP}}$-mediated ubiquitination is extremely rapid; multiple groups have estimated the Cdc25A protein half-life in interphase HeLa cells as less than 10 minutes (110, 111). Recognition of Cdc25A by $SCF^{\beta\text{-TrCP}}$ is a complex process that is not fully understood, but requires two independent phosphorylation events. The first is likely a priming phosphorylation at Ser76, which is catalyzed by GSK-3β during G_1 (76) and by Chk1 during S-phase and G_2 (74, 112). The second event is subject to debate, but appears to require phosphorylation of Ser82 and at least one of serines 79 and 88 (77, 78). Phosphorylation of these serines creates a phosphodegron surrounding a DSG amino acid motif, which is a common recognition motif for β-TrCP-binding (113). The kinase(s) responsible for this second phosphorylation event remains unknown, although Cdk2 has been proposed as a potential candidate kinase on the basis that chemical or genetic inhibition of Cdk2 kinase activity

increases Cdc25A half-life (110). The kinase(s) responsible for the second phosphorylation event would have to be active in G_1, S, and G_2 phases, which is consistent with the temporal profile of Cdk2 kinase activity. Additionally, phosphorylation of Cdc25A by Cdk2/cyclin E increases Cdc25A activity (48), which would result in a self-attenuating regulation of Cdk2 activity. This type of autoregulatory system is attractive because it would prevent transient fluxes in Cdc25 or Cdk2 activity from prematurely triggering DNA synthesis or progression through G_2.

The $SCF^{\beta\text{-}TrCP}$ ubiquitin ligase is also responsible for the accelerated proteolysis of Cdc25A following checkpoint activation in G_1, S and G_2 cells (76-78). In response to checkpoint activation, Cdc25A is phosphorylated on a number of serines in its N-terminus, which promotes more efficient recognition of Cdc25A by $SCF^{\beta\text{-}TrCP}$ and enhanced ubiquitination and degradation. Several reports have identified Chk1, Chk2, GSK-3β, and p38 as the kinases that phosphorylate Cdc25A following checkpoint signaling by replication stress, DNA damage, or osmotic stress (76, 114). The sites of phosphorylation differ among these kinases (reviewed in (114)), but can include Ser76, Ser124, Ser178, Ser279, and Ser293. The function(s) of these serine phosphorylations (with the exception of phospho-Ser76) is poorly understood. It has been hypothesized that phosphorylation of serines 124, 178, 279, and 293 in response to stress may change the conformation of Cdc25A, enhancing ubiquitylation kinetics and thus Cdc25A degradation, although this model remains to be evaluated (114).

In contrast to interphase Cdc25A, mitotic Cdc25A is much more stable with an apparent half-life of at least 20 minutes (57, 111). Once Cdk1/cyclin B becomes activated at the G_2-M transition, Cdc25A is uncoupled from $SCF^{\beta\text{-}TrCP}$-mediated degradation by phosphorylation at Ser18 and Ser116 (and perhaps Ser320) by Cdk1/cyclin B (57, 115). Dephosphorylation of (at

least) Ser116 and Ser320 is mediated by Cdc14A, although the physiological significance is not known (115). Regardless, phospho-Ser18/Ser116-mediated Cdc25A accumulation is necessary to achieve threshold activation of Cdk1/cyclin B to trigger the irreversible commitment to mitosis, as a high threshold for Cdc25 activity would prevent minor fluctuations in Cdc25 activity from triggering mitosis prematurely (57). This stable form of Cdc25A persists until mitotic exit, at which point the cell cycle machinery must be reset to prevent aberrant progression through the G_1-S transition. During mitotic exit the Anaphase-promoting complex, or cyclosome (APC/C), is activated. Like the $SCF^{\beta\text{-}TrCP}$ complex, the APC/C is a RING-finger family multi-protein ubiquitin ligase that recognizes and ubiquitinates proteins involved in mitosis for degradation by the proteasome (113). Targeting of Cdc25A by the APC/C is mediated by a KEN-box motif in the N-terminus (111). Destruction of Cdc25A during late mitosis and early G_1 ensures that it does not trigger activation of Cdk4 and Cdk2 complexes prematurely during the subsequent cell cycle. An additional level of Cdc25A control is mediated by Chk1 phosphorylation and occurs in interphase cells. Phosphorylation of Cdc25A at Ser178 and T507 by Chk1 promotes binding of 14-3-3 to Cdc25A and restricts its activity toward Cdk1/cyclin B to prevent premature mitotic entry (37).

1.4.1.2 Biochemical regulation

Elucidation of the crystal structure of the Cdc25A catalytic domain unexpectedly revealed a disulfide bond between the active site Cys431 and Cys385 in some crystals (42). The authors originally postulated that the enzyme may be self-inhibited under conditions of oxidative stress. Enzymatic analysis of Cdc25B later revealed that the pK_a of the catalytic cysteine is extremely low (5.6 vs. 8.3 for free cysteine), indicating it exists primarily as a thiolate anion at physiological pH (44). Given the high identity in the primary sequence and the nearly-identical

three dimensional structures of the Cdc25A and B catalytic domains, it is anticipated that the Cdc25A catalytic cysteine also exists as a thiolate. Whereas thiols are not particularly reactive with oxidants such as H_2O_2, thiolates react with H_2O_2 with rates from approximately 10^1 to 10^5 $M^{-1}s^{-1}$ (116). Based on these observations it was hypothesized that the activity of Cdc25 phosphatases would be inhibited by oxidation of the catalytic cysteine in response to oxidative stimuli such as H_2O_2. A thorough kinetic analysis confirmed this hypothesis indicating rates of inactivation of all three Cdc25 isoforms by H_2O_2 on the order of 100 $M^{-1}s^{-1}$, more than 400-fold faster than the oxidation of the major cellular reductant glutathione (GSH)(117). Loss of activity was accompanied by the formation of a disulfide bond between the catalytic cysteine and a three-dimensionally adjacent cysteine (now referred to as the back-door cysteine) as determined by mass spectrometry (MS). This study also discovered that the back-door cysteine acts to protect the catalytic cysteine from more severe oxidation (presumably by disulfide formation) in response to mild oxidative conditions, as mutation of this residue resulted in the loss of disulfide formation and the appearance of the "irreversible" catalytic sulfinic acid (117). Most interestingly, whereas up to 50 mM GSH failed to significantly restore Cdc25B activity following H_2O_2 treatment, the low molecular mass (LMM) dithiol protein thioredoxin (Trx) was able to restore Cdc25B containing this intramolecular disulfide bond to the reduced active form at a rate 2000 times greater than DTT, indicating that Trx is likely the intracellular agent responsible for maintaining Cdc25 enzymes in their reduced active form *in vivo* (117). As this enhanced activity toward Cdc25 cannot be explained merely by reduction potentials (-270 mV for Trx (118) vs. -330 mV for DTT (119)), other forces (likely protein-protein interactions) must enhance Trx activity toward Cdc25.

Cdc25C from HeLa cells treated with H_2O_2 undergoes a redox-sensitive change in migration that is dependent upon the integrity of the catalytic cysteine and the predicted back-door cysteine (120). Oxidation of Cdc25C is accompanied by a shortening of its protein half-life and an increase in association with 14-3-3, suggesting that the oxidized form of Cdc25C is removed from cellular circulation and subsequently degraded (120). Reports also abound of loss of Cdc25A expression following H_2O_2 treatment, but the mechanism is subject to debate (108, 121). Generation of a STAT3-Rb complex that represses transcription of Cdc25A has been described following H_2O_2 treatment. Cdc25A protein levels are also decreased by H_2O_2 in HeLa cells, which have inactivated Rb due to the human papilloma virus (122, 123), and treatment with the peroxide-generating isoquinoline Caulibugulone A shortened Cdc25A protein half-life via activation of p38 (121), questioning whether a transcriptional mechanism is involved.

Although the mechanisms governing Cdc25 activity following oxidants and reactive oxygen species (ROS), relatively little attention has been paid to other families of reactive species such as nitric oxide (•NO) and •NO-derived reactive species (RNS), which have gone essentially unexamined.

1.5 NITROGEN OXIDES

Nitrogen makes up approximately 78% of the Earth's atmosphere, and is the fourth most common element by mass in living systems.[4] Incorporation of nitrogen into biomolecules is

[4] Nelson, David L., and Cox, Michael M. Principles of Biochemistry. 4th Ed. New York: Lehninger, 2005.

essential for all living species, yet most life forms cannot utilize elemental nitrogen. Instead, fixation of atmospheric dinitrogen to usable forms such as NO_3^- and NH_3 by nitrogen-fixing life forms known as diazotrophs (generally bacteria) must occur. These fixed nitrogen sources are absorbed by plants, which then transfer nitrogen to herbivores and omnivores, and subsequently to carnivores via their respective ingestions of nitrogen-containing species.[5] Nitrogen is contained in DNA, RNA, and every amino acid, and is utilized in various forms both macro- and unimolecularly for cellular signaling. This section will familiarize the reader with the role of oxygen-containing forms of nitrogen (nitrogen oxides) in physiological and pathological control of cellular processes with a focus on the mammalian cell cycle.

1.5.1 •NO and RNS: origin, properties, and fate

Nitric oxide (•NO) is a diatomic free radical molecule produced in many eukaryotic organisms that is involved in processes ranging from bioluminescence to vasodilation. In fact, •NO was first described as "endothelium-derived relaxation factor" due to its potent vasodilatory effects on vascular smooth muscle (124, 125). In humans, the most well-recognized source of •NO is the nitric oxide synthase (NOS) enzymes endothelial NOS (eNOS), neuronal NOS (nNOS) and inducible NOS (iNOS). •NO is produced differentially by the NOS enzymes; eNOS and nNOS generally elicit production of low quantities of •NO while iNOS generally produces high quantitites of •NO. These enzymes catalyze the O_2- and reduced nicotinamide adenine dinucleotide phosphate (NADPH)-dependent five-electron oxidation of the imino nitrogen of *L*-arginine to produce •NO and *L*-citrulline (and oxidized NADPH, or $NADP^+$)(126). The NOS

[5] http://users.rcn.com/jkimball.ma.ultranet/BiologyPages/N/NitrogenCycle.html

enzymes function as homodimers and are dependent upon the tight binding of several cofactors, namely flavin mononucleotide, flavin adenine dinucleotide, tetrahydrobiopterin, and heme iron, which pass electrons from NADPH to the imino nitrogen of *L*-arginine (126). Additionally, nNOS and eNOS are Ca^{2+}-dependent enzymes, as they bind calmodulin. The reaction stoichiometry is generally thought to occur as displayed in scheme 1:

$$L\text{-Arg} + 1.5\ NADPH + 1.5\ H^+ + 2\ O_2 \rightarrow \bullet NO + L\text{-Citrulline} + 1.5\ NADP^+ + 2\ H_2O \quad (1)$$

There is some debate as to whether or not the NOS enzymes truly produce •NO or some other species; it has been suggested that peroxynitrite ($ONNO^-$)(127), nitroxyl (NO^-/HNO)(127), H_2O_2 (128), and/or superoxide ($\bullet O_2^-$)(129-131) could be formed from NOS enzymes. Alternatively, it may be necessary for closely-associated superoxide dismutase (SOD) activity to generate •NO from NOS enzymes by Cu(II)-SOD-mediated oxidation of NO^- to •NO (127). For the purposes of this thesis, I will not discriminate between the possible nitrogen oxide(s) and ROS that may initially be produced by NOS enzymes; instead I will consider •NO the primary product of NOS enzymes under physiological conditions, as the bulk of the literature suggests this is the primary product and I have no evidence to suggest otherwise.

It should be mentioned that there are other biological sources of •NO aside from the NOS enzymes; release of •NO by *S*-nitrosothiols (RSNOs) in the circulatory system is well-documented, and it has been suggested that RSNOs may act as a physiological storehouse for •NO bioactivity in the bloodstream (132). Under hypoxic conditions, xanthine oxidase catalyzes the nicotinamide adenine dinucleotide-dependent reduction of NO_3^- and NO_2^- (as well as organic nitrates such as nitroglycerin) to •NO (133). Reduction of NO_2^- by deoxyhemoglobin and eNOS under oxygen-deficient conditions have also recently been reported (134, 135). Nitrated lipids

are also capable of donating •NO in protic solvents (136) by homolysis and/or transition metal/ascorbate-assisted reduction (137).

•NO is a relatively stable radical with a half-life of 5 to 15 seconds, and is readily soluble in both aqueous and hydrophobic phases (with more favorable partitioning into hydrophobic phases), allowing its diffusion into and out of cells, with a radius up to 100 – 200 μm through biological milieu (138). •NO can thus execute both autocrine and paracrine signaling. •NO has an unpaired electron, and it can both accept and donate an electron (e^-) to generate the non-radicals NO^-/HNO and nitrosonium (NO^+), respectively (139). •NO is surprisingly unreactive considering that it is a free radical, and reacts only with other paramagnetic species such as transition metals and free radicals. Many of these reactions are relatively unstable with the ultimate end-products of •NO formation *in situ* generally being considered NO_2^- and NO_3^-.

•NO reacts readily with the diradical O_2 in 2:1 empirical stoichiometry to generate nitrogen dioxide, $•NO_2$. The $•NO_2$ product, also a radical, is readily reactive with numerous biomolecules including additional $•NO_2$, •NO, thiols, ascorbate, tyrosine, tryptophan, and unsaturated fatty acids (140), and elicits primarily oxidation of targets and/or formation of nitrated biomolecules via one-electron oxidations, radical recombination, or addition across double bonds (140, 141). Recombination of $•NO_2$ with •NO yields the potent nitrosant N_2O_3. The formation of this species in biologically relevant amounts has been questioned due to the relatively slow autooxidation rate of •NO at physiologically relevant concentrations (142). Nonetheless, recent experiments have shown acceleration of •NO autooxidation in lipid membranes, as the local •NO and O_2 concentrations are higher than in aqueous medium due to their preferential solubility in hydrophobic environments (142, 143). In addition, it has recently been demonstrated that hemoglobin is capable of reducing nitrite to N_2O_3 via catalytic reaction

of metheme-bound NO_2^- (which shows partial Fe(II)-•NO_2 character) with •NO, regenerating hemoglobin and releasing N_2O_3 (144). These studies raise the possibility that N_2O_3 may accumulate and thus have significant biological effects *in vivo*; it has recently been hypothesized that N_2O_3 accounts for up to 90% of nitrosation in cells (145), and evidence demonstrating quenching of *N*-nitrosation by azide (which reacts selectively with N_2O_3) upon cogeneration of •NO and $•O_2^-$ support this hypothesis under some conditions (146).

Reaction of •NO with $•O_2^-$ occurs at a diffusion-limited rate of 1.9×10^{10} $M^{-1}s^{-1}$ (147). The product is $ONOO^-$, which upon protonation (the pK_a is altered by solution composition, but ranges from 6.5 to 7.5, (147, 148)) decomposes either via homolysis to •NO_2 and hydroxyl radical (•OH), or by intramolecular rearrangement to $NO_3^- + H^+$ (149). $ONOO^-$ itself is a strong oxidant (E^o(ONOOH, H^+ / •NO_2) at pH 7 = 1.4 V, (150)) and is a potent oxidant of thiols and lipids (151, 152). $ONOO^-$ can also be rapidly scavenged by CO_2, which is present in high soluble concentrations in many tissues, generating the unstable species nitrosoperoxocarbonate ($ONOOCO_2^-$), which subsequently undergoes homolytic cleavage to •NO_2 and $CO_3^{•-}$ (153) or rearranges to nitrate and CO_2. The result of shunting of $ONOO^-$ into nitrosoperoxocarbonate appears to be two-fold: a relative detoxification of $ONOO^-$ by disproportionation to NO_3^-, and a reequilibration of $ONOO^-$-mediated two-e^- oxidations to one-e^- oxidations mediated by •NO_2 and/or $CO_3^{•-}$ (154).

Direct •NO recombination with thiyl radicals (RS•) has also been described, but will be discussed in Section 1.5.2.3. One additional well-studied interaction of •NO is with transition metals. Interaction of •NO with transition metals fall into three categories: 1) direct reaction of •NO with the metal center to generate metal-nitrosyls, 2) •NO oxidation of metals in dioxygen metal complexes, and 3) reduction of high valence metal-oxo complexes. The most common

form of metal-nitrosyl is a mononitrosyl, in which •NO reacts 1:1 with a metal ion (155). Although in theory •NO can bind many transition metals to form a complex, only a few

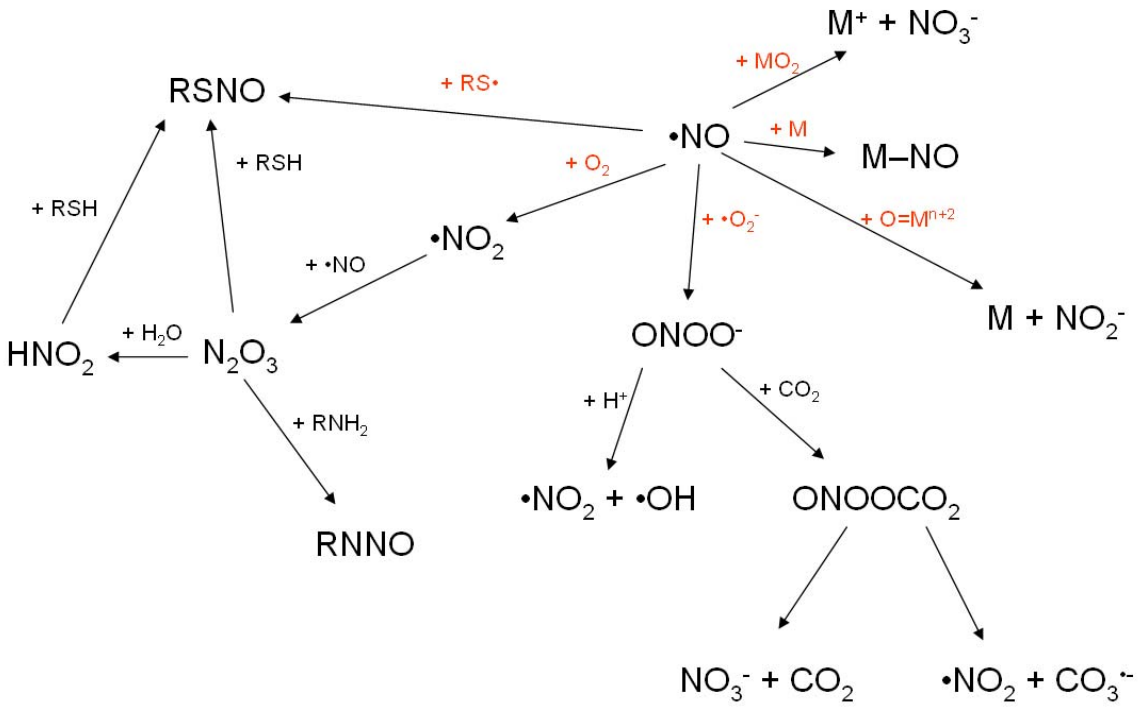

Figure 9. Interactions of •NO with biologically relevant molecules.

In biological milieu, reactions of •NO are largely limited to reactions with transition metal complexes, oxygen radicals (either molecular oxygen or $•O_2^-$), and with other radicals (largely lipid radicals, thiyl radicals). The downstream products of these reactions are known as •NO-derived reactive species. Molecules with which •NO reacts directly are shown in red type, and direct and indirect downstream products are shown in black type. This figure is a simplified schematic of •NO reactions with biological molecules. M, metal ion.

complexes are formed in significant quantity in biological systems due to metal availability and energetic requirements (156). The prototypical example of this type of •NO binding is the binding of •NO to the heme-histidyl-pentacoordinated Fe^{2+} moiety in soluble guanylate cyclase (157). Interaction of •NO with oxygenated metal complexes, such as the oxyheme moiety in oxyhemoglobin and oxymyoglobin, results in oxidation of •NO to NO_3^- and oxidation of the

Fe(II) heme to metheme (Fe(III))(144). Finally, high-valence metal-oxo complexes such as Fe(IV)=O and Fe(V)=O are reduced by •NO to ferric heme and NO_2^-, thus detoxifying these potent oxidants (158, 159).

As reaction of •NO is largely limited to interactions with other radicals (including dioxygen) and transition metals, the products of these reactions are largely either the relatively stable species NO_2^- and NO_3^-, or oxidants/nitrating agents ($ONOO^-$, $ONOOCO_2^-$, $•NO_2$) and nitrosants (N_2O_3 and RSNO). The breadth of species generated by •NO reaction coupled to the number of potential sites of generation allows for a staggering number of potentially independent signaling events. Deciphering the biochemical regulation of •NO and RNS is therefore quite complex, although several well-studied models exist that delineate the common themes. •NO and RNS can regulate protein function through covalent and non-covalent mechanisms; non-covalent regulatory mechanisms are relatively rare. The activities of RNS such as N_2O_3, $ONOO^-$, and $•NO_2$ toward proteins can generally be divided into three areas: nitros(yl)ation, nitration, or oxidation. The relative proportions of each of these activities is dependent on many factors determined both by the characteristics of the individual species formed as well as the environment in which the substrate and reactive species is located. It is becoming increasingly apparent that the bias between oxidative/nitrative events and nitrosative events may be dependent upon the relative proportions of •NO to $•O_2^-$ being formed in close proximity to one another (146, 160).

1.5.2 Biochemical regulation of protein function by nitrogen oxides

The high reactivity of •NO/RNS allots them a miniscule half-life in biological milieu, which suits them well for transducers of cellular signaling, as the relative levels of RNS can be rapidly

altered in response to changes in •NO and/or $•O_2^-$ production. Proteins mediate many signaling pathways in cells and thus are targets for and transducers of •NO-dependent signaling. Transduction of signaling by proteins can be enacted by •NO either directly or indirectly through the activities of •NO-derived reactive species. Direct regulation of proteins by •NO is typically mediated either by •NO-bonding with a protein-complexed transition metal, or by direct recombination with a protein radical center. Direct regulation of proteins by •NO is typically associated with low levels of •NO production, as is the case for soluble guanylate cyclase (sGC) (157).

1.5.2.1 Direct modulation of protein signaling by •NO

One of the best-studied examples of protein regulation via direct •NO binding is that of sGC, which regulates smooth-muscle relaxation in response to •NO via its cyclization of guanosine triphosphate to cyclic guanosine monophosphate (cGMP)(157). Binding of cGMP by cGMP-dependent protein kinase then occurs, resulting in its activation and subsequent transduction of the •NO signal (161). sGC exists as a heterodimer of an α-subunit and a heme-binding β-subunit. The heme group contains a penta-coordinated heme-histidyl-Fe^{2+} complex, which acts as the •NO sensor. Upon binding of •NO to the heme-Fe^{2+}, a covalent bond is formed that disrupts interaction of the histidine with the iron atom, resulting in a conformational change in the protein that increases its activity ~200-fold (162). According to kinetic modeling, the inactivation of sGC (due to •NO dissociation) proceeds primarily via *trans*-nitrosation (described below) of thiols, and is approximately an order of magnitude slower than its activation (163)

Another example more relevant to cell cycle is the inactivation of mammalian ribonucleotide reductase (RR) by •NO. RR is responsible for reducing (via deoxygenation) the 2' hydroxyl of the ribose sugar in ribonucleotides to generate deoxyribonucleotides, an essential

and rate-limiting step in DNA synthesis (164). Mammalian RR contains at its active site a diiron site which upon O_2-binding generates a tyrosyl radical (this residue acts as the "storage" site for the radical until ribonucleotide binding) whose function is to abstract an e^- from the catalytic cysteine. The thiyl radical in turn abstracts an electron from carbon-3 of the ribose sugar, triggering double bond formation between carbon-2 and carbon-3. The leaving group for this rearrangement is the 2'-hydroxyl, thus generating the deoxyribonucleotide (165). Indeed, inactivation of RR by •NO gas has been reported (166) and quenching of the tyrosyl radical of RR in tumor cells overexpressing RR has been observed following activating macrophage co-culture experiments (167). The mechanism by which this occurs is not clear, and may involve either direct addition of •NO to the tyrosyl radical (168) or direct •NO binding to the diiron complex, preventing tyrosyl radical formation (169).

1.5.2.2 Regulation of protein function by RNS

In contrast to direct regulation of proteins by •NO, indirect regulation of proteins by •NO occurs largely through RNS, and falls into three major categories as described above: oxidation, nitration, and nitros(yl)ation. Nitros(yl)ation will be discussed in section 1.5.2.3. In most cases, regulation of protein activity by RNS is induced biochemically by modifying one or more amino acids responsible for protein activity. These modifications can change the enzymatic activity of a protein or alter its interaction with other biomolecules (170-173).

The best-described regulatory targets of protein nitration and oxidation are aromatic amino acids such as phenylalanine and tyrosine, and thiols, respectively. Nitration of tyrosine is generally considered to occur via a two-step process, in which an e^- is first abstracted from the tyrosyl side chain of tyrosine, generating a tyrosyl radical (Figure 10). This step can be catalyzed by a number of RNS and oxidizing species, including $•NO_2$, $CO_3^{•-}$, and •OH (149).

Subsequently, $\bullet NO_2$ from •NO autooxidation or peroxynitrous acid decomposition will recombine with tyrosyl radical at near diffusion-limited rates ($k = 3x10^9\ M^{-1}s^{-1}$) to yield nitrotyrosine (NT) (174). The highly reactive nature of $\bullet NO_2$ implies that tyrosine nitration will be observed only in sites proximally localized to $\bullet NO_2$ formation, and this is supported by empirical evidence *in vivo* (175). Although there is some evidence of "denitrase" activity in cells (176, 177), tyrosine nitration is regarded largely as irreversible; thus, if nitration of tyrosines essential for protein activity occurs the protein is irreversibly inhibited. Nitration of proteins often stimulates their proteolytic degradation, allowing the turnover of damaged or irreversibly inhibited proteins (178). Nitration and inhibition of protein activity has been well-described for several proteins, including human manganese-superoxide dismutase (Mn-SOD). Tyr34, which is located at the vertex of a molecular funnel that guides $\bullet O_2^-$ to the active site Mn atom, is nitrated by $ONOO^-$, resulting in a loss of SOD activity due to steric blockade of the active site and/or perturbation of the active site electronic environment (172).

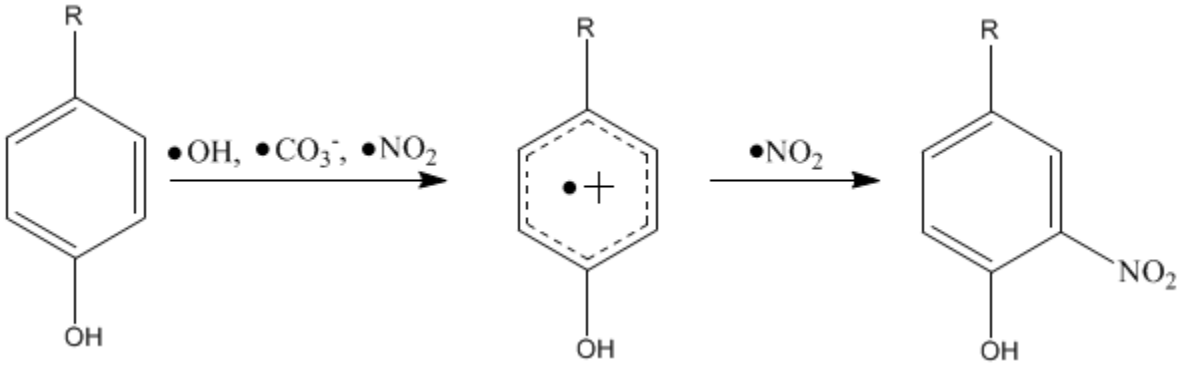

Figure 10. Formation of 3-nitrotyrosine.

Formation of 3-nitrotyrosine is thought to occur via a two-step mechanism: 1) abstraction of an e^- from the tyrosyl ring, followed by 2) adduction of $\bullet NO_2$ at the electronically-favored 3- and 5-positions on the ring. R, amino acid backbone.

Oxidation of thiols either by one-e^- or two-e^- processes has been reported in response to a number of RNS (Figure 11), including •NO_2 (174), RSNOs (179), and $ONOO^-$ (180). Oxidation of thiols is a common mechanism observed in biological regulation of proteins, and examples of protein regulation by intermolecular (*S*-thiolation) (181) and intramolecular disulfide formation (182), sulfenylamide generation (183, 184), terminally oxidized sulfinic or sulfonic acid generation (183, 184), and addition of glutathione to cysteines (*S*-glutathionylation) (185, 186) has been reported. Generation of these protein products is dependent upon the individual location, environment, the reactive species mediating the modification, and biochemical properties of the thiol being modified. Vicinal thiols as are found in thioredoxin, for example, often are oxidized to an intramolecular disulfide in response to ROS and RNS resulting in loss of enzymatic activity (187), whereas loss of activity due to modification of unprotected thiols is often due to generation of "terminally" oxidized to sulfinic or sulfonic acids, as was observed for creatine kinase in response to peroxynitrite (180). *S*-thiolation has also been reported in response to RNS (173). Treatment with the •NO-donating prodrug PABA/NO induced nitrosative stress and accumulation of PTP1B that had been *S*-glutathionylated, which inhibits its activity (173, 186).

1.5.2.3 *S*-nitros(yl)ation as a prototypical signaling paradigm

A mechanism of cysteine-dependent protein regulation that has garnered increased attention recently is *S*-nitros(yl)ation, or the reversible addition of NO to a thiol to generate RSNO. Cysteine composes on average 4% of protein amino acid sequence, and many enzyme families contain catalytic cysteine residues necessary for their enzymatic activity. Thus *S*-nitros(yl)ation of cysteines by •NO and RNS provides a convenient biochemical mechanism to regulate enzymatic activities and protein-protein interactions in response to •NO-dependent

signaling. Regulation of protein interaction and function by *S*-nitros(yl)ation has been described for proteins from numerous families, including phosphatases, GTPases, oxygenases, proteases, transcription factors, and ion channels (188-193).

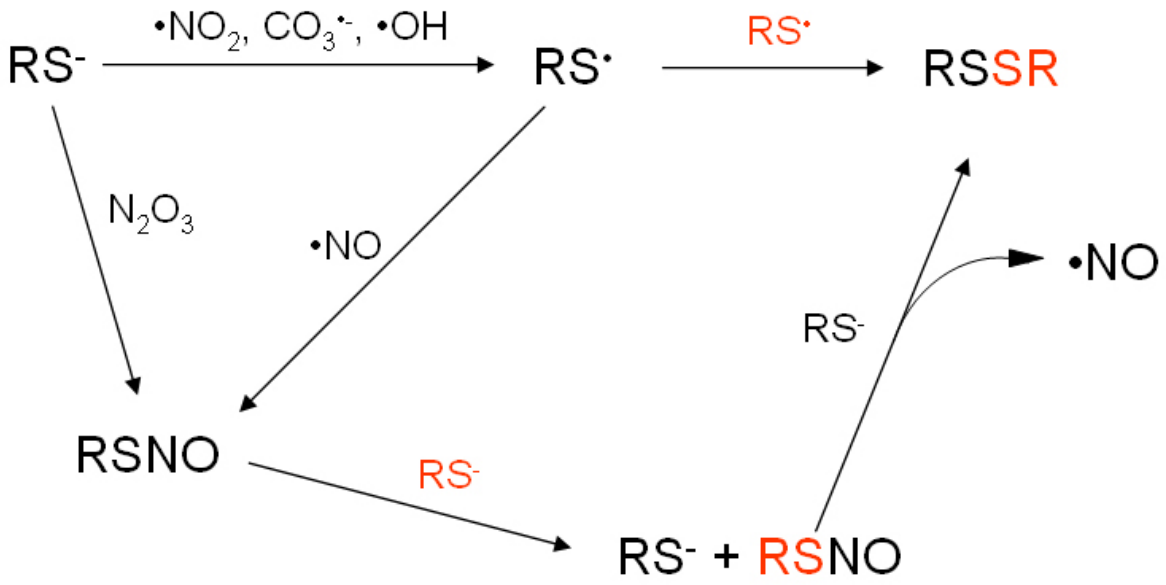

Figure 11. Reversible oxidation and *S*-nitrosation reactions of thiols.

In response to RNS, thiolates can be oxidized, *S*-nitrosated, or oxidatively nitrosylated. Upon exposure to nitrosating agents such as RSNOs or N_2O_3, thiolates can receive NO^+, generating RSNO. Alternatively, exposure to one-e^- oxidizing agents such as $•NO_2$, •OH, or $CO_3^{•-}$ can abstract an e^- from thiolates, generating thiyl radicals. Thiyl radicals can in turn recombine with other thiyl radicals to generate disulfides, or interact with •NO to produce RSNO via oxidative nitrosylation. Additionally, thiolate can reductively cleave •NO from RSNO, generating •NO and disulfide. Different thiolates and/or their reaction products are shown in black and red for clarity.

Nitros(yl)ation of protein cysteines can occur through a variety of mechanisms (Figure 11), with the two most studied being *S*-nitrosation (addition of NO^+ to a thiolate) and oxidative nitrosylation (one-e^- oxidation of cysteine to RS• followed by •NO addition) as these are the most likely mechanisms *in vivo* (146, 159). Upon coproduction of •NO and $•O_2^-$, peroxynitrite

decomposition products are thought to mediate e^- abstraction from thiols, promoting oxidative nitrosylation (direct •NO addition) (146). Disproportionate generation of •NO vs. $•O_2^-$ favors •NO autooxidation and *S*-nitrosation via production of the nitrosating species N_2O_3 as evidenced by the quenching of intracellular nitrosation by azide treatment (146). An alternative source of nitrosation is *trans*-nitrosation, the direct transfer of NO^+ from RSNO to thiolate as shown in equation 2:

$$R_1S^- + R_2S\text{-}NO \rightarrow R_1S\text{-}NO + R_2S^- \quad (2)$$

The relative contribution of *trans*-nitrosation to biological nitros(yl)ation is unclear; speculation exists that given the relative concentration of GSH vs. total cellular thiols, *trans*-nitrosation of GSH will be essentially unidirectional (194). This implies that in the absence of additional mechanisms of selectivity, GSH will act as a sink for NO^+ equivalents, essentially precluding intracellular *trans*-nitrosation. However, recent experiments demonstrating catalytic *trans*-nitrosation (188) have revived debate over whether it is a significant source of RSNO *in vivo* (see below).

Given the frequency of cysteine in protein sequences, how specificity of protein *S*-nitros(yl)ation is achieved has been the subject of debate. Evidence exists that the biochemical and environmental characteristics of the cysteine to be modified may play an important role in targeting specific residues for *S*-nitros(yl)ation. Cysteines targeted by *S*-nitros(yl)ation often exist in hydrophobic pockets of proteins (171). Given that •NO autooxidation to nitrosating species such as N_2O_3 is accelerated in hydrophobic regions (143), it is reasonable to posit that proteins may selectively catalyze the nitrosation of hydrophobically constrained cysteines by proximally concentrating •NO and/or O_2. Cysteines that are selectively nitros(yl)ated often display a characteristic low pK_a compared to that of free cysteine (free Cys $pK_a \approx 8.3$) as a result

of surrounding environmental factors. For hepatic methionine adenosyltransferase, sterically adjacent basic arginines reduce the pK_a of Cys121, increasing its nucleophilicity, which makes it a more attractive target for NO^+ donation from GSNO (195). In fact, a recent sequence analysis of 20 *S*-nitrosylated proteins identified in a proteomic screen found flanking of *S*-nitrosylated cysteines by basic groups (histidine, lysine, arginine) either in the primary protein sequence or the tertiary structure (within ≈ 7 Å of the cysteine) of the proteins (196). Additionally evidence now exists that targeted nitros(yl)ation of proteins by proteins occurs, but it has been convincingly demonstrated only for cyclooxygenase-2 and caspase-3 (188, 192). Nonetheless, these studies identified direct and indirect mechanisms mediating target-specific *S*-nitrosylation: iNOS binds and directly *S*-nitrosylates cyclooxygenase-2, resulting in its activation, while *S*-nitrosothioredoxin *trans*-nitrosates caspase-3 *in vitro*, although this is yet to be observed *in vivo*.

For *S*-nitrosylation to fit the requirements of a biological signaling mechanism, it must be reversible (197). The chemistry of denitrosylation is well-defined in the test tube; RSNOs are decomposed via photolytic homolysis (194), reduction to thiol and •NO by Cu^+ (198) and by Hg^{2+}-mediated release of •NO, generating disulfide likely by thiyl recombination (199). Additionally, thiols can catalyze the reduction of RSNOs either by maintaining Cu^+ in a reduced state (200) or by releasing NO^- with generation of disulfide (194). In cells, photolytic and Hg^{2+}-catalyzed decomposition is presumably negligible due to poor penetration of tissues by light and the trace amounts of unchelated Hg^{2+}. These characteristics, however, make this chemistry useful for determination of RSNO content in the laboratory (199, 201). In cells, denitros(yl)ation appears to be mediated primarily by the Trx/Trx-reductase system (187, 202, 203) and by GSNO-reductase (204), although protein disulfide isomerase (PDI) and CuZn-SOD can denitrosate LMM RSNOs *in vitro* (205, 206).

1.5.3 Initiation and cellular effects of nitrosative stress

Although RSNOs exist in unperturbed cells, the levels are normally low; the basal concentration of GSNO in rat cerebellum for example is estimated at 6 - 8 μM (207). Under conditions of high •NO production accumulation of intracellular nitroso species can occur, and when production of these species exceeds the cellular requirements or buffering systems, nitrosative stress ensues (145). Accumulation of RSNOs and *N*-nitrosamines (RNNOs) alters cell signaling via *S*-nitros(yl)ation of cysteine-containing proteins and *N*-nitrosation of biomolecules, and the depletion of thiols associated with RSNO formation decreases cellular resistance to further oxidative and nitrosative insult. Indeed, activation of the respiratory burst in macrophages increases intracellular RSNOs and RNNOs via generation of N_2O_3 (208, 209), and is followed by apoptosis (209). Similarly, chemical induction of nitrosative stress in HL-60 cells induced phosphatidylserine externalization by inhibition of the aminophospholipid translocase and induced subsequent engulfment and clearance by macrophages (210). These studies indicate that overproduction of •NO and/or $•O_2^-$ and accumulation of nitroso species occurs in cells and has pathophysiological consequences. In contrast, several studies have reported prevention of apoptosis in response to nitrosative stimuli by reversible *S*-nitros(yl)ation of caspases, suggesting that different durations or intensities of nitrosative stress may exert differential effects on cell survival (211, 212).

Numerous disease states are associated with increased nitrosative stress, including neurodegeneration (213, 214), migraine headaches (215), and diabetes (216). Considering that many cancer cells and preneoplastic lesions derived from chronic inflammatory diseases are exposed to high •NO produced either endogenously due to iNOS overexpression or exogenously by inflammatory mediators (reviewed in (217)), it is not surprising that markers of nitrosative

stress have been observed in cancer patients (218) and patients with chronic inflammatory diseases (219). The sustained production of potentially mutagenic RNNOs, in fact, may contribute to carcinogenesis (220).

1.5.4 Nitrogen oxides and the cell cycle

Numerous reports have correlated the generation of •NO or RNS with cytostasis or cell proliferation in a variety of tissues. Most early studies examined the role of •NO in regulation of vascular smooth muscle proliferation, stemming from the discovery that endothelium-derived relaxation factor was •NO. The mid-nineties yielded several seemingly contradictory reports that •NO derived from various sources could either suppress (221-223) or stimulate (224) vascular cell proliferation. Although in hindsight these studies can likely be explained by the concentrations and kinetics of •NO administration, to the cell cycle researcher "in the moment," they undoubtedly provided ample source of confusion. What is apparent from these studies is that administration of sufficiently high levels of •NO during a given time course results in cell cycle arrest via inhibition of DNA synthesis (221-223, 225-227). Subsequent studies examining the molecular mechanisms of •NO-mediated cell cycle arrest frequently identified suppression of Cdk2 activity and decreased cyclin A expression in •NO-treated cells (225-227). Although these studies provided an explanation for the failure of vascular cells to exit S-phase upon •NO treatment, it did not explain the failure of these cells to synthesize DNA, as cyclin E expression was not affected significantly (225-227) and therefore was not responsible for suppressed Cdk2 activity.

The picture of •NO/RNS-mediated cell cycle regulation became cloudier when the effects of •NO/RNS on tumor cells were examined. In cell culture, •NO administration to MDA-MB-

231 breast cancer cells suppressed DNA synthesis (as implied by failure of cells to cross the G_1-S transition), and again the expression of cyclin E and Cdk2 was unchanged (228). The authors attributed this to suppression of cyclin D_1 in response to •NO, but the high expression of cyclin E would preclude this explanation as Cdk2/cyclin E drives the G_1/S transition (46, 228). More detailed cell cycle analysis of •NO-mediated cell cycle arrest using isogenic cell lines deficient in the cell cycle regulators p53 and p21 excluded a role for these proteins in prevention of S-phase progression by •NO, as $p53^{-/-}$ and $p21^{-/-}$ cells failed to synthesize DNA identically to wild-type cells (219). Moreover, different RNS may enact S-phase arrest via different mechanisms. Treatment of cells with nitrating agents $•NO_2$ and SIN-1 activated ATM, and initiated S-phase arrest concurrent with accrual of DNA damage (229).

Whereas the effects of •NO/RNS in cell culture is largely consistent across cell types with suppression of DNA synthesis being the primarily observed phenotype, data from mouse studies have contradicted the *in vitro* observations. Colon cancer cells engineered to constitutively express iNOS grew much slower than wild-type cells in culture, as would be expected. However the same iNOS-expressing cells produced significantly larger tumors in nude mice than did the wild-type cells, suggesting that •NO production can have different effects on tumor cell growth *in vitro* and *in vivo* (228). Furthermore, numerous examples of pro- and anti-tumor effects of iNOS expression either in the tumor cells or in the host animal exist, further complicating the interpretation of whether or not •NO production is beneficial or detrimental to tumor formation (230-235).

1.6 STATEMENT OF THE PROBLEM AND HYPOTHESIS

The existing body of evidence clearly demonstrates that •NO and/or RNS suppress S-phase activity in normal and cancerous cells; however, the exact mechanism(s) by which this occurs remain unclear. The observation that Cdk2 activity is suppressed even in the presence of its cognate S-phase cyclin suggests an alternative activator of Cdk2 is the target of •NO-mediated S-phase suppression. Cdc25A enzymatically activates Cdk2 at the G_1-S transition (46-48), so suppression of Cdc25A either at the level of expression or enzymatic activity represents an attractive target for •NO-mediated cell cycle signaling.

Structural and biochemical analysis of Cdc25A indicates that its catalytic cysteine exists as a highly reactive thiolate anion (43, 182, 236) and is situated in an acid-base motif within a hydrophobic substrate-binding pocket (42), flagging it as a potential target of regulation by *S*-nitros(yl)ation. Direct chemical regulation of Cdc25A by •NO/RNS could rectify the observed perturbation to cell cycle progression and Cdk2 activity in response to •NO/RNS. In support of this hypothesis, the endogenous reducing agent for Cdc25 catalytic cysteine, Trx (117), has been recently reported catalyze *S*-nitrosation of target proteins (188). Morever, in light of frequent Cdc25A overexpression in human cancers (91) and the apparent ability of tumors *in vivo* to bypass •NO-mediated cell cycle arrest and thrive (228), I hypothesized that **Cdc25A represents the unidentified target of •NO-dependent cell cycle signaling, and that loss of Cdk2 activity in cells exposed to •NO is limiting for progression through S-phase.** Thus, the specific aims of this dissertation were to 1) probe the susceptibility of Cdc25A to enzymatic regulation by •NO/RNS, 2) interrogate the effects of •NO/RNS production on Cdc25A expression in tumor cells and 3) determine whether reintroduction of Cdk2 activity in •NO/RNS-challenged tumor cells restores DNA synthesis.

2.0 EXPERIMENTAL METHODS

2.1 REAGENTS

L-Cysteine ethyl ester hydrochloride (CEE), etoposide, OMFP, Na_3VO_4, β-mercaptoethanol, diethylene triamine pentaacetic acid (DTPA), $CuSO_4$, (+)-sodium-*L*-ascorbate, $NaNO_2$, *cis*-diamineplatinum (II) dichloride (cisplatin, CDDP) and ethyl nitrite were from Sigma-Aldrich (St. Louis, MO). Cycloheximide (CHX), dithiothreitol (DTT), glutathione (GSH), Hoechst 33342, iodoacetamide (IAC), N^G-monomethyl-*L*-arginine monoacetate (*L*-NMMA), MG-132, *N*-ethylmaleimide (NEM), roscovitine, and salubrinal were from Calbiochem (La Jolla, CA). *S*-Nitrosoglutathione (GSNO), Nitrate/Nitrite Colorimetric Assay Kit and nitrotyrosine BSA were from Cayman Chemical (Ann Arbor, MI). ThioGlo-1 was from Covalent Associates, Inc. (Corvallis, OR). Chelex-100 was purchased from Bio-Rad (Hercules, CA). SNCEE was synthesized and quantified using its extinction coefficient (1019 $M^{-1}cm^{-1}$ at 343 nm in methanol) as previously described (237). SNCEE was allowed to decompose for ≥ 24 hours to generate decomposed SNCEE, which was verified spectroscopically by loss of the S-N bond absorbance at 343 nm before use. LipofectAMINE PLUS and *E. coli* strain DH5α Supercompetent cells, were obtained from Invitrogen (Carlsbad, CA). *E. coli* strain BL21(DE3) and the pET28a bacterial expression plasmid were from Novagen (Madison, WI). Cdc25A (sc-7389), Cdc25C (sc-327), and Cdk1 (sc-54) antibodies, normal mouse IgG (sc-2025), Protein A/G-PLUS agarose

(sc-2003) and anti-cyclin B_1-agarose (sc-245 AC) were obtained from Santa Cruz Biotechnology (Santa Cruz, CA). Cdc25A DCS-120 antibody was from Thermo-Fisher Scientific (Fremont, CA). Antibodies against Cdc25B (610528) and iNOS/NOS Type II (610332) were from BD Transduction Laboratories (Lexington, KY). Antibodies recognizing phospho-Thr180/Thr182-p38 MAP kinase (#9211), p38 MAP kinase (#9212), phospho-Tyr15 Cdk1 (#9111), PARP (#9542), phospho-Ser51 eIF-2α (#9722), and eIF-2α (#9721) were from Cell Signaling Technology (Danvers, MA), the caspase-3 antibody (AAP-113) was from Assay Designs (Ann Arbor, MI), the β-tubulin antibody (CLT9003) was from Cedarlane Laboratories (Hornby, Ontario, Canada) and the 3-nitrotyrosine antibody (#189540) was from Cayman Chemical. HA.11 affinity matrix was purchased from Covance Research Products, Inc. (Princeton, NJ). Horseradish peroxidase-conjugated secondary antibodies were from Jackson Immunoresearch (West Grove, PA). ECL Western blotting substrate was purchased from Pierce Biotechnology (Rockford, IL). Dialyzed FBS was from Hyclone (Logan, UT). EasyTag™ EXPRESS [^{35}S] Protein Labeling Mix and [γ^{33}P]-ATP were purchased from Perkin-Elmer (Waltham, MA). Recombinant Cdk2/cyclin A was from New England Biolabs (Ipswich, MA).

The pCMV-HA-Cdc25A and pCMV-HA-C431S vectors were supplied by Alexander Ducruet (University of Pittsburgh) and were created by ligating the Cdc25A WT or C431S cDNA into the Eco R1 and Xho I sites of the pCMV-HA vector. The pcDNA3-Cdc25A vector was provided by Thomas Roberts (Dana-Farber Cancer Institute, Boston, MA) and has been described previously (238). The pET28a-rHis-Cdc25A vector was created by ligating the human *CDC25A* cDNA into the Bam H1 and Xho I sites of the pET28a vector. The pcDL-Cdk2AF-HA vector encodes a double mutant (Thr14Ala and Tyr15Phe) Cdk2 that cannot be phosphorylated on these residues, and thus does not require Cdc25 activity to be catalytically active (71, 105,

239) and was provided by David Morgan (University of California, San Francisco, CA). The pcDNA3-HA-ASK-1 vector has been described previously (240) and was provided by Peter Houghton (St. Jude Children's Research Hospital, Memphis, TN) Ad-LacZ and Ad-iNOS adenoviruses encoded the β-galactosidase and human iNOS cDNAs, respectively (241), and were supplied by Paul Robbins (University of Pittsburgh).

2.2 CELL CULTURE, TREATMENTS, AND RADIOLABEL INCORPORATION

Wild-type, Chk2$^{-/-}$, p53$^{-/-}$, and p21$^{-/-}$, HCT116 cells were provided by Bert Vogelstein (The Johns Hopkins University), and HIF-1α$^{-/-}$ HCT116 cells were provided by Long Dang (University of Michigan). HCT116 wild-type and isogenic cells were maintained in McCoy's 5A medium plus *L*-glutamine supplemented with 10% fetal bovine serum (Cellgro, Manassas, VA), 100 U/mL penicillin/streptomycin (Invitrogen) in a humidified incubator at 37^{o}C with 5% CO_2. HeLa cells (ATCC, Manassas, VA) were maintained in Dulbecco's modified eagle medium supplemented with 10% fetal bovine serum (Cellgro), 100 U/mL penicillin/streptomycin (Invitrogen) in a humidified incubator at 37^{o}C with 5% CO_2.

All compounds were either dissolved into DMSO or directly into medium for cell treatment. To metabolically label newly synthesized proteins, I washed HCT116 cells twice with PBS and incubated them with priming medium (Dulbecco's Modified Eagle Medium lacking *L*-cysteine or *L*-methionine (Invitrogen), supplemented with 10% dialyzed fetal bovine serum and 100 U/mL penicillin/streptomycin) for one hour before addition of 300 μCi/mL of EasyTag™ EXPRESS [^{35}S] Protein Labeling Mix (Perkin-Elmer, Waltham, MA).

For exposure to UV irradiation, cells were washed once in 37°C PBS, and the PBS was aspirated. The dish of cells was then placed on top of the lid to elevate it, and irradiated using a UVC Crosslinker, (Stratagene, La Jolla, CA), followed by addition of fresh medium before incubation for the indicated times and cell harvesting.

2.3 PLASMID TRANSFECTION AND ADENOVIRAL INFECTION OF HUMAN TUMOR CELL LINES

HCT116 cells were transfected at 25 to 40% confluence using Lipofectamine PLUS according to the manufacturer's instructions in serum-containing medium. Three hours after transfection, medium was aspirated to remove DNA-lipid complexes and fresh medium was added to cells. When replating of cells to attain target confluence was necessary after transfection, cells were trypsinized 8 hours post-transfection and replated in fresh medium at 25 – 30% density. Estimation of transfection efficiency was performed visually by inspection of a tandem sample transfected with vectors encoding green fluorescent protein and were routinely 40-50%.

HCT116 cells were infected with 10 MOI of adenoviruses encoding either β-galactosidase or human iNOS in 1.2 mL PBS, yielding > 99% infection. One hour after infection, 4 mL of medium was added to plates, and they were incubated for 24 hours before harvest. No apparent cytotoxicity was observed either in LacZ- or iNOS-infected cells up to 48 hours post-infection.

2.4 PURIFICATION OF RECOMBINANT HUMAN CDC25A AND TYR15-PHOSPHORYLATED CDK1/CYCLIN B_1

His-tagged Cdc25A was expressed from *E. coli* strain BL21(DE3) using 1 mM isopropyl-β-*D*-1-thiogalactopyranoside from bacterial OD_{600} 0.4 to 0.8. Protein was purified using nickel-nitrilotriacetic acid (His_6) resin as described previously (242), except that the protein was eluted in the absence of reducing agents.

Tyr15-hyperphosphorylated Cdk1 was generated by treating subconfluent (25 – 30% confluent) HeLa cells with 40 μM etoposide for one hour, and 23 hours later cells were harvested in RSNO- and phosphatase assay-compatible RIPA buffer (50 mM Tris pH 7.6, 1% Triton X-100, 0.1% SDS, 150 mM NaCl, 1 mM DTPA, 10 mM NaF, 10 μg/mL aprotinin, 10 μg/mL leupeptin, 100 μg/mL 4-(2-aminoethyl)-benzenesulfonylfluoride hydrochloride, 10 μg/mL soybean trypsin inhibitor, and 1 mM phenylmethylsulfonyl fluoride; prepared with Chelex-100-treated, deionized H_2O). Cdk1/cyclin B_1 complexes were immunoprecipitated as described below, and stored as a pellet at -80°C until use.

2.5 WESTERN BLOTTING, DOT BLOTTING, AND IMMUNOPRECIPITATION

For Western blotting, cells were harvested by scraping into a modified RIPA buffer (50 mM Tris pH 7.6, 1% Triton X-100, 0.1% SDS, 150 mM NaCl, 1 mM EDTA, 2 mM Na_3VO_4, 12 mM β-glycerol phosphate, 10 mM NaF, 10 μg/mL aprotinin, 10 μg/mL leupeptin, 100 μg/mL 4-(2-aminoethyl)-benzenesulfonylfluoride hydrochloride, 10 μg/mL soybean trypsin inhibitor, and 1 mM phenylmethylsulfonyl fluoride). Cells were lysed either by incubation on ice for 30 minutes

with frequent vortexing or by sonication at 50% amplitude for 6 x 2 seconds on ice with a 2 second pause between pulses using a GEX-130 ultrasonic processor with a VC-50 2 mm microtip (Gene Q, Montreal, Quebec, Canada). Lysates were cleared by centrifugation at 13,000 x g for 15 minutes, and protein content of the supernatant was determined by the method of Bradford. Total cell lysates (30 – 50 μg protein) were resolved by SDS-PAGE and transferred to nitrocellulose membranes at 4°C overnight at 35 V to maximize protein transfer. Membranes were then blocked in 5% non-fat milk or 5% BSA as recommended by the primary antibody manufacturer, and incubated with primary antibodies overnight at 4°C. After washing 3 times for 5 minutes with 25 mL TBS-T, horseradish peroxidase-conjugated secondary antibodies were added for one hour before 3 additional TBS-T washes visualization with ECL reagent. Densitometric analysis was performed on films using an Amersham Biosciences SI densitometer and analyzed using ImageQuant software (Amersham Biosciences, Piscataway, NJ) for quantification.

For dot blotting, 1 μg of total protein or 50 – 100 ng of 3-nitrotyrosine BSA was added directly to nitrocellulose membranes and allowed to dry completely before Western blotting as above with an antibody to nitrotyrosine.

Immunoprecipitation of cyclin B_1 and associated proteins was performed by lysing cells as described in RSNO- and phosphatase assay-compatible RIPA buffer as described above. Immunoprecipitation of Cdc25A and ASK-1 was performed by lysing cells in HEPES buffer (103). Total protein (250 μg per sample for cyclin B_1, 1000 - 1500 μg for Cdc25A and ASK-1) was diluted to 1 mL in the above buffer and pre-cleared with 2 μg of normal mouse IgG and 50 μL Protein A/G PLUS-agarose for one hour at 4°C on a rotating mixer. Agarose beads were pelleted by centrifugation for 5 minutes at 1500 x g, and the supernatant was transferred to a new

tube containing 50 µL of anti-cyclin B_1-agarose antibody, Cdc25A antibody (DCS-120) plus 50 µL of Protein A/G PLUS-agarose, or 50 µL of HA.11 affinity matrix (for cyclin B_1, Cdc25A, and ASK-1, respectively) and incubated on the rotating mixer overnight at 4°C. After centrifugation at 1500 x g for 5 minutes, the pellet was washed 3 times with 1 mL of the above buffer.

2.6 QUANTIFICATION OF NITRITE, NITRATE, *S*-NITROSOTHIOLS, AND FREE THIOLS

Nitrite and nitrate in culture medium from iNOS-infected cells was measured using a colorimetric nitrite/nitrate detection kit (Cayman Chemical) based on the Greiss assay. To measure *S*-nitrosothiols, I washed cells twice with ice-cold PBS, scraped them into RSNO stabilization buffer (100 mM sodium phosphate, pH 7.4, 100 µM DTPA and 10 mM NEM), and sonicated them as described above. Lysates were cleared by centrifugation at 13,000 x g for 10 minutes, and supernatants were collected. RSNOs in each lysate were analyzed immediately by ozonolysis-based chemiluminescence. A 10 µL aliquot of each lysate was injected into the helium-purged reaction chamber of a Sievers Model 280 NO analyzer (Sievers, Inc., Boulder, CO), which contained 3 mL sodium phosphate buffer, pH 7.4, 40 µM $CuSO_4$, and 50 mM sodium ascorbate. A 10 µL injection of up to 100 µM $NaNO_2$ produced no discernible signal, and pretreatment of an aliquot of each sample with 10 mM DTT completely ablated any signal, suggesting that this method was specific for RSNOs. Area under the curve for each injection was normalized to a GSNO standard curve and then for protein content. To quantify free thiols, cell lysates (200 µL) were prepared as described for measurement of *S*-nitrosothiols and mixed

with 100 µL of a 30 µM solution of ThioGlo-1, were incubated for 5 minutes at ambient temperature, and assayed for fluorescence (ex 388 nm, em 505 nm) using a SpectraMAX M5 (Molecular Devices Corp., Sunnyvale, CA) in a 96-well black polystyrene assay plate (Corning, Lowell, Massachusetts). Fluorescence values were normalized for protein content and to a GSH standard curve.

2.7 PHOSPHATASE AND KINASE ASSAYS

Dephosphorylation of Cdk1^{Tyr15}/cyclin B_1 was measured by incubating 500 ng of rHis-Cdc25A that had been pretreated for 15 minutes with the indicated compounds with 250 µg of cyclin B_1 immunoprecipitate in a 50 µL final volume for 60 minutes at 37^{o}C in assay buffer (30 mM Tris pH 7.4, 75 mM NaCl, 100 µM DTPA in Chelex-100-treated deionized H_2O). Laemmli buffer was then added and samples were boiled to halt the reaction. Levels of Cdk1^{Tyr15} phosphorylation were determined by Western blotting as above using a phospho-Cdk1^{Tyr15} antibody.

Phosphatase activity toward the artificial substrate *O*-methylfluorescein phosphate (OMFP) was measured at the K_m (40 µM) and pH 7.4 at ambient temperature in a 96-well microtiter plate assay based on previously described methods (242). rHis-Cdc25A (500 ng) was pretreated for 15 minutes to 1 hour with the indicated compounds in assay buffer, after which OMFP was added. Fluorescence emission was measured after a 60 minute incubation period with a Molecular Devices M5 Spectrophotometer (ex 485 nm, em 525 nm).

Cdk2/cyclin A kinase activity toward recombinant human Histone H1.2 (Calbiochem) was measured by radiolabel incorporation from [γ^{33}P]-ATP (Perkin-Elmer). Cdk2/cyclin A (1 U,

New England Biolabs) was incubated in 1X kinase buffer (500 mM Tris pH 7.5, 100 mM $MgCl_2$, 10 mM EGTA, 0.10% Brij-35 in Chelex-100-treated deionized H_2O) with 20 µg Histone H1.2, and the indicated compounds for 15 minutes before addition of 0.62 µCi [γ^{33}P]-ATP in a total concentration of 200 µM ATP to bring the total reaction volume to 60 µL and initiate the kinase reaction. After 20 minutes, 25 µL of each sample was transferred to a P81 phosphocellulose square, air dried for 5 minutes, and washed 3 times for 5 minutes with 0.75% phosphoric acid. Squares were then rinsed in acetone, air dried, transferred to scintillation vials containing 4 mL scintillant, and ^{33}P signal was counted using a Beckman-Coulter LS6500 Multi-purpose Scintillation Counter (Beckman-Coulter, Fullerton, CA). Total phosphate incorporation was kept below 5% of theoretical maximum to maintain linear kinase reaction kinetics.

2.8 FLOW CYTOMETRY AND MICROSCOPY

DNA synthesis and DNA content were measured by bromodeoxyuridine (BrdU) and 7-aminoactinomycin D (7-AAD) staining, respectively, using the FITC-BrdU flow cytometry kit from BD Pharmingen (San Diego, CA) according to the manufacturer's instructions. Cells were incubated with 10 µM BrdU in medium for 30 minutes before harvesting and preparation according to the manufacturuer's instructions. Cell fluorescence was measured in the FITC and PI channels with appropriate compensation using a BD FACScalibur flow cytometer (BD, San Diego, CA) or a Guava EasyCyte flow cytometer (Guava Technologies, Inc., Hayward, CA). Data analysis was performed using Cytosoft 5.0.2 (Guava Technologies, Inc.) for data aquired on the EasyCyte, and WinMDI 2.8 (acquired from http://facs.scripps.edu/software.html as freeware) for data acquired on the FACScalibur to determine BrdU-positive cells.

To measure apoptosis, cells were washed once with PBS and fixed for 10 minutes at room-temperature in 4% formaldehyde in PBS. One mL of PBS containing 10 µg/mL Hoechst 33342 was added to each sample, and nuclei were visualized by standard fluorescence microscopy. Nuclei that were fragmented or condensed but not mitotic were considered apoptotic.

2.9 CYSTEINE REDOX-MODIFICATION PROFILING BY MASS SPECTROMETRY

Profiling of the post-translational and/or redox state of protein cysteines was performed using a modified version of the biotin-switch method (243) based on the selectivity of RSNO reduction by ascorbate (overview in Figure 12) coupled with MS. Recombinant Cdc25A (50 µg) or recombinant human Trx (50 µg) was treated with 50 µM SNCEE (or 50 µM CEE) in assay buffer at 37^{o}C for 30 minutes before removal of excess SNCEE (or CEE) by centrifugation using a 6 kDa cutoff filter equilibrated in assay buffer (Bio-Rad). A 1:100 volume of 25% sodium dodecyl sulfate in chelex-treated dH_2O was added to each sample, followed by 1 µL of 2 M IAC to alkylate free thiols. Samples were incubated at 50^{o}C for 1 hour to promote denaturation and alkylation. Samples were then cooled on wet ice, and 4 volumes of -80^{o}C acetone were added to each sample to precipitate protein overnight at -80^{o}C. The following day, proteins were subjected to centrifugation at 10,000 x g at 4^{o}C for 10 minutes, and washed twice in 500 µL of -80^{o}C acetone. Pellets were redissolved in 100 µL assay buffer, and 1µL of 1 M sodium ascorbate and 1 µL of 2 M NEM were added to each sample to promote reduction and NEM alkylation of RSNOs. Samples were incubated at 50^{o}C for 2 hours, after which 33.3 µL of 4X

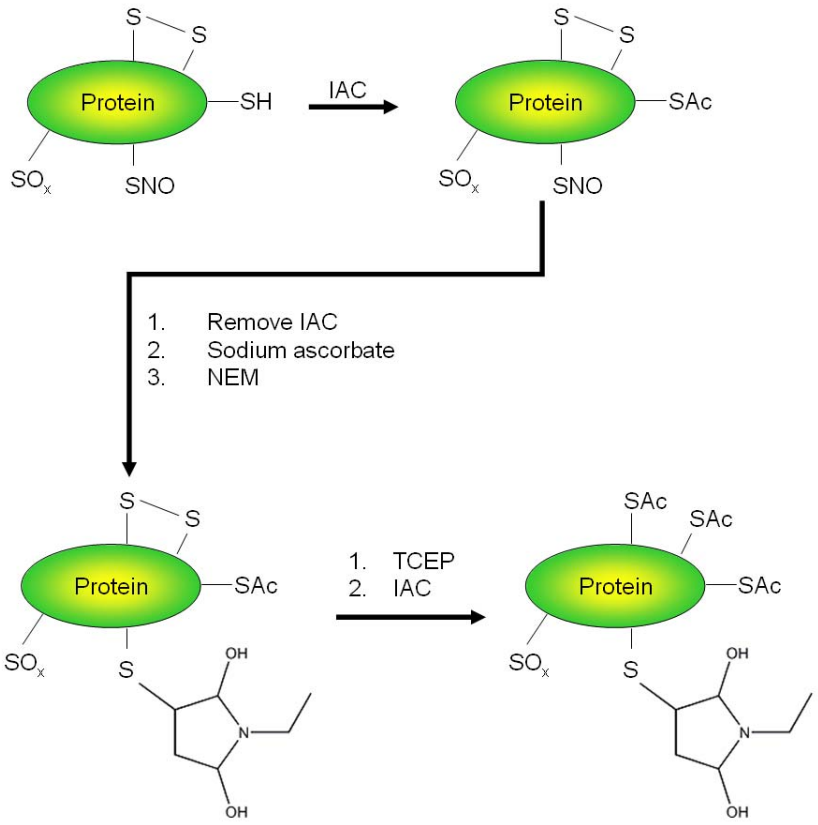

Figure 12. Redox-profiling of protein cysteines by selective reduction and alkylation.

I used redox state-selective reducing agents with the alkylating agents NEM and IAC to distinguish potential *S*-nitrosothiols (-SNO) from stable, terminally oxidized cysteines (-SO_x, sulfinic or sulfonic acids) and thiols/disulfides. TCEP, tris-carboxyethylphosphine.

Laemmli buffer was added. The mix (50 µL) was separated by SDS-PAGE. Samples were excised and in-gel digested using 200 ng Trypsin Gold (Promega, Madison, WI) in 20 µL NH_4HCO_3 overnight at 37°C. Digested peptides were extracted in 1% trifluoroacetic acid / 50% acetonitrile at room temperature, dried, and resuspended in 0.1% trifluoroacetic acid. Peptides were purified by reverse-phase Ziptip (Millipore, Danvers, MA) chromatography and eluted into 0.3% trifluoroacetic acid/50% acetonitrile. Peptide solution (2 µL) was mixed with 2 µL of a supersaturated α-cyano-4-hydroxycinnamic acid solution, and 0.75 µL was spotted onto a

Matrix-assisted laser desorption/ionization (MALDI) plate. Mass spectra were acquired over a *m/z* = 800 - 4000 acquisition range (focus *m/z* = 1570) using an Applied Biosystems 4700 Proteomics Analyzer (Applied Biosystems, Foster City, CA) in positive ion MS mode with reflectron engaged. Mass spectra were calibrated using the mass standards kit for the 4700 proteomics analyzer (Applied Biosystems). Predicted *m/z* ratios were calculated using predominant isotope elemental masses with Protein Prospector's MS-Digest software (accessed from http://prospector.ucsf.edu/cgi-bin/msform.cgi?form=msdigest).

3.0 ENZYMATIC REGULATION OF CDC25A BY NITROSATIVE INSULT

3.1 INTRODUCTION

•NO and •NO-derived reactive species (RNS) suppress DNA synthesis and Cdk2 activity, yet the mechanisms that enforce these observations remain poorly defined. Regulation of phosphatase activity by redox stimuli has recently emerged as a mechanism regulating cell signaling. Oxidative inactivation of the Cdc25 phosphatases has been reported by our group and others, but the effects of •NO and RNS on Cdc25A activity have not been examined. Other tyrosine phosphatases including PTP1B and CD45 are regulated by RSNOs (244), and the structural Cdc25 homolog rhodanese is regulated by *S*-nitrosothiols *in vitro* (245). The phosphatase activity of Cdc25A is dependent upon the integrity of the catalytic thiolate. Structural analysis indicates the Cdc25A catalytic cysteine (Cys431) is in a relatively shallow hydrophobic cleft, leaving it exposed to its environment. Cys431 is predicted to be much more reactive with electrophiles than that of typical cysteines, as the catalytic cysteine pK_a is estimated at 5.6 – 6.3, compared to 8.33 for free cysteine. These features likely render it susceptible to nitrosative attack, inhibiting its activity and providing a potential linkage between •NO and cell cycle arrest.

In this study, the effects of •NO-derived species in the form of *S*-nitrosothiols on Cdc25A phosphatase activity were examined. I found that *S*-nitrosothiols directly inhibited Cdc25A phosphatase activity, and that Cdc25A activity could be restored upon treatment with reductants.

Cdc25A was *S*-nitrosated with two molar equivalents of cysteine per mole protein upon treatment with SNCEE, providing a plausible explanation for the observed loss of phosphatase activity. I used selective chemical modification of Cdc25A cysteines based on their redox modifications (*S*-nitrosated vs. terminally oxidized vs. thiol/disulfide, see Figure 12) coupled with mass spectrometric analysis to profile the redox state of Cdc25A cysteines after SNCEE treatment. Mass spectrometric analysis identified peptides containing 9 of 12 Cdc25A cysteines, all as either thiols or disulfides, and failed to detect any terminally oxidized or *S*-nitrosated cysteines. The three cysteine-containing peptides that were not detected resided in the catalytic domain (Cys442) and the regulatory domain (Cys85 and Cys115). Collectively, these experiments indicate that Cdc25A is *S*-nitrosated and inactivated by low molecular mass (LMM) RSNOs, and identify a novel mechanism regulating Cdc25A activity in response to •NO-derived reactive species. These studies implicate the cellular balance of RSNOs as a potential mediator of Cdc25A activity.

3.2 RESULTS

3.2.1 Low molecular mass RSNOs decreased Cdc25A phosphatase activity toward OMFP and phospho-Cdk1^{Tyr15}/cyclin B

I determined whether the phosphatase activity of Cdc25A was sensitive to *S*-nitrosothiols *in vitro*. Treatment with the LMM RSNOs *S*-nitrosoglutathione (GSNO) or *S*-nitrosocysteine ethyl ester (SNCEE) inhibited Cdc25A phosphatase activity toward OMFP in a concentration-dependent manner (Figure 13). The IC_{50} values for GSNO and SNCEE were 969 ± 126 and 22.5

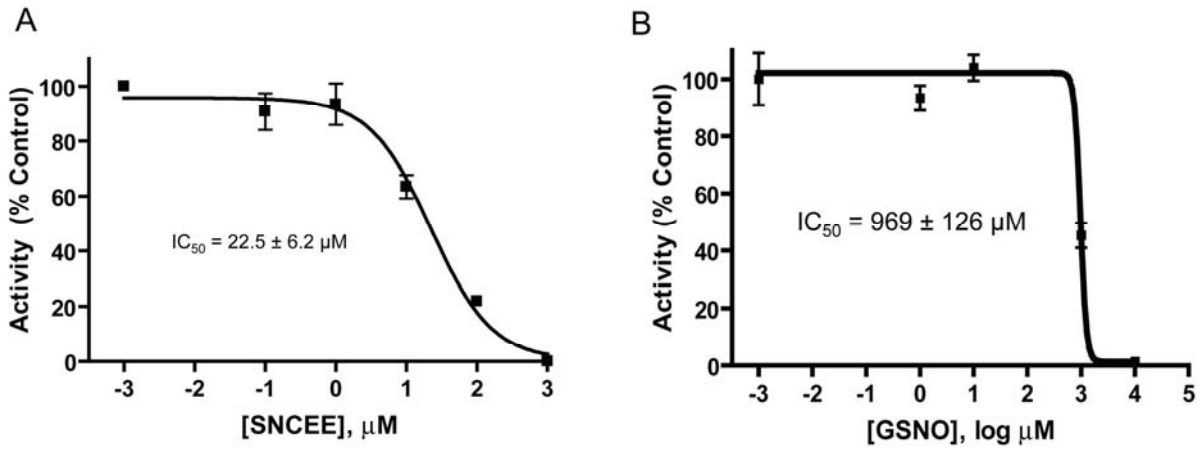

Figure 13. LMM RSNOs inhibited Cdc25A phosphatase activity toward OMFP.

Cdc25A (500 ng) was incubated with the indicated concentrations of SNCEE (*A*) or GSNO (*B*) and phosphatase activity toward OMFP was measured as described in *Experimental Methods* section 2.7. Results were normalized to untreated Cdc25A phosphatase activity and were expressed as percent control. Error bars indicate SEM, N=4.

± 6.2 μM, respectively, indicating that SNCEE was more potent toward inhibition of Cdc25A phosphatase activity.

I next probed the effects of SNCEE on dephosphorylation of an endogenous Cdc25A substrate, phospho-Cdk1^{Tyr15}/cyclin B (Figure 14). DTT maintains a reduced Cdc25A catalytic thiol, so DTT-treated Cdc25A added to phospho-Cdk1^{Tyr15}/cyclin B served as a positive control for maximal dephosphorylation. Cdc25A dephosphorylated Cdk1/cyclin B on tyrosine 15, and treatment of Cdc25A with SNCEE attenuated Cdc25A-mediated dephosphorylation of Cdk1/cyclin B similarly to the nonspecific tyrosine phosphatase inhibitor Na_3VO_4. Together, these results indicated that LMM RSNOs inhibited Cdc25A phosphatase activity toward artificial and endogenous substrates.

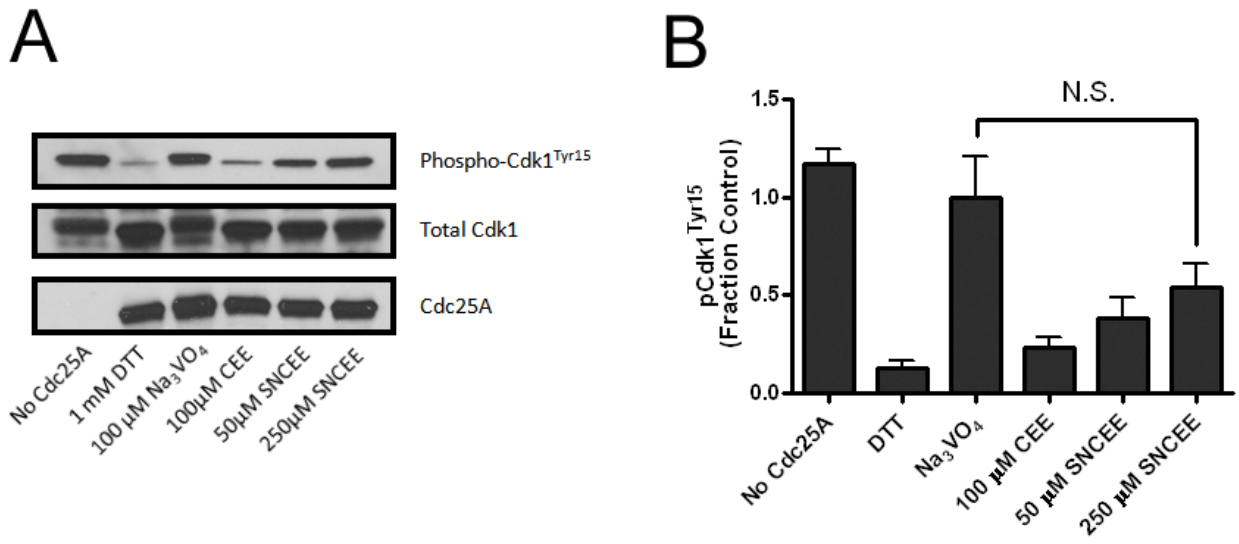

Figure 14. SNCEE inhibited dephosphorylation of Cdk1^{Tyr15}/cyclin B by Cdc25A.

A, Cdc25A (500 ng) was incubated with the indicated compounds before addition of 250 µg of Cdk1/cyclin B immunoprecipitate from etoposide-treated cells as described in *Experimental Methods* section 2.7. The phosphorylation status of Cdk1^{Tyr15} (top panel), total Cdk1 levels (middle), and Cdc25A levels (bottom) were measured by Western blotting. N=4. *B*, Quanitification of *A*. N.S., not significant.

3.2.2 SNCEE was stable during the Cdc25A phosphatase activity assay

S-nitrosothiols are typically unstable in aqueous solutions, as trace Cu^+ ions and exposure to light catalyze the release of •NO and thiol in the case of transition metal ions and •NO and thiyl radical (RS•) upon photolysis. RS• reacts rapidly with LMM RS• and protein RS• to generate mixed disulfides. •NO can autooxidize upon exposure to aqueous O_2, generating the nitrosating species N_2O_3, which can *S*-nitrosate protein cysteines. Thus, decomposition of SNCEE may generate several chemical agents capable of regulating Cdc25A activity, and it was important to determine whether significant decomposition of SNCEE occurred under our assay conditions. 100 µM SNCEE, a concentration that readily inhibited Cdc25A activity, was incubated in assay buffer and SNCEE absorbance at 343 nm was measured at various timepoints to quantify

remaining SNCEE (Figure 15*A*). No significant breakdown of SNCEE was detected over the time course of our assay, indicating that loss of Cdc25A activity was elicited by intact SNCEE. Consistent with this conclusion, treatment of Cdc25A with decomposed SNCEE did not decrease Cdc25A activity as fresh SNCEE did (Figure 15*B*). Together, these results indicate intact SNCEE, and not SNCEE decomposition products, mediates Cdc25A inhibition.

3.2.3 SNCEE treatment induced a reductant-sensitive change in Cdc25A migration by SDS-PAGE

S-Nitrosation and *S*-thiolation are redox-reversible post-translational modifications (PTMs), and PTMs often change the migration of their targets as assessed by SDS-PAGE. I thus investigated whether SNCEE treatment altered the migration of Cdc25A by SDS-PAGE under reducing and non-reducing conditions. Cdc25A was treated either with decomposed SNCEE or fresh SNCEE, and subjected to SDS-PAGE in the prescence or absence of β-mercaptoethanol (β-ME). SNCEE-treated Cdc25A migrated faster in SDS-PAGE compared to decomposed SNCEE-treated Cdc25A (Figure 16, lanes 1 and 2), and addition of β-ME to samples before electrophoresis ablated this accelerated migration in response to SNCEE treatment (Figure 16, lanes 3 and 4). Interestingly, the β-ME-treated Cdc25A appeared more finely resolved than that of even decomposed SNCEE-treated Cdc25A electrophoresed under non-reducing conditions (Figure 16, lane 1 vs. lane 3), suggesting that multiple oxidation states or conformations of Cdc25A may exist under basal conditions. This observation is consistent with reports of Cdc25A oxidation to a disulfide under non-reducing conditions (42). Two additional Cdc25A antibody-reactive bands with molecular masses > Cdc25A were apparent in lane 1 (Figure 16) but not under the reducing conditions in lane 3. The identity of the proteins constituting these

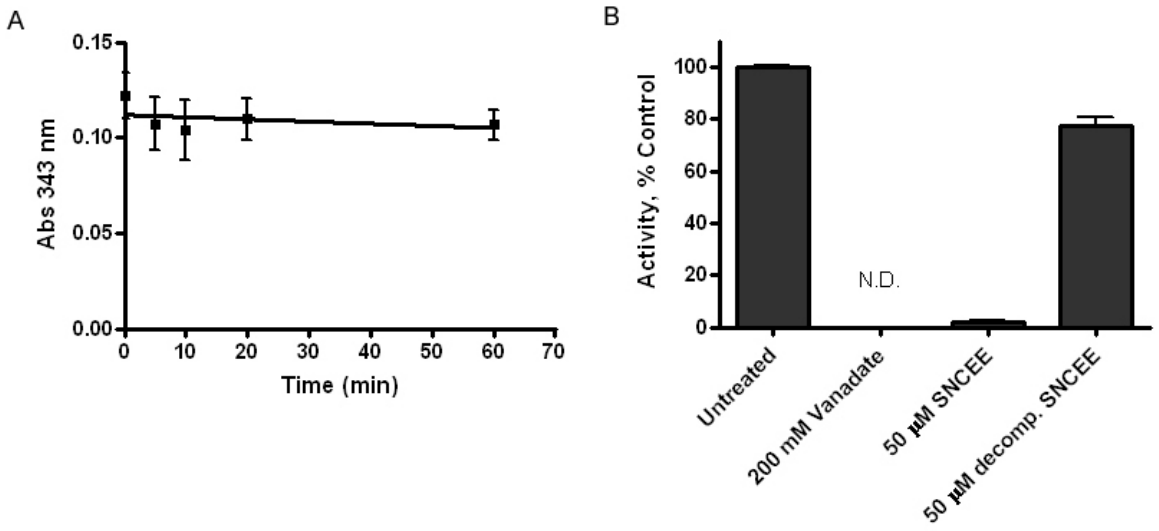

Figure 15. Intact SNCEE mediated Cdc25A inhibition.

A, SNCEE was diluted in assay buffer and the stability of SNCEE was monitored via its absorbance at 343 nm. SNCEE did not degrade significantly by one hour, the length of a typical phosphatase assay. Error bars indicate SEM, N=3. *B*, Cdc25A was treated with the indicated compounds before the phosphatase activity was assayed. Phosphatase activity is expressed as percent of untreated control. Error bars indicate SEM, N=4. N.D., not detectable.

bands was not known, but the molecular masses of these bands were not multiples of the Cdc25A molecular mass, indicating they were not multimers. Together, these results suggest that SNCEE induces a reductant-sensitive change in Cdc25A under conditions that inhibit its activity.

3.2.4 DTT treatment restored the activity of SNCEE-treated Cdc25A

Vicinal dithiols such as α-lipoic acid, thioredoxin, and DTT can denitrosate protein RSNOs (187, 202). Disulfide bonds as are found in protein-disulfides and mixed protein disulfides are also

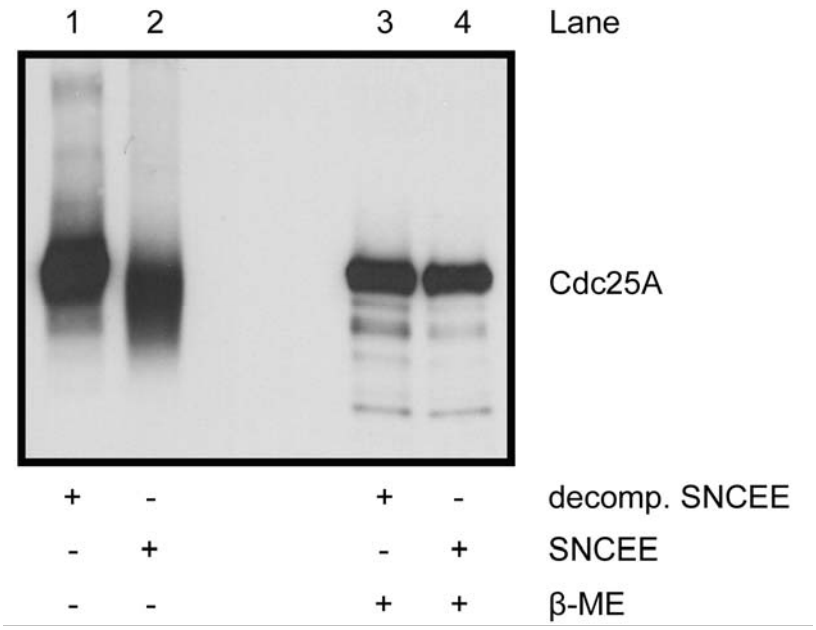

Figure 16. SNCEE reversibly changed Cdc25A migration by SDS-PAGE.

Cdc25A was treated with either decomposed or fresh SNCEE, and then electrophoresed in the presence or absence of the thiol reducing agent β-ME. Cdc25A was then detected by Western blotting.

sensitive to reduction with DTT. To determine a potential linkage between the β-ME-sensitive change in Cdc25A migration following SNCEE treatment and SNCEE-induced loss of Cdc25A activity, I exposed SNCEE-treated Cdc25A to 20 mM DTT (which has been shown previously to efficiently cleave RSNOs (211)) or vehicle, and immediately measured its phosphatase activity after DTT. Figure 17 shows that addition of 20 mM DTT restored > 60% of Cdc25A activity after SNCEE treatment. Although Cdc25A activity was not totally restored, the complete ablation of Cdc25A migration change following SNCEE suggested that irreversible PTM of Cdc25A did not occur and therefore was not responsible for failure to restore complete activity. It was possible that reduction of Cdc25A PTMs was time-dependent, and the incomplete restoration of activity reflected such. Regardless, Cdc25A inhibition by SNCEE was at least

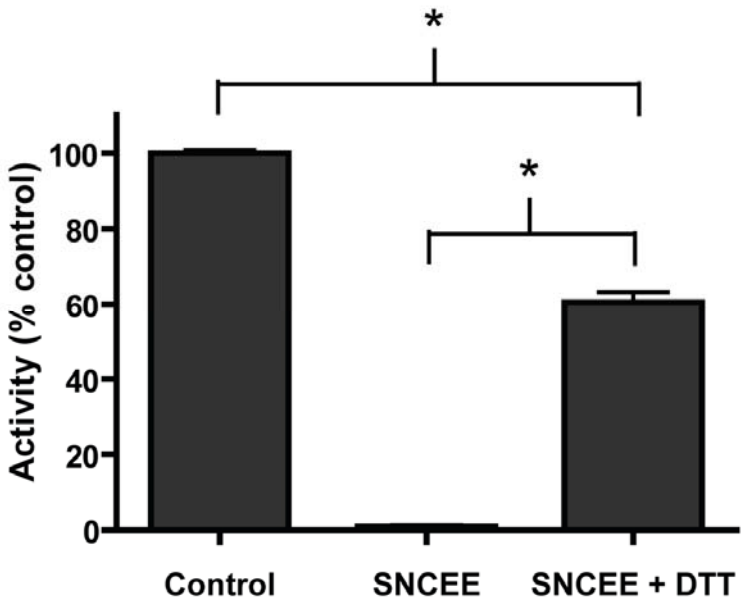

Figure 17. DTT restored Cdc25A phosphatase activity after SNCEE treatment.

Cdc25A was treated with SNCEE, and then exposed or not to 20 mM DTT immediately before assay of phosphatase activity. Cdc25A activity was expressed as percent untreated control. Error bars indicate SEM, N=4. *, $p < 0.001$.

partially redox-reversible, consistent with a model where SNCEE S-nitrosated the active site cysteine of Cdc25A.

3.2.5 SNCEE induced S-nitrosation of Cdc25A

To determine whether *S*-nitrosation of Cdc25A by SNCEE may induce the observed loss of activity, I measured Cdc25A-associated RSNOs after treatment with SNCEE. The divalent cation Hg^{2+} selectively releases •NO from RSNOs, which can be captured using a number of •NO-reactive "traps." I treated Cdc25A with SNCEE, removed unreacted SNCEE, and treated Cdc25A with or without $HgCl_2$ in buffer containing diaminofluorescein-2 (DAF-2), a •NO trap

that fluoresces upon reaction with •NO. Addition of $HgCl_2$ to SNCEE-treated Cdc25A increased DAF-2 fluorescence correlating to 2 mol of •NO release per mol Cdc25A, indicating that two Cys equivalents per Cdc25A molecule were *S*-nitrosated. In agreement with the literature (188, 246), *trans*-nitrosation of recombinant human thioredoxin at pH 7.2 resulted in only one modified cysteine using this method, suggesting that our detection of 2 mol RSNOs per mol Cdc25A was authentic.

3.2.6 Mass spectrometric analysis of SNCEE-treated Cdc25A did not detect *S*-nitrosothiols

I next wanted to identify the cysteines that were *S*-nitrosated following SNCEE exposure to understand how LMM RSNOs were regulating Cdc25A enzymatic activity. I used a modification of the biotin switch assay (243) to analyze the status of Cdc25A cysteines (Figure 12). First, free thiols are blocked with an alkylating agent (namely, IAC) after which RSNOs are selectively reduced with ascorbate and labeled with a thiol-alkylating agent (namely, NEM). Disulfides then were reduced and alkylated with IAC, allowing differentiation between RSNOs and other thiol modifications by MS.

Using this approach, peptides by MALDI-TOF MS containing 9 of 12 Cdc25A cysteines from SNCEE-treated Cdc25A were identified (Table 1), all of which were IAC-alkylated, indicating they existed either as thiols or disulfides following SNCEE treatment. I also did not detect any cysteine-containing peptides with cysteine sulfinic or sulfonic acids (Table 1), which indicates that SNCEE did not induce terminal oxidation of cysteines. This is congruent with my enzymatic and migration data in which I observed that the migration change of SNCEE-treated Cdc25A (Figure 16) and inhibition of Cdc25A activity by SNCEE (Figure 17) were reversible.

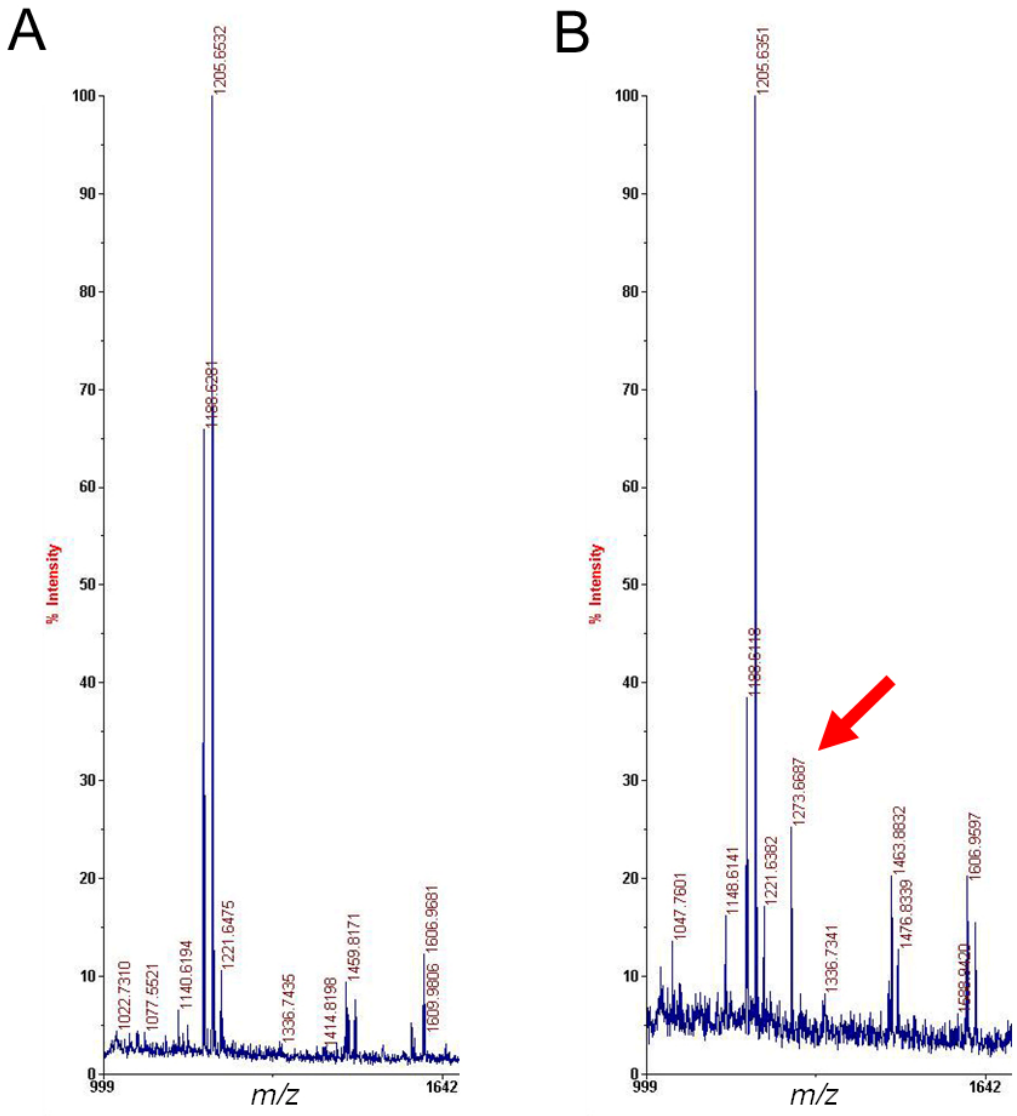

Figure 18. SNCEE *S*-nitrosated Trx Cys73.

Recombinant human Trx was incubated with 50 μM SNCEE (*B*) or vehicle (*A*) and analyzed by MALDI-TOF MS after preparation for cysteine redox-modification profiling as described in *Experimental Methods* section 2.9. The predicted *m/z* of the tryptic peptide containing iodoacetylated Cys73 (indicative of a thiol or disulfide), which was observed as 1205.6532 (*A*) and 1205.6361 (*B*), is 1205.5482. The red arrow indicates the appearance of an ion with observed *m/z* of 1273.6687, corresponding to NEM-modified Cys73-containing peptide (predicted *m/z* = 1273.5744) indicating SNCEE *S*-nitrosated Cys73.

Surprisingly, I did not detect any NEM-alkylated (*S*-nitrosated) Cdc25A peptides (Table 1). I was able to successfully detect an ion with an observed *m/z* correlating to the tryptic NEM-alkylated peptide containing Trx Cys73 from SNCEE-treated Trx (Figure 18*B*) but not vehicle-treated Trx (Figure 18*A*), suggesting that my failure to detect NEM-alkylated Cdc25A peptides did not stem from detection error. The three cysteine-containing peptides that were not identified by MS analysis contained cysteines 85, 115, and 442, which lie in the regulatory domain (Cys85 and Cys115) and catalytic domain, respectively (Cys442).

In summary, I have determined that LMM RSNOs inhibit Cdc25A activity towards artificial and endogenous substrates, and that inhibition of Cdc25A activity was associated with a change in its post-translational modification state and/or protein conformation. Moreover, Cdc25A was *S*-nitrosated on two moles cysteine equivalents per mole protein following SNCEE treatment, providing a potential explanation for SNCEE-induced loss of Cdc25A activity. Together, these results identify a novel redox-sensitive mechanism controlling Cdc25A activity following nitrosative challenge.

	IAC-labeled peptide (Thiol or disulfide)		NEM-labeled peptide (*S*-nitrosothiol)		Irreversibly oxidized peptide (sulfinic or sulfonic acid)	
Cysteine	**Pred. *m/z***	**Obs. *m/z***	**Pred. *m/z***	**Obs. *m/z***	**Pred. *m/z***	**Obs. *m/z***
17	1710.9247	1711.0325	1778.9510	N/A	1685.8931 / 1701.8880	N/A
85	2273.9537	N/A	2341.9799	N/A	2248.9220 / 2264.9169	N/A
115	958.539	N/A	1026.5652	N/A	933.5074 / 949.5023	N/A
159	1322.627	1322.7094	1390.6532	N/A	1297.5953 / 1313.5902	N/A
236	2322.0563	2322.2019	2390.0825	N/A	2297.0246 / 2313.0195	N/A
256	2150.1209	2150.1746	2218.1471	N/A	2125.0892 / 2141.0841	N/A
265	1456.6737	1456.7809	1524.6999	N/A	1431.6420 / 1447.6369	N/A
385	1051.5241	1051.6046	1119.5503	N/A	1026.4924 / 1042.4873	N/A
431	1608.7839	1608.8966	1676.8101	N/A	1583.7522 / 1599.7471	N/A
442	1398.6365	N/A	1466.6627	N/A	1373.6048 / 1389.5997	N/A
477	2468.0216	2468.1997	2604.0741	N/A	2417.9584 / 2449.9482	N/A
481	2468.0216	2468.1997	2604.0741	N/A	2417.9584 / 2449.9482	N/A

Table 1. Predicted and observed *m/z* of Cdc25A peptides by MALDI-TOF-MS.

Recombinant human Cdc25A was incubated with 50 μM SNCEE before redox-profiling by MALDI-TOF MS as described in *Experimental Methods* section 2.9. Data for the Cdc25A regulatory domain cysteines, catalytic domain cysteines, and catalytic cysteine are displayed in black, green, and red, respectively. N/A, not observed.

3.3 DISCUSSION

Because Cdc25A depends upon a highly reactive thiolate for its activity and because this thiolate exists as part of an acid-base motif in a readily accessible hydrophobic pocket, we hypothesized Cdc25A activity would be inhibited by *S*-nitrosation in response to LMM RSNOs. Our studies indicated that Cdc25A is *S*-nitrosated and reversibly inhibited by LMM RSNOs *in vitro*, partially confirming our hypothesis. The implications of these studies are that Cdc25A may be an intracellular target for nitrosative regulation in addition to the previously described oxidative regulation. LMM RSNOs are generated in cells producing •NO from iNOS and in

experimental models of nitrosative stress; under these circumstances it could be anticipated that inhibition of Cdc25A phosphatase activity would halt the cell cycle, providing the logical link between the observed cell cycle inhibition and •NO signaling.

Cdc25A was more sensitive to inhibition by SNCEE than GSNO (IC_{50} = 969 μM compared to 22.5 μM). This difference in sensitivity may reflect molecular size or hydrophobicity and thus access of the molecule to the Cdc25A active site. It is possible that release of •NO into solution and subsequent autooxidation to the nitrosant N_2O_3 is required for Cdc25A inhibition; GSNO is a remarkably stable RSNO and its high IC_{50} compared to that of SNCEE may reflect this. Although these RSNOs are less potent than many Cdc25 inhibitors, the concentrations necessary for inhibition may not be outside the physiological (or pathological) concentrations in cells. The basal concentration of GSNO in the rat cerebellum was estimated at 6-8 μM, or 0.3 to 0.7% of total GSH (207). The authors did not measure the levels of protein-associated RSNOs or other LMM RSNOs such as CysNO, and did not examine the levels in cells expressing iNOS or under inflammatory stress, where RSNO levels are much higher (209). Thus, the total basal level of intracellular RSNOs is low, allowing retention of Cdc25A phosphatase activity for normal cellular functions. Under inflammatory conditions stimulated by iNOS activity, however, total RSNO levels can climb as high as 220 nmol / g protein, of which greater than 75% is protein-SNO (209). The concentration of GSNO in unperturbed rat cerebellum is estimated at 15.4 to 21.8 nmol / g protein (207), indicating that intracellular RSNO levels may climb at least 10-fold during inflammation. These conditions would be consistent with our observed enzymatic inhibition of Cdc25A by RSNOs, as a 10-fold increase in intracellular RSNOs would be predicted to result in 60 - 80 μM intracellular RSNO (207). Dependent upon the specific RSNO(s) formed, enzymatic inhibition of Cdc25A is feasible.

Our studies used a model of *trans*-nitrosation to inhibit Cdc25A activity. N_2O_3 and peroxynitrite (in the absence of excess $\bullet O_2^-$) are also potent nitrosating agents (146), and it has been hypothesized that N_2O_3 is the major nitrosating agent in cells when $\bullet O_2^-$ production is low (145). N_2O_3 forms and partitions selectively in the hydrophobic cores of membranes (143), and Cdc25A has been observed to localize to the plasma membrane (247), indicating Cdc25A, or at least a specifically-localized subpopulation of Cdc25A, could be exposed to very high local concentrations of nitrosating agents *in vivo* under conditions of nitrosative stress that would be sufficient to inhibit its enzymatic activity.

How do LMM RSNOs inhibit Cdc25A phosphatase activity? SNCEE did not degrade significantly in our assay, and decomposed SNCEE did not inhibit Cdc25A very potently. Together these results argue against a role of RSNO decomposition in Cdc25A inhibition by RSNOs. To our knowledge, no binding of intact nitrosothiols by proteins has been reported in the literature, making direct binding and steric interference with Cdc25A phosphatase activity another unlikely cause of inhibition. Regulation of tyrosine phosphatase activity by *S*-nitrosation in response to RSNOs has been described for PTP1B, SHP-1, and SHP-2 (189, 248), and inhibition of tyrosine superfamily phosphatase activity by RSNOs has been described for PTP1B and the lipid phosphatase PTEN *in vivo*, and *Yersinia* protein tyrosine phosphatase *in vitro* (244, 249, 250). It should be noted that *S*-nitros(yl)ation of the active site cysteine was confirmed only for SHP-1 (189), and oxidation appears to be the mechanism by which inactivation occurs for PTP1B and PTEN *in vivo*, as inhibition is reversible with DTT, but not with ascorbate (244, 250). Our results are consistent with a redox-reversible modification to Cdc25A that inhibits its activity. Inhibition of Cdc25A toward two structurally and biochemically distinct substrates as measured using separate analytical methods indicated that RSNOs exerted their effects through

Cdc25A and not the substrate. As I found Cdc25A was *S*-nitrosated on two molar equivalents of cysteine, the simplest explanation is that one or more cysteines whose integrity is critical for Cdc25A activity is *S*-nitrosated by RSNOs.

Cleavage of RSNOs in the prescence of ascorbate is dependent upon Cu^{+} ions, which are kept in the reduced state by ascorbate (198, 200). This chemistry, which forms the basis of the biotin-switch assay, thus depends upon the prescence of copper ions in the RSNO cleavage solution. Evidence for this copper dependence is supported by recent work indicating that variance in the biotin switch assay reported by groups may be due to trace contamination of laboratory water supplies with copper ions (251). I used chelex-treated, deionized H_2O and the ion chelator DTPA in my redox-profiling experiments, which may have prevented successful reduction and thus alkylation and detection of *S*-nitrosated cysteines on Cdc25A. Thioredoxin binds two cupric ions in its crystal structure (252), which may have provided a source of reducing equivalents in the prescence of ascorbate that were not available in experiments with Cdc25A. This would potentially explain the facile detection of Trx-Cys73-NO as well as detection of Cdc25A-associated RSNOs using Hg^{2+}-catalyzed •NO realease and trapping, but failure to identify Cdc25A-associated RSNOs using the modified biotin switch assay herein.

My failure to detect *S*-nitroso-Cys431-containing (or other *S*-nitrosated) peptides by mass spectrometry and my facile detection of reduced and IAC-thioalkylated Cys431-containing peptides under conditions where Cdc25A phosphatase activity was totally inhibited suggested that Cys431 was not *S*-nitrosated in response to LMM RSNOs. I failed to detect peptides containing 3 of 12 Cdc25A cysteines; these could be the cysteines that were *S*-nitrosated by SNCEE. Modification of cysteines in the N-terminus of Cdc25A would not be expected to impact its phosphatase activity, as the N-terminus is not necessary for its activity (30). Only one

catalytic domain cysteine remained unaccounted for by MS, Cys442. In the crystal structure of Cdc25A, Cys442 is buried and not readily accessible (42); this does not preclude the possibility of Cys442 *trans*-nitrosation by SNCEE, as a crystal structure of human thioredoxin in which a buried cysteine (Cys62) is *S*-nitrosated has been reported (246).

Finally, an additional explanation for the loss of Cdc25A activity consistent with our MS data would be that Cys431 existed as a disulfide after RSNO exposure. As mentioned above, other tyrosine superfamily phosphatases are oxidatively inhibited by RSNOs (244, 249, 250). Generation of an intra- or intermolecular disulfide bond with another Cdc25A cysteine, or a mixed disulfide with the CEE moiety of SNCEE could inhibit Cdc25A activity. Western blotting on SNCEE-treated Cdc25A did not reveal any antibody-reactive proteins or protein complexes with molecular masses greater than Cdc25A even under non-reducing conditions in SNCEE-treated samples (Figure 16); this evidence discourages intermolecular disulfide formation as the effecting mechanism. Generation of an intramolecular disulfide bond between the catalytic cysteine (Cys431) and a 3-dimensionally adjacent cysteine (Cys385) was observed in the crystal structure of Cdc25A (42), and treatment H_2O_2 inactivates the enzyme quite rapidly (k_{inact} = 69 ± 9 $M^{-1}s^{-1}$) (117). These observations suggest that intramolecular disulfide formation may be the most likely mechanism of inactivation, and that the *S*-nitrosation of Cdc25A cysteines observed may simply be auxiliary, or provide some additional regulatory role. Consistent with this hypothesis, a Cdc25A Cys431 disulfide would be detected by MALDI-TOF MS as a reduced, IAC alkylated peptide with predicted *m/z* 1608.7839, which we readily detected (obs. *m/z* 1608.8966). Further studies will be centered on identifying the type and location of the PTM regulating Cdc25A activity in response to LMM RSNOs.

4.0 CELLULAR REGULATION OF CDC25A BY NITROSATIVE STRESS

4.1 INTRODUCTION

In light of my studies on Cdc25A activity in response to RSNOs *in vitro*, I aimed to determine the effects of nitrosative stress on Cdc25A in cells. I hypothesized that induction of cellular nitrosative stress would suppress the activity of Cdc25A, resulting in hyperphosphorylation of Cdc25A targets such as $Cdk2^{Tyr15}$ and would subsequently induce cell cycle checkpoint. Importantly, I observed suppression of Cdc25A expression using two different models of nitrosative stress, treatment with the cell-permeable *S*-nitrosating agent SNCEE, and adenoviral expression of iNOS in cancer cells. I used SNCEE to control the molar and temporal release of •NO-equivalents to characterize Cdc25A suppression and probe the molecular mechanism governing Cdc25A loss following nitrosative stress. Cdc25A loss was time- and concentration-dependent, and occurred in cell lines derived from tumors of different tissue types. Ectopically expressed Cdc25A was also suppressed following SNCEE, suggesting a post-transcriptional mechanism of suppression. Cdc25A protein half-life was not decreased following SNCEE, and pre-treatment of cells with the proteasomal inhibitor MG-132 failed to prevent Cdc25A loss following SNCEE, indicating that increased protein degradation was not the mechanism by which Cdc25A loss occurred. Global protein synthesis was inhibited following SNCEE exposure, and I observed hyperphosphorylation and inhibition of the translational regulator

eIF2α with kinetics consistent with protein synthesis inhibition and Cdc25A loss. Indeed, the eIF2α inhibitor salubrinal was sufficient to suppress Cdc25A protein levels, indicating that eIF2α was responsible for SNCEE-induced Cdc25A loss. Collectively, these studies identified and delineated the first known translational mechanism governing Cdc25A protein levels, and indicated that Cdc25A was a target of •NO and RNS signaling in cells. In light of the oncogenic and anti-apoptotic role of Cdc25A in tumor cells, these studies provide evidence that loss of Cdc25A may mediate the pro-apoptotic and/or cytostatic effects of •NO signaling.

4.2 RESULTS

4.2.1 SNCEE induced nitrosative stress

We next investigated the effects of nitrosative insult to cellular Cdc25A. As nitrosative stress elicits multiple effects on endogenous thiol buffering systems including thiol depletion and *S*-nitrosation (209, 210), we first characterized the effects of nitrosative insult on cells. We used SNCEE to induce nitrosative stress in HCT116 cells. The monovalent cation Cu^{+} rapidly releases •NO from *S*-nitrosothiols at catalytic concentrations in the presence of a reducing agent such as ascorbic acid, which maintains the ion in its reduced form (198, 200). Thus, we utilized $CuSO_4$ in excess ascorbate to selectively reduce *S*-nitrosothiols to •NO for detection by ozone-mediated chemiluminescence. The basal level of RSNOs in vehicle-treated HCT116 cells was estimated at 32.3 ± 57.2 pmol/mg protein (Figure 19*A*, column 1), similar to that reported for other cell lines (210). SNCEE treatment induced intracellular RSNO accumulation within 30 minutes with maximal RSNO formation occurring in cells treated with 100 μM SNCEE, yielding

3.8 ± 0.9 nmol RSNOs per mg protein. Pretreatment with the denitrosating agent DTT reduced the level of intracellular RSNOs nearly to that of vehicle-treated cells (202.6 ± 6.9 pmol/mg protein), suggesting that DTT could protect against or reverse intracellular nitrosative stress.

An increase in intracellular RSNOs would be anticipated to decrease intracellular thiols, as nitrosation converts free thiols to –SNO. The fluorogenic maleimide thiol-alkylating agent ThioGlo-1 reacts selectively and quantitatively with free thiols at physiological pH generating an increase in its quantum fluorescence yield. I used ThioGlo-1 to quantify intracellular thiols in cell lysates following SNCEE treatment (Figure 19*B*). As a control, cells were treated with 100 μM decomposed SNCEE, and I detected 43.6 ± 0.8 nmol free thiols per mg protein (Figure 19*B*). This was in agreement with free thiol concentrations published for other cell lines (210). SNCEE decreased intracellular thiols in a concentration-dependent manner (Figure 19*B*). These results were consistent with *S*-nitrosation of intracellular proteins resulting in a decrease in intracellular thiols. As reported previously the loss of thiols exceeded the generation of RSNOs, which implies that thiol oxidation may be occurring in response to SNCEE treatment (210).

Regulation of •NO and RNS is complex in cells and generation of numerous RNS is possible, including the oxidizing and nitrating agents $ONOO^-$ and $•NO_2$ (253). Because I observed thiol depletion in excess of the observed RSNO generation, I queried whether significant amounts of $•NO_2$ and $ONOO^-$ were being formed. A convenient biomarker of $•NO_2$ and $ONOO^-$ formation is 3-nitrotyrosine (3-NT) because it is a relatively stable post-translational protein modification, is specifically generated by nitrating reactions, and because reagents against 3-NT are readily available (253). Therefore, I utilized a 3-NT-specific antibody to determine whether SNCEE increased the intracellular levels of 3-NT. In control cells (Figure 20,

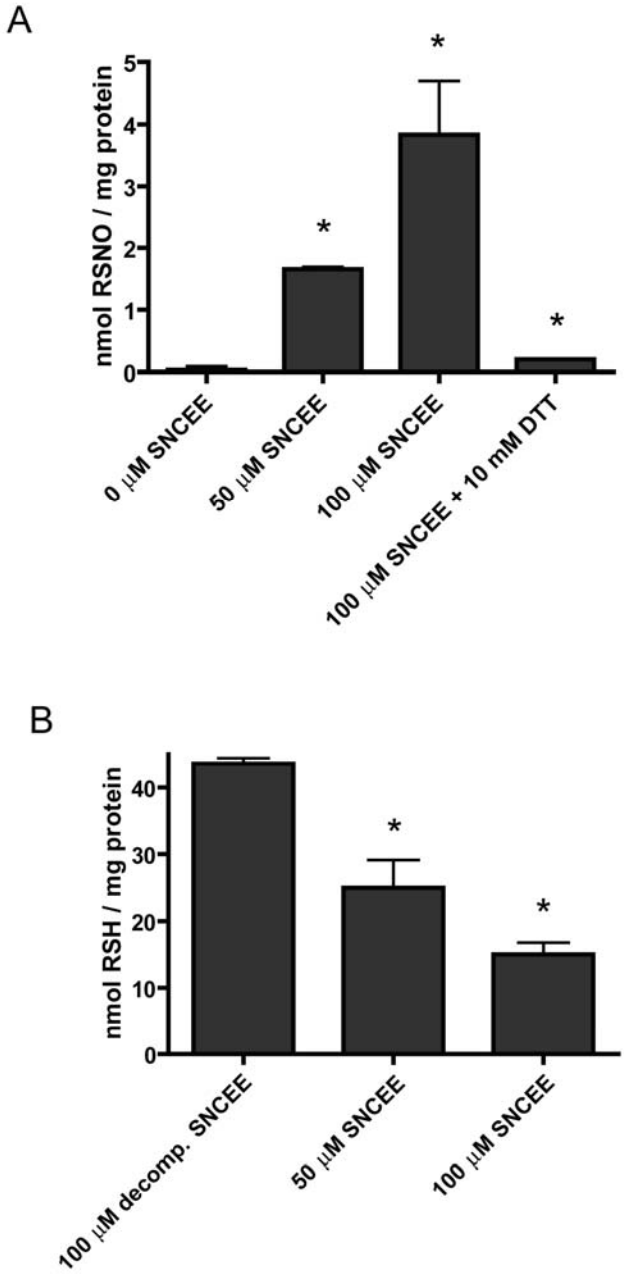

Figure 19. SNCEE induced intracellular RSNO accumulation and thiol depletion.

A, HCT116 cells were treated with the indicated compounds for 30 minutes, at which time lysates were prepared and analyzed for RSNO content as described in *Experimental Methods* section 2.6. *B*, HCT116 cells were treated with the indicated compounds for 30 minutes, at which time lysates were prepared and analyzed for thiol content as described in *Experimental Methods* section 2.6. *, $p < 0.05$.

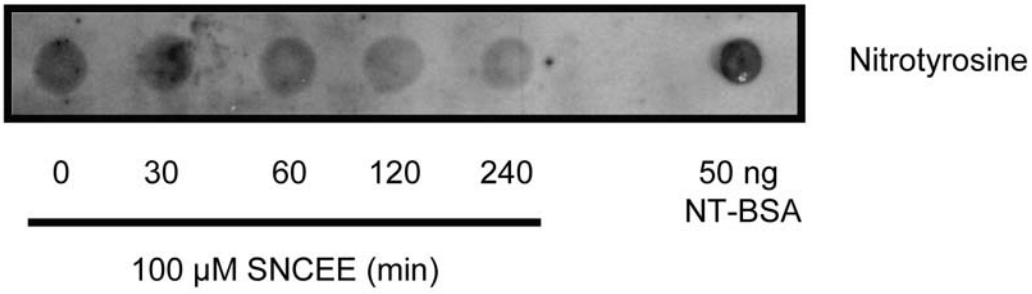

Figure 20. SNCEE did not induce significant biomolecule nitration.

HCT116 cells were treated with 100 μM SNCEE for the indicated time periods and 1μg of protein per sample was subjected to dot blotting for nitrotyrosine. Nitrotyrosine-BSA is shown as a control for antibody activity.

0 minutes) 3-NT levels were low compared to the positive control lane (Figure 20, NT-BSA), although there was a 20-fold higher amount of protein present. Notably, no change in the levels of 3-NT were detected following treatment of HCT116 cells with 100 μM SNCEE up to 4 hours following treatment. Collectively, these results suggest SNCEE selectively induced intracellular biomolecule nitrosation.

4.2.2 SNCEE decreased Cdc25A protein levels in HCT116 cells

I next determined the effects of SNCEE-induced nitrosative stress on Cdc25A activity in cells. I treated HCT116 cells with 100 μM SNCEE or the control compounds *L*-cysteine ethyl ester (CEE) or decomposed SNCEE, as 100 μM SNCEE induced significant accumulation of intracellular RSNOs but did not generate any detectable 3-nitrotyrosine (Figures 19 and 20). Surprisingly, treatment for two hours with SNCEE but not decomposed SNCEE or CEE decreased Cdc25A protein levels, whereas the protein levels of β-tubulin were unaffected (Figure

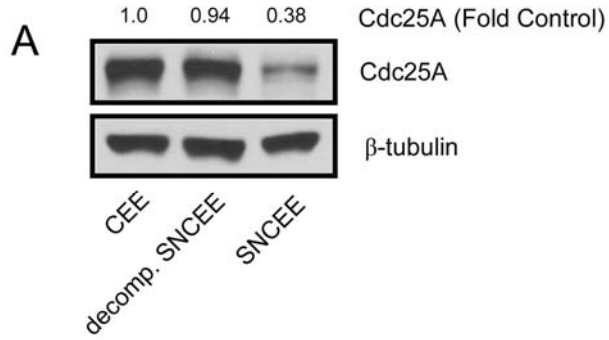
A
1.0
0.94
0.38
Cdc25A (Fold Control)
Cdc25A
β-tubulin
CEE
decomp. SNCEE
SNCEE

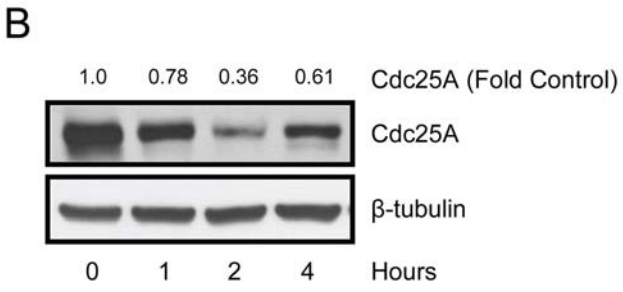
B
1.0
0.78
0.36
0.61
Cdc25A (Fold Control)
Cdc25A
β-tubulin
0
1
2
4
Hours

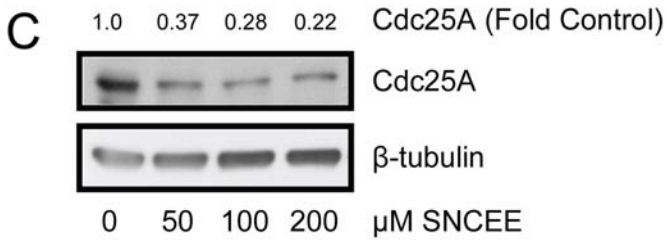
C
1.0
0.37
0.28
0.22
Cdc25A (Fold Control)
Cdc25A
β-tubulin
0
50
100
200
μM SNCEE

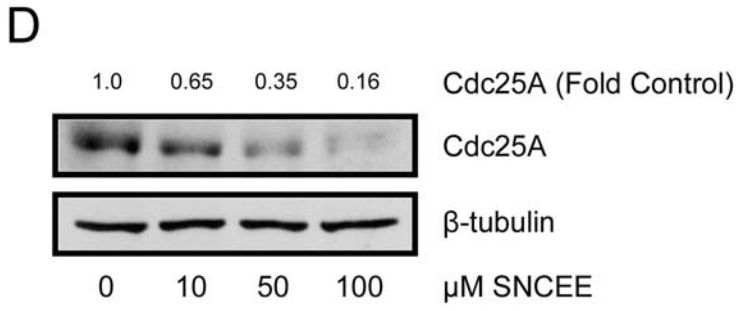
D
1.0
0.65
0.35
0.16
Cdc25A (Fold Control)
Cdc25A
β-tubulin
0
10
50
100
μM SNCEE

Figure 21. Characterization of Cdc25A suppression following SNCEE treatment.

A, HCT116 cells were treated with 100 μM of the indicated compounds and harvested two hours later for Western blotting. *B*, HCT116 cells were treated with 100 μM SNCEE and samples were harvested at the indicated time points for Western blotting. *C* and *D*, HCT116 cells (*C*) and HeLa cells (*D*) were treated with the indicated concentrations of SNCEE and harvested two hours post-treatment for Western blotting.

21). I observed no significant change in the protein levels of Cdk2 or GAPDH (Figure 22), indicating some specificity for Cdc25A. Cdc25A loss was time-dependent with the lowest Cdc25A levels occurring approximately 2 hours after treatment and rebounding by 4 hours post-treatment (Figure 21*B*). Cdc25A suppression following SNCEE was concentration-dependent; treatment of HCT116 cells with 50 μM SNCEE resulted in loss of greater than 60% of Cdc25A by 2 hours after treatment (Figure 21*C*). A similar concentration-dependent loss of Cdc25A protein levels in response to SNCEE was observed in HeLa cervical carcinoma cells (Figure 21*D*) indicating that SNCEE decreased Cdc25A levels in cells derived from multiple tumor types. As HeLa cells are functionally deficient in p53- and Rb-pathway signaling due to the presence of human papilloma virus-associated oncogenes (122, 123), this also indicated these pathways were not required for loss of Cdc25A following SNCEE. Recognition of Cdc25A by the antibody used for Western blotting was unaffected by RSNOs directly by SNCEE (Figure 17), suggesting a *bona fide* decrease in Cdc25A protein levels.

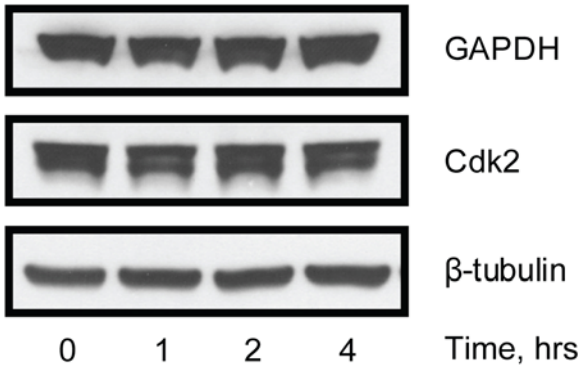

Figure 22. GAPDH and Cdk2 were not affected by SNCEE treatment.

HCT116 cell lysates from Figure 21*B* were subjected to Western blotting for the indicated proteins.

4.2.3 SNCEE did not decrease Cdc25A protein stability

I next aimed to determine the mechanism by which nitrosative stress suppressed Cdc25A protein levels. Cdc25A is a labile protein with a short half-life (57, 110, 111). The basal half-life of Cdc25A is controlled by ATR/Chk1-mediated ubitquitination and proteasomeal degradation (74, 112). In response to various stresses, Cdc25A becomes hyperphosphorylated by several stress-dependent kinases including p38, Chk1, and Chk2, subsequently targeting Cdc25A for degradation via ubiquitin-mediated proteolysis (114). The resultant decreased protein levels and thus Cdc25 phosphatase activity promotes accumulation of hyperphosphorylated, inactive Cdk complexes (72). Loss of Cdk activity slows or stops cell cycle progression, allowing time for repair of cellular damage. To determine whether nitrosative stress suppresses Cdc25A by decreasing its protein half-life, I treated HCT116 cells with UV irradiation, which decreases Cdc25A half-life (72), or either decomposed SNCEE or SNCEE, and monitored its half-life after blockade of new protein synthesis with cycloheximide (Figure 23*A* and *B*). Logarithmic regression analysis of the data indicated half-lives of 25.1 and 15.5 minutes for Cdc25A in

decomposed SNCEE- and UV-treated cells, respectively, consistent with UV irradiation-accelerated Cdc25A turnover. Whereas Cdc25A levels decreased by 120 minutes in SNCEE-treated cells to a level similar to that in response to decomposed SNCEE, the half-life was not shortened; rather, no significant decrease in protein levels was detected until 120 minutes after SNCEE treatment. These results suggested that Cdc25A stability was not decreased in response to SNCEE treatment. Similarly, pretreatment of HCT116 cells with the proteasomal inhibitor MG-132 (Figure 22*C*) or the ATR/ATM inhibitor caffeine (Figure 24) failed to prevent Cdc25A loss following SNCEE treatment, although the absolute levels of Cdc25A were increased (Figure 22*C*, Figure 24). Collectively, these results argued against a proteasomal mechanism of Cdc25A loss.

4.2.4 Post-transcriptional Cdc25A suppression by SNCEE

Transcription from the Cdc25A promoter is negatively regulated by several stress-responsive proteins, including p53, p21, and HIF-1α (84, 85, 109). •NO or nitrosative stress have been reported to activate and/or stabilize the expression of several of these proteins (219, 254, 255); thus, I investigated whether the Cdc25A promoter region was essential for SNCEE-mediated Cdc25A suppression. I generated mammalian expression vectors containing the *CDC25A* cDNA but not the *CDC25A* promoter or 3'-untranslated region. These vectors drive expression of Cdc25A from the cytomegalovirus promoter, and express a influenza hemaglutinin (HA) epitope-Cdc25A fusion protein, allowing differentiation between endogenous and ectopically expressed Cdc25A. I transfected these vectors into HCT116 cells, and measured the effects of SNCEE on HA-Cdc25A. As observed in Figure 25, SNCEE but not decomposed SNCEE or CEE decreased HA-Cdc25A levels as was observed with protein transcribed from the

endogenous gene. This implied that suppression of Cdc25A following SNCEE was a promoter-independent, post-transcriptional effect.

4.2.5 Protein translation was inhibited following SNCEE treatment

Attenuation of protein translation provides a functional mechanism to decrease the protein levels of a rapidly synthesized protein. The short half-life of Cdc25A indicated a rapid synthetic rate for Cdc25A, so we investigated whether SNCEE affected protein synthesis. I treated HCT116 cells with radiolabeled [^{35}S]-*L*-cysteine and [^{35}S]-*L*-methionine for different time periods following decomposed SNCEE or SNCEE treatment, and monitored total radioisotope incorporation into proteins via SDS-PAGE and autoradiography (Figure 26). Total protein loading was equal as assessed by β-tubulin levels; radiolabeled amino acid incorporation into protein from SNCEE-treated cell lysates, however, was reduced during both the first and second hour, consistent with the time course of Cdc25A decrease (Figure 21B). In addition, the magnitude of protein synthesis repression was consistent with the expression levels of Cdc25A in SNCEE-treated cells. Together, these results suggested that SNCEE treatment decreased Cdc25A protein translation.

4.2.6 Suppressed eIF2α activity was responsible for loss of Cdc25A following SNCEE treatment

SNCEE decreased global protein synthesis. Stress-dependent global translational inhibition is mediated primarily through phosphorylation and inhibition of the translational regulator eIF2α

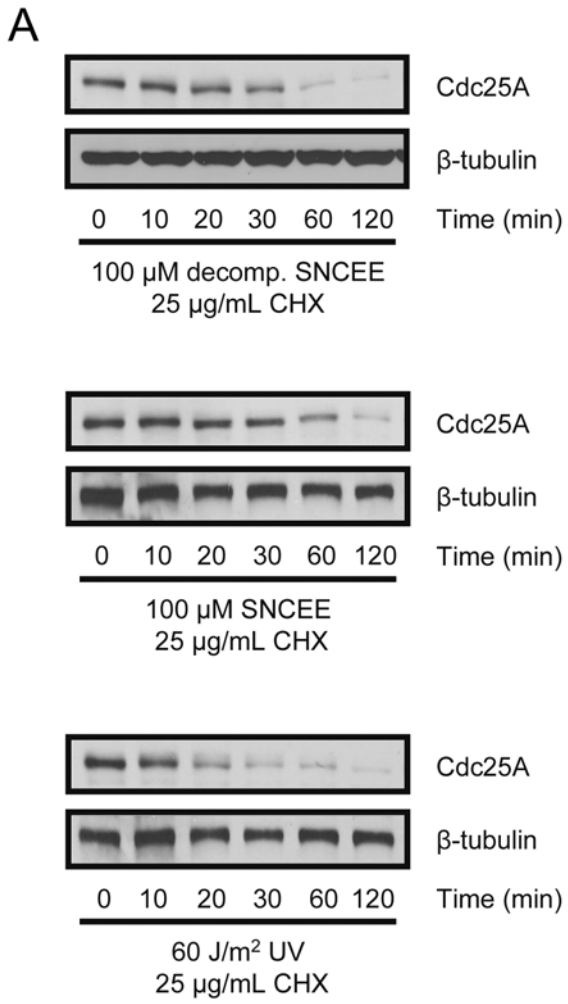
A
Cdc25A
β-tubulin
0 10 20 30 60 120
Time (min)
100 μM decomp. SNCEE
25 μg/mL CHX
Cdc25A
β-tubulin
0 10 20 30 60 120
Time (min)
100 μM SNCEE
25 μg/mL CHX
Cdc25A
β-tubulin
0 10 20 30 60 120
Time (min)
60 J/m2 UV
25 μg/mL CHX

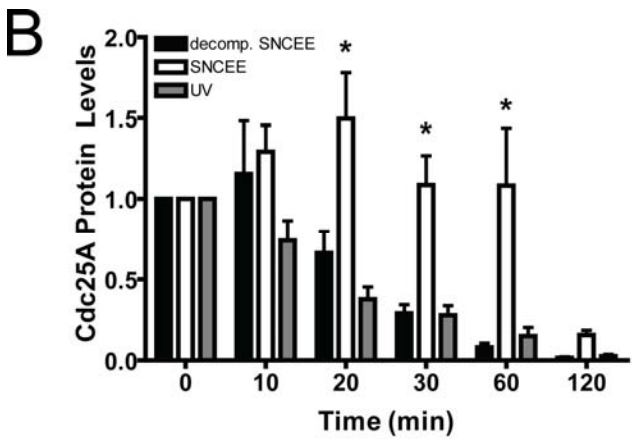
B
decomp. SNCEE
SNCEE
UV
Cdc25A Protein Levels
2.0
1.5
1.0
0.5
0.0
0
10
20
30
60
120
Time (min)
*
*
*

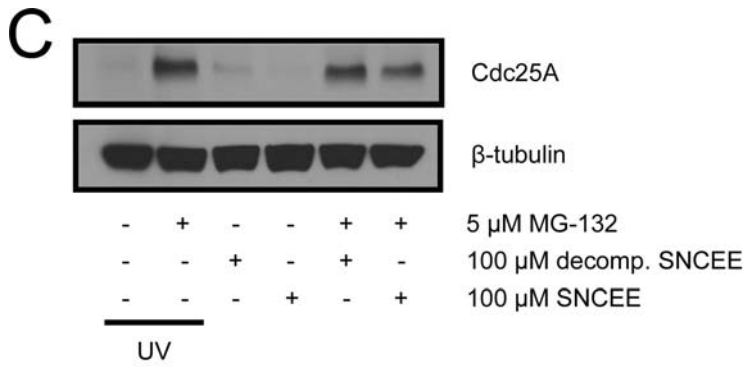

Figure 23. Cdc25A half-life was not decreased following SNCEE treatment.

A, HCT116 cells were co-treated with 25 μg/mL cycloheximide and either 100 μM decomposed SNCEE, 100 μM SNCEE, or 60 J/m^2 UV. Cells were harvested at the indicated timepoints for Western blotting. N=5. *B*, Western blots from A were densitometrically scanned, and remaining Cdc25A levels were expressed as fraction Cdc25A at time = 0 after normalization to β-tubulin. Black, gray, and white bars represent Cdc25A levels from decomposed SNCEE-, SNCEE-, and UV-treated cells, respectively. *, $p < 0.05$. *C*, HCT116 cells were pretreated with 5 μM MG-132 for 8 hours before treatment with 100 μM of the indicated compounds. Two hours later, cells were harvested for Western blotting. N=4.

(256). In response to various stresses, eIF2α is phosphorylated on Ser51 by stress-sensitive kinases (257). Phosphorylation of eIF2α at Ser51 increases its affinity for the eIF2B subunit, whose release from the eIF2 complex is necessary for GTP-GDP recycling, and subsequent tRNA recruitment and binding (256). Thus, eIF2α^{Ser51} hyperphosphorylation results in a general decrease in protein translation. To investigate whether SNCEE altered the activity of eIF2α, I treated cells with 100 μM SNCEE and monitored phosphorylation of eIF2α^{Ser51} using phospho-specific antibodies (Figure 27*A*). Although the total levels of eIF2α were not changed in response to SNCEE, the pool of phosphorylated eIF2α^{Ser51} increased in a time-dependent manner with phospho-eIF2α^{Ser51} appearing as soon as 30 minutes after SNCEE treatment and persisting for at least two hours after treatment. The onset of eIF2α hyperphosphorylation was consistent

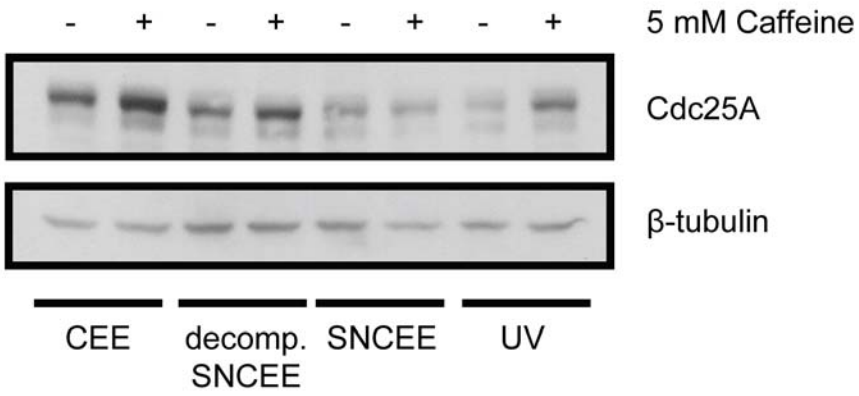

Figure 24. Caffeine did not block Cdc25A loss following SNCEE treatment.

HCT116 cells were incubated for 30 minutes in medium containing 5 mM caffeine before treatment with 100 μM of the indicated compounds or with 60 J/m^2 UV irradiation as described in *Experimental Methods*. Cells were harvested two hours later for Western blotting.

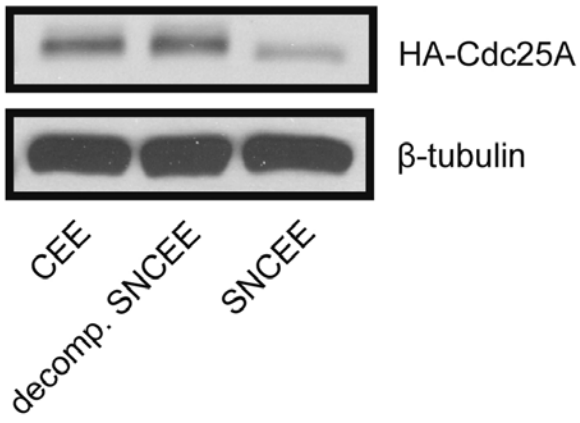

Figure 25. Cdc25A promoter-independent suppression of Cdc25A by SNCEE.

HCT116 cells were transfected with plasmids encoding HA-tagged Cdc25A as described in *Experimental Methods*. After 24 hours, cells were treated with 100 μM of the indicated compounds. Two hours later, cells were harvested for Western blotting.

both with the loss of Cdc25A protein, as well as attenuation of protein synthesis in response to SNCEE.

To determine whether inhibition of eIF2α was sufficient to suppress Cdc25A protein levels, I treated HCT116 cells with the eIF2α inhibitor salubrinal (258) or vehicle, and determined the effects on Cdc25A expression by Western blotting (Figure 27*B*). In response to eIF2α inhibition, Cdc25A levels decreased to levels similar to those observed in SNCEE-treated cells. This implied that eIF2α was a regulator of basal Cdc25A protein levels and suggested that eIF2α inhibition in response to SNCEE was a mechanism by which Cdc25A was decreased following nitrosative stress.

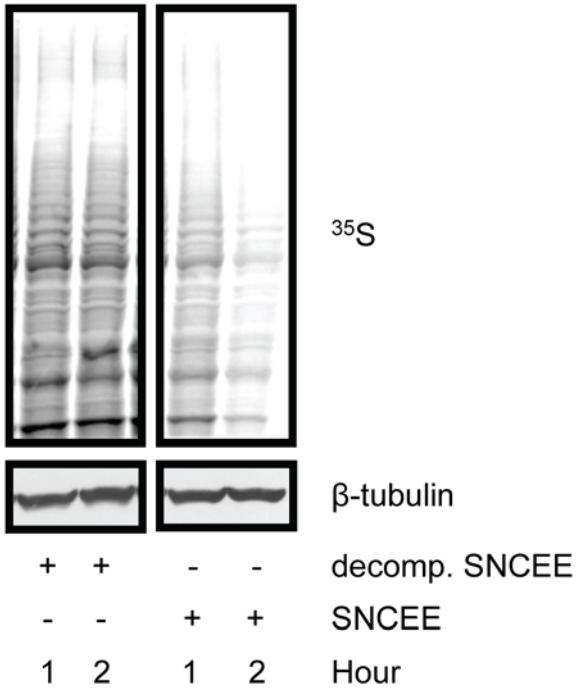

Figure 26. SNCEE inhibited global protein translation.

HCT116 cells were incubated for 1 hour in medium lacking *L*-Cys and *L*-Met, and then treated with 100 μM decomposed SNCEE, or 100 μM SNCEE for 2 hours. I added 300 μCi/mL [^{35}S]-*L*-Cys and [^{35}S]-*L*-Met to the medium at the start of the indicated hour post-SNCEE treatment and cells were harvested for autoradiography and Western blotting 60 minutes later. Non-adjacent lanes are shown from the same gel.

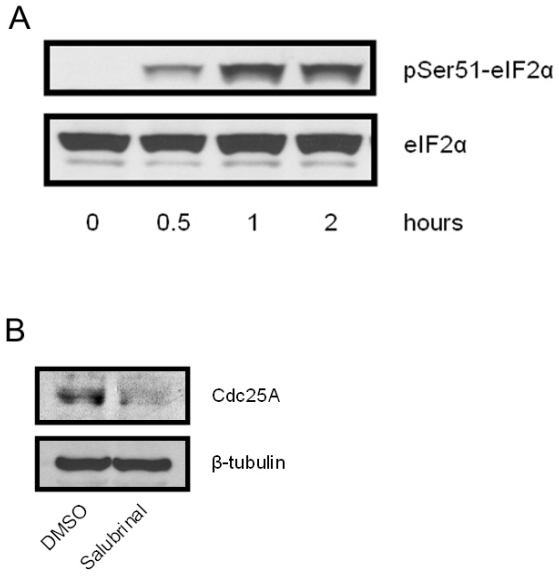

Figure 27. eIF2α controlled Cdc25A protein levels.

A, HCT116 cells were treated for the indicated times with 100 μM SNCEE and harvested for Western blotting. *B*, HCT116 cells were treated for 24 hours with DMSO or with 75 μM salubrinal (Sal) and were then harvested for Western blotting.

4.2.7 •NO derived from iNOS decreased Cdc25A protein levels

Induction of nitrosative stress decreased Cdc25A protein levels. In cells iNOS catalyzes RSNO production and initiates nitrosative stress (209). To investigate whether intracellular production of •NO from an endogenous source affected Cdc25A expression, I infected HCT116 cells with adenoviruses encoding the human iNOS cDNA. Measurement of NO_2^- and NO_3^- formation indicated that iNOS induced •NO formation similar to the concentrations of SNCEE utilized above (Figure 28*B*). Expression of iNOS decreased Cdc25A protein levels but did not affect Cdc25B or Cdc25C (Figure 28*A*). Blockade of •NO production by the NOS inhibitor *L*-NMMA prevented •NO generation, and restored Cdc25A levels (Figure 28*A* and *B*).

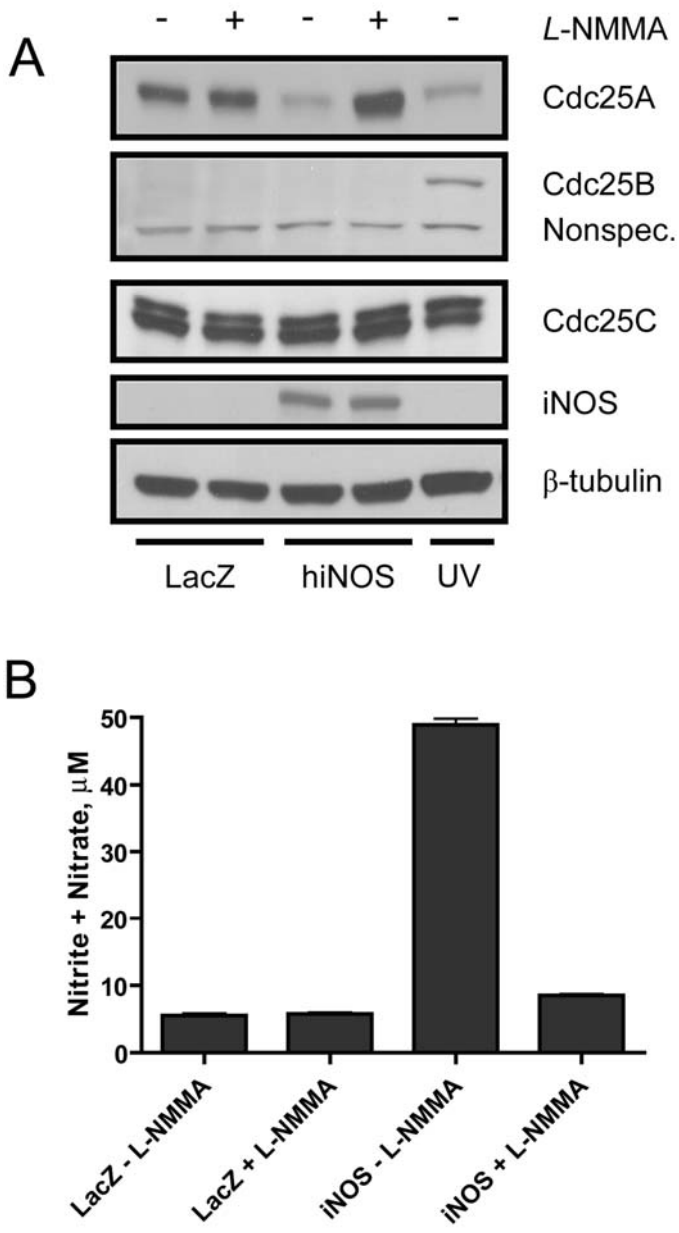

Figure 28. iNOS-derived •NO suppressed Cdc25A expression.

A, HCT116 cells were infected with 10 MOI of adenoviruses encoding the β-galactosidase gene (LacZ) or human the iNOS cDNA in the prescence or absence of 1 mM *L*-NMMA. 24 hours later, cells were harvested for Western blotting. *B*, The concentration of NO_2^- and NO_3^- in the medium (from *A*) was determined using a colorimetric detection kit from Cayman Chemical according to the manufacturer's instructions.

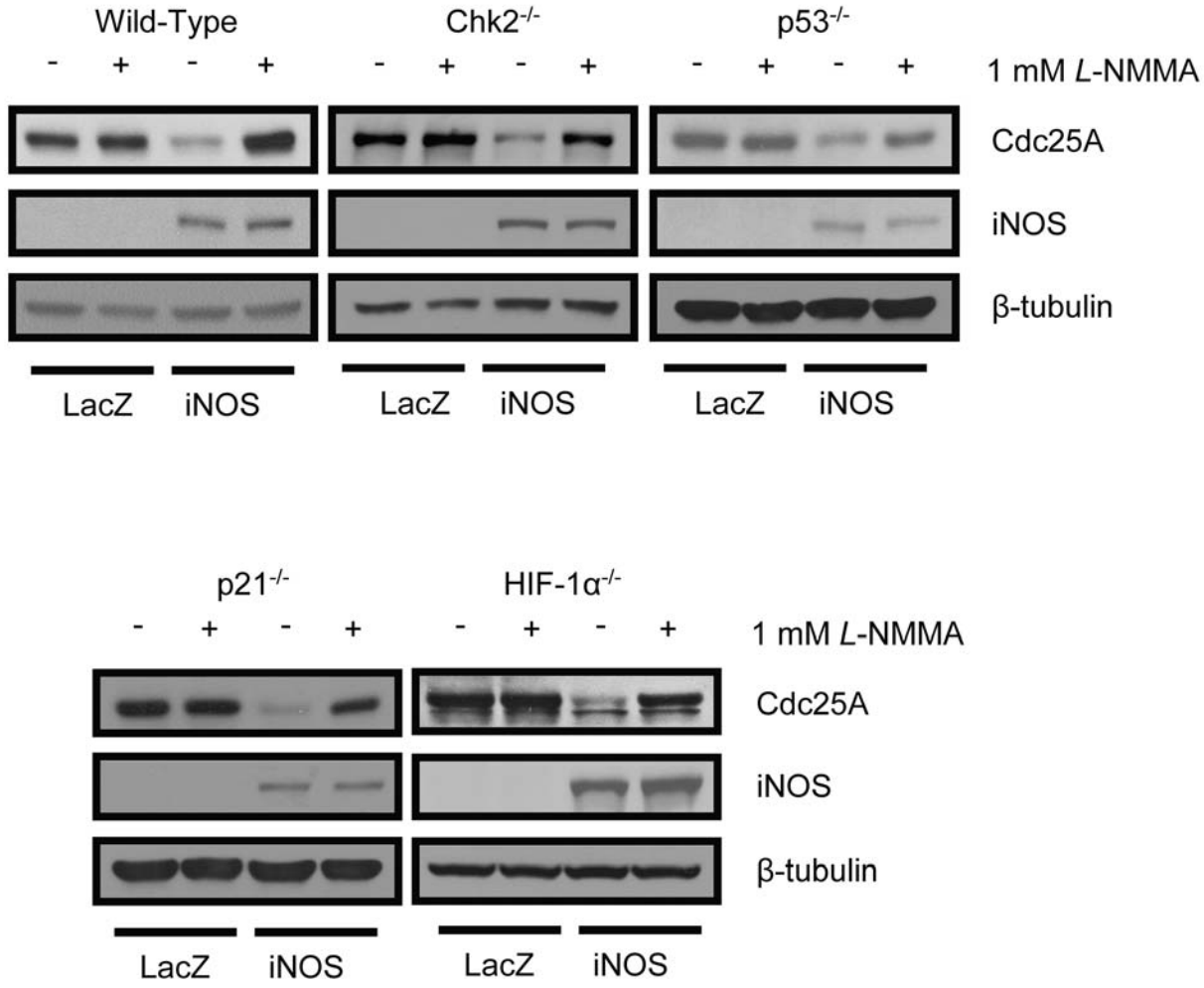

Figure 29. Genetic profiling of Cdc25A suppression by iNOS-derived •NO.

Wild-type or isogenic HCT116 cells deficient in the indicated gene products were infected with 10 MOI of adenoviruses encoding the β-galactosidase gene (LacZ) or human the iNOS cDNA in the prescence or absence of 1 mM *L*-NMMA. Cells were harvested 24 hours later for Western blotting.

It is difficult to perform mechanistic studies in iNOS-expressing cells because the temporal and quantal production of •NO by iNOS are not easily regulated. Also, viral infection induces eIF2α^{Ser51} phosphorylation via protein kinase R activation (257), confounding interpretation of eIF2α^{Ser51} phosphorylation state in adenovirally-infected cells. Thus, we used a panel of isogenic HCT116 cells with homozygous deletions in a number of previously reported Cdc25A regulators to confirm or refute the roles of several reported Cdc25A regulators. As shown in Figure 29, HCT116 cells deficient in Chk2, p53, p21, and HIF-1α suppressed Cdc25A in response to iNOS activity as was observed for the wild-type cells, consistent with a translational mechanism of Cdc25A loss following induction of nitrosative stress. Collectively, these results corroborate the observed loss of Cdc25A in response to SNCEE treatment, and demonstrate that endogenously generated •NO decreased Cdc25A protein levels similar to that observed in cells subjected to chemically-induced nitrosative stress.

4.3 DISCUSSION

Stringent Cdc25A regulation is critical for cell growth without unwarranted proliferation. High Cdc25A activity and expression are hallmarks of human cancers, likely conveying resistance to apoptosis and to anti-growth signals. Thus, mechanisms have evolved to rapidly suppress Cdc25A following normal and stress-mediated cellular signaling. Previous research uncovered transcriptional and proteasomal control of Cdc25A following stress; herein I described a distinct and novel mechanism regulating Cdc25A following exposure to •NO and RNS: translational suppression of Cdc25A activity by nitrosative stress triggered by low molecular mass RSNOs and by iNOS-derived •NO. This mechanism may be most prevalent in tumor tissues expressing

iNOS or in tissues derived from chronic inflammatory diseases, as •NO generated from iNOS was sufficient to suppress Cdc25A levels (Figure 28).

Translational Cdc25A suppression following nitrosative stress can be distinguished from previous reports examining Cdc25A regulation by RNS (229). In response to nitrating agents, Cdc25A loss was paralleled by activation of the upstream kinase ATM and was sensitive to okadaic acid. Protein phosphatase 5 (PP5) activity is required for ATM activity (259), and PP5 is inhibited by okadaic acid (260). These data imply the traditional DNA damage pathway mediates Cdc25A loss following $\bullet NO_2$ or SIN-1 treatment. In contrast, SNCEE did not decrease Cdc25A half-life, nor was Cdc25A loss blocked by proteasome inhibition. Also, pre-treatment with the ATM/ATR inhibitor caffeine did not block Cdc25A loss following SNCEE treatment, though UV-induced Cdc25A loss was inhibited (Figure 24). This further distinguished SNCEE-mediated Cdc25A downregulation from the traditional DNA damage pathway. Collectively, this work and previous studies (229) reinforce the concept that distinct RNS mediate discrete intracellular signaling (Figure 30).

eIF2α^{Ser51} is phosphorylated by the stress-responsive eIF2 kinases PKR-like endoplasmic reticulum kinase (PERK), heme-regulated inhibitor (HRI), GCN2, and RNA-dependent protein kinase (257), and is dephosphorylated by protein phosphatase 1 (PP1) (258, 261). How eIF2α becomes hyperphosphorylated in response RNS is unknown, although several candidate mediators exist. PP1 is inhibited by H_2O_2 in PC12 cells and suppression of PP1 activity in H_2O_2-treated cells correlated with phosphorylation of eIF2α^{Ser51} (262). H_2O_2 can deplete thiols by oxidation to inter- and intra-molecular disulfides or higher order cysteine oxides. SNCEE depleted thiols (Figure 19B), indicating that this could be responsible for eIF2α^{Ser51} hyperphosphorylation in response to RSNOs.

Perturbations to the ER redox status either in response to reductants (263) or RNS (264) are reported to initiate ER stress, and thus generate phospho-eIF2α^{Ser51}, presumably through activation of PERK. Whereas •NO-derived species have not been reported to directly activate PERK, *S*-nitrosation of the ER-localized protein disulfide isomerase results in protein misfolding, which is a well-characterized ER stress (213). This could initiate eIF2α hyperphosphorylation and subsequent translational inhibition. Although PERK-mediated translational inhibition can occur rapidly in response to several stimuli (263), it remains undetermined whether PERK is activated in response to RNS, or whether S-nitrosation of protein disulfide isomerase and subsequent ER stress is mediated rapidly enough to elicit •NO- and SNCEE-induced loss of Cdc25A.

In addition to PERK activation, HRI kinase activity has previously been reported to be activated in response to •NO. HRI may not be the major target of SNCEE-induced eIF2α hyperphosphorylation in HCT116 cells, as HRI protein is expressed primarily in erythroid precursor cells, and HRI is essentially undetectable in many other cell types (265). Nonetheless, it remains possible that HRI mediated eIF2α activation.

Cdc25A inhibits apoptosis by binding to and inhibiting the pro-apoptotic MAP kinase family member ASK-1 (103). Overexpression of Cdc25A attenuates ASK-1 activation and subsequent apoptosis in response to H_2O_2, suggesting that dissociation of Cdc25A from ASK-1 is a required step for stimulation of ASK-1 kinase activity (103). I have not excluded the possibility that loss of Cdc25A following nitrosative or oxidative stress is an essential step for activation of ASK-1 and subsequent downstream signaling via p38 and/or JNK kinases. I have observed activation of p38 after SNCEE treatment with kinetics that slightly trail loss of Cdc25A (unpublished observations) and found that Cdc25A and ASK-1 coimmunoprecipitate as reported

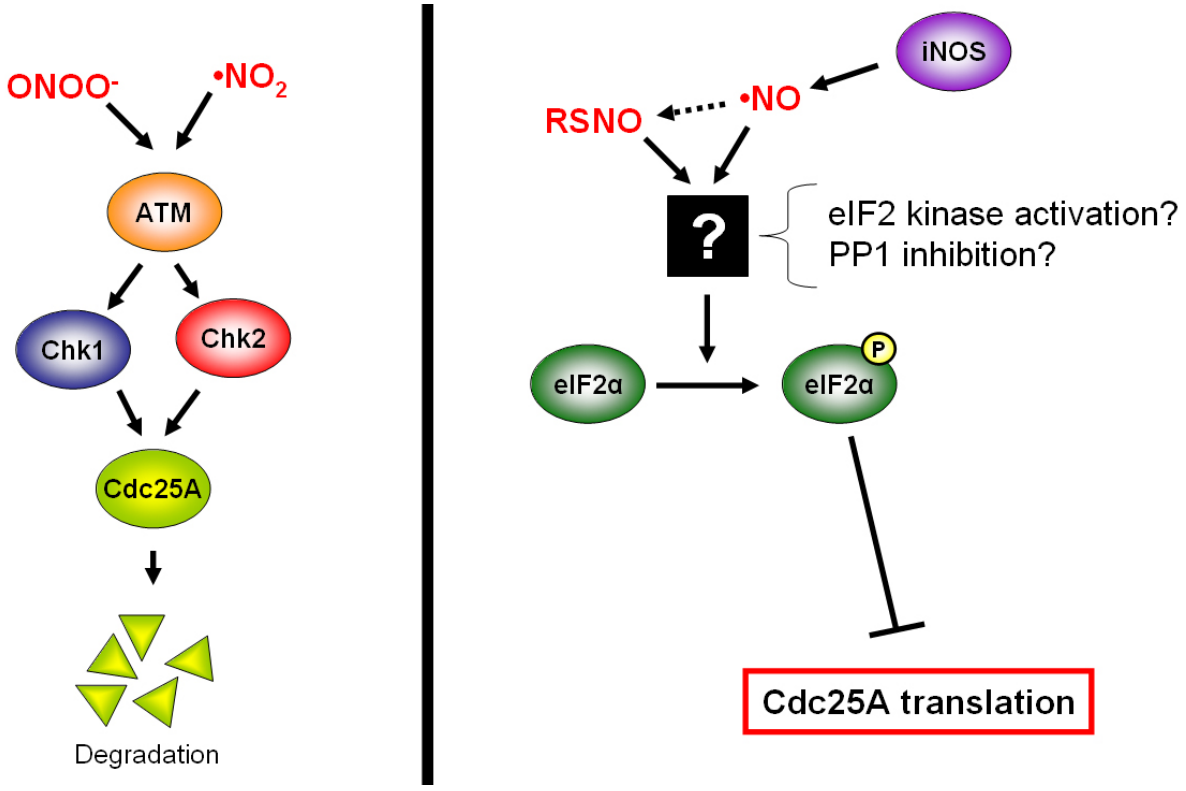

Figure 30. Regulation of Cdc25A protein levels by •NO and RNS.

In response to nitrating species such as $ONOO^-$ and $•NO_2$, activation of ATM is observed coincident with loss of Cdc25A protein levels. This loss of Cdc25A is sensitive to okadaic acid, which inhibits the essential ATM cofactor PP5. Thus, nitrating agents appear to activating the traditional checkpoint signaling machinery to suppress Cdc25A. In contrast, RSNOs and •NO derived from iNOS (which may ultimately generate RSNOs) trigger suppression of eIF2α activity and subsequent translational inhibition of Cdc25A. The mechanism by which eIF2α is inhibited remains to be determined (see text for detailed discussion).

previously ((103) and Figure 37), consistent with a model where translational suppression of Cdc25A following stress generated by high •NO primes the cell for ASK-1 activation and signaling through the p38 pathway. Alternatively, in response to shorter or less severe nitrosative stress, Cdc25A enzymatic activity may be inhibited, allowing for cellular regulation of Cdc25A phosphatase-dependent vs. independent activities in response to nitrosative insult (Figure 31). Future studies are centered on this hypothesis.

In summary I have described novel regulation of Cdc25A in response to •NO and •NO-derived species, RSNOs reversibly inhibit Cdc25A phosphatase activity while inhibition of eIF2α suppresses translation of Cdc25A protein. These results highlight the importance of stringent control of Cdc25A expression to regulate cellular activities. I speculate that this bipartite control of Cdc25A allows a cellular "stopwatch" function, where rapid inhibition of Cdc25A phosphatase activity protects against cell cycle progression, while prolonged or severe •NO-mediated cell stress suppresses Cdc25A levels and attenuates non-enzymatic Cdc25A functions such as apoptosis suppression.

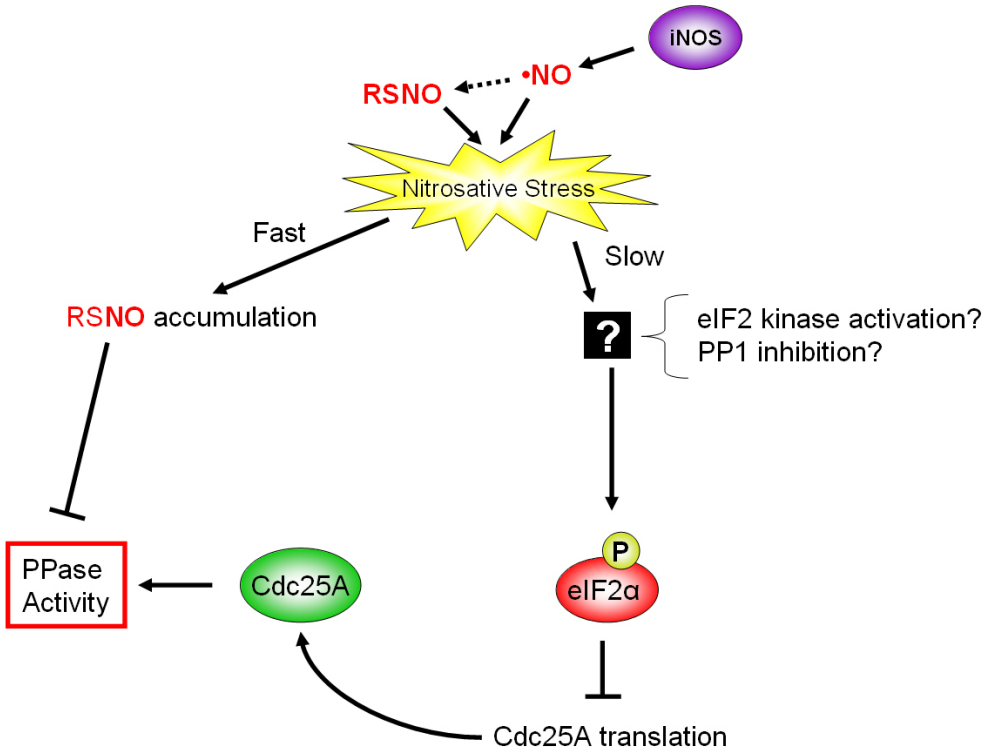

Figure 31. Bipartite control of Cdc25A by nitrosative stress.

Nitrosative stimuli are capable of both inhibiting Cdc25A enzymatic activity and inhibiting the translation of the protein. Enzymatic inhibition of Cdc25A by LMM RSNOs occurred rapidly *in vitro*, whereas suppression of Cdc25A protein levels following nitrosative stress required several hours. Thus, both the duration and intensity of nitrosative insult may dictate the Cdc25A-dependent biological outcome of the stress.

5.0 EXAMINATION OF THE PHYSIOLOGICAL SIGNIFICANCE OF CDC25A SUPRESSION IN RESPONSE TO NITROSATIVE INSULT

5.1 INTRODUCTION

Cdc25A dephosphorylates and activates Cdk2 complexes and thus drives the G_1-S transition and progression through S-phase (46, 48). Overexpression of Cdc25A accelerates dephosphorylation of Cdk2 complexes and accelerates the G_1-S transition (46). Conversely, suppression of Cdc25A attenuates DNA synthesis in a manner dependent upon Cdk2 dephosphorylation (266), and suppression of Cdc25A is required for S-phase checkpoint in response to DNA damage (71, 74, 105). Similarly, overexpression of Cdc25A bypasses checkpoint initiation and results in radioresistant DNA synthesis (RDS)(71, 74, 78) . This requirement for Cdc25A suppression for checkpoint initiation is supported by studies in which expression Cdk2AF (a Cdk2 double mutant in which the inhibitory Thr14 and Tyr15 residues are mutated to alanine and phenylalanine, respectively, and thus is not dependent upon Cdc25 activity) bypassed the S-phase checkpoint and resulted in RDS (71, 105). Thus, dephosphorylation of Cdk2 by Cdc25A is rate-limiting for DNA synthesis in normal and DNA-damaged cells.

Our observation that nitrosative stress in the form of iNOS-mediated •NO production or SNCEE treatment decreased Cdc25A activity and levels in conjunction with previous studies reporting •NO/RNS-mediated S-phase arrest concurrent with suppressed Cdk2 activity (226,

227) suggests that Cdc25A could be the causal link between •NO production and cellular inhibition of DNA synthesis. Overexpression of Cdc25A by tumor cells provides a logical explanation for the paradoxical high •NO production in many tumors and the apparent insensitivity to •NO/RNS-mediated S-phase inhibition.

I tested the role of Cdc25A expression and activity in the regulation of S-phase checkpoint in response to •NO/RNS. I found that iNOS-derived •NO or SNCEE treatment potently and rapidly inhibited DNA synthesis as measured by BrdU incorporation into DNA. Expression of Cdc25A was not sufficient to restore DNA synthesis in response either to iNOS-derived •NO or SNCEE. Morever, expression of Cdk2AF failed to restore DNA synthesis in SNCEE-treated cells, and did not alter the kinetics of S-phase inhibition or recovery. SNCEE did not significantly inhibit Cdk2 activity *in vitro*, suggesting that Cdk2 is not a direct target for nitrosative signaling. Thus, I conclude that Cdc25A and Cdk2 activity are not sufficient to restore DNA synthesis in response to nitrosative stimuli; thus, nitrosative stress-induced S-phase inhibition is distinct from the DNA damage-induced intra-S-phase checkpoint, as ectopic Cdk2 activity cannot bypass it.

Because Cdc25A did not appear limiting for DNA synthesis following nitrosative insult, I examined whether other known Cdc25A activities were altered in nitrosatively-challenged cells. I found that Cdc25A interacted with ASK-1, and that the downstream target of ASK-1, p38 MAP kinase, was activated in SNCEE-treated cells with kinetics that roughly coincided with Cdc25A suppression. Moreover, whereas SNCEE did not cause apoptosis alone, cotreatment of cells with SNCEE and the cytotoxic agent cisplatin caused an approximately two-fold increase in apoptosis compared to decomposed SNCEE and cisplatin-treated cells. Together, these results indicate

that Cdc25A suppression in nitrosatively-challenged cells may decrease the apoptotic threshold in response to genotoxic stimuli.

5.2 RESULTS

5.2.1 SNCEE and iNOS-derived •NO inhibited DNA synthesis

I first determined the intensity and kinetics of DNA synthesis inhibition of HCT116 cells expressing iNOS or treated with SNCEE. Expression of iNOS in HCT116 cells simultaneously decreased Cdc25A (Figure 32*B*) and incorporation of BrdU into DNA compared to cells expressing LacZ (Figure 32*A*, top-right panel vs. top-left panel). Notably, cells still incorporated some BrdU (Figure 32*A*, bottom-left panel), although to a lesser level than LacZ-expressing cells. Although *L*-NMMA had no effect on Cdc25A expression or DNA synthesis in LacZ-expressing cells, treatment of iNOS-expressing cells with *L*-NMMA restored both Cdc25A expression (as observed previously) and DNA synthesis (Figure 32*A*, bottom-right panel vs. bottom-left panel), indicating that production of •NO was required for suppression of Cdc25A and DNA synthesis. Together, these results indicate that iNOS-derived •NO triggered S-phase arrest, and that Cdc25A suppression and DNA synthesis inhibition were temporally correlated.

I next examined the effects of SNCEE on DNA synthesis in HCT116 cells. I exposed cells to 100 μM SNCEE, and monitored DNA synthesis at various timepoints post-treatment by BrdU incorporation. As shown in Figure 33, treatment with SNCEE suppressed DNA synthesis within two hours of treatment, and rebounded by six hours post-treatment. Comparison of the kinetics of DNA synthesis inhibition to Figure 21*B* suggested that inhibition of DNA synthesis

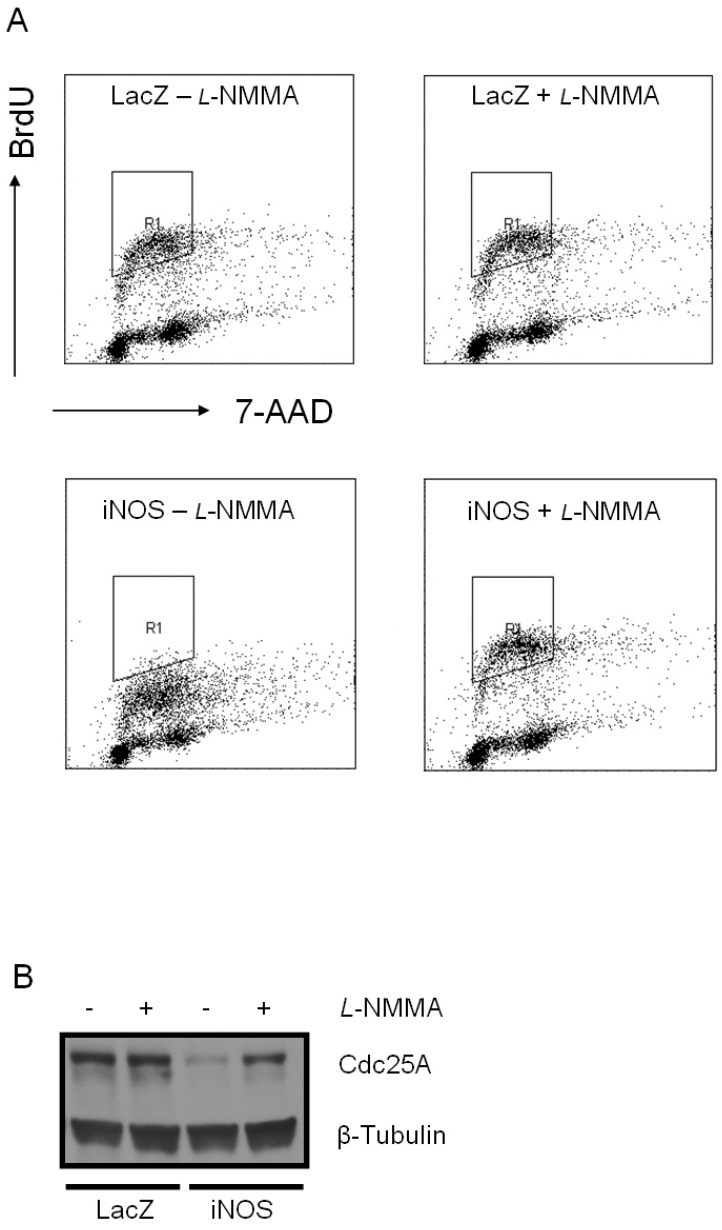

Figure 32. iNOS-derived •NO simultaneously suppressed Cdc25A and DNA synthesis.

A, HCT116 cells were infected with adenoviruses encoding LacZ or iNOS and incubated in medium with or without 1 mM *L*-NMMA for 24 hours. Cells were labeled with BrdU for 30 minutes, and harvested for flow cytometry. The y-axis depicts log-BrdU fluorescence, while the x-axis depicts 7-AAD fluorescence as a measure of DNA content. *B*, Duplicate plates of cells were infected as above and harvested 24 hours post-infection for Western blotting.

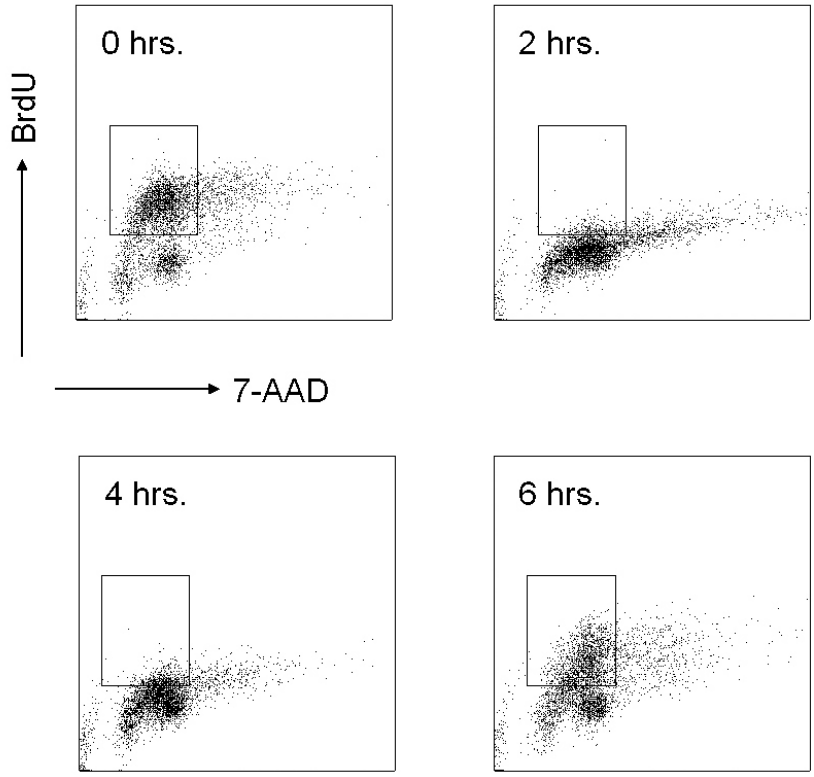

Figure 33. SNCEE time-dependently inhibited DNA synthesis.

HCT116 cells were treated with 100 μM SNCEE, and cells were labled with 10 μM BrdU 30 minutes before harvesting at the indicated time periods for flow cytometric analysis.

correlated with loss of Cdc25A, and recovery of DNA synthesis trailed recovery of Cdc25A expression, consistent with a role for Cdc25A in stimulating S-phase activity.

5.2.2 DNA synthesis was not restored by Cdc25A expression in iNOS-expressing cells.

If Cdc25A activity is limiting for S-phase, restoration of Cdc25A activity in iNOS-expressing cells would be anticipated to restore DNA synthesis. I ectopically expressed Cdc25A in cells expressing iNOS or LacZ as a control and measured the effect on iNOS-induced DNA synthesis

inhibition by BrdU incorporation (Figure 34). Again, iNOS expression reduced Cdc25A protein levels (Figure 34*B*) and suppressed DNA synthesis (Figure 34*A*, upper-right panel). Despite the high Cdc25A levels in Cdc25A-transfected cells expressing iNOS (Figure 34*B*), DNA synthesis was not increased compared to vector-transfected cells (Figure 34*A*, bottom-right panel vs. top-right panel). Although I do not know if the ectopic Cdc25A phosphatase activity remained after iNOS expression and I cannot rule out the possibility that high expression of Cdc25A in nitrosatively-challenged cells may negatively impact DNA synthesis, the results in Figure 34B suggest that restoration of Cdc25A expression alone is not sufficient to restore S-phase progression in iNOS-expressing cells.

5.2.3 Neither Cdc25A, C431S-Cdc25A, nor Cdk2AF altered the induction, duration, or recovery from S-phase arrest in response to SNCEE

It is possible that Cdc25A expression accelerates recovery from S-phase checkpoint rather than restores DNA synthesis. Also, Cdc25A activity is attenuated by RSNOs *in vitro*, and RSNOs are generated by iNOS-derived •NO in cells (209). Therefore it is possible that Cdc25A expression alone is not able to activate Cdk2 because RNS inactivate Cdc25A phosphatase activity. To test these hypotheses, I expressed Cdc25A, catalytically inactive Cdc25A (C431S), or a Cdk2 Thr14Ala/Tyr15Phe mutant that cannot be phosphorylated at Thr14/Tyr15 and is thus active independent of Cdc25A (Cdk2AF) and monitored the kinetics of S-phase checkpoint initiation, duration, and recovery following SNCEE treatment. As shown in Figure 35, expression of Cdc25A, C431S, or Cdk2AF had no significant effect on induction of S-phase arrest, duration of arrest, or recovery from arrest. These results indicate that while Cdk2 activity (and thus Cdc25A

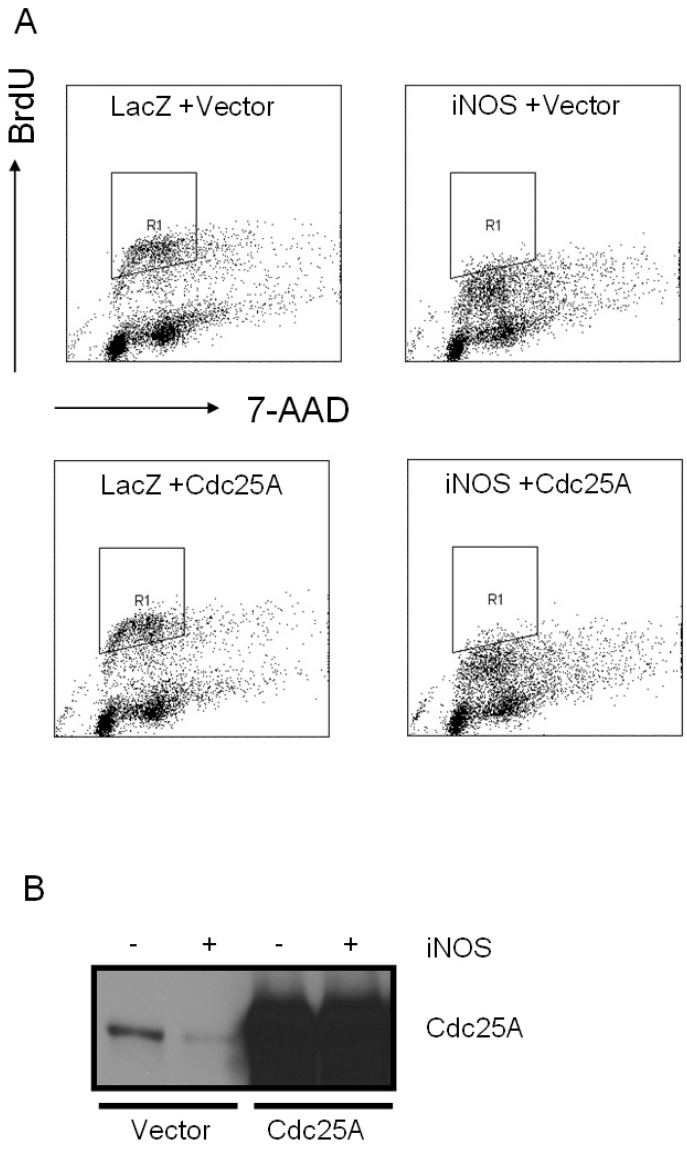

Figure 34. Cdc25A expression did not restore DNA synthesis in iNOS-expressing cells.

A, HCT116 cells were transfected with vectors encoding HA-Cdc25A and replated at low density. The following day, cells were infected with adenoviruses encoding LacZ or iNOS, incubated for 24 hours, and labeled with 10 μM BrdU for 30 minutes before harvesting for flow cytometry. *B*, HCT116 cells were transfected and infected as above, and incubated for 24 hours before harvesting for Western blotting.

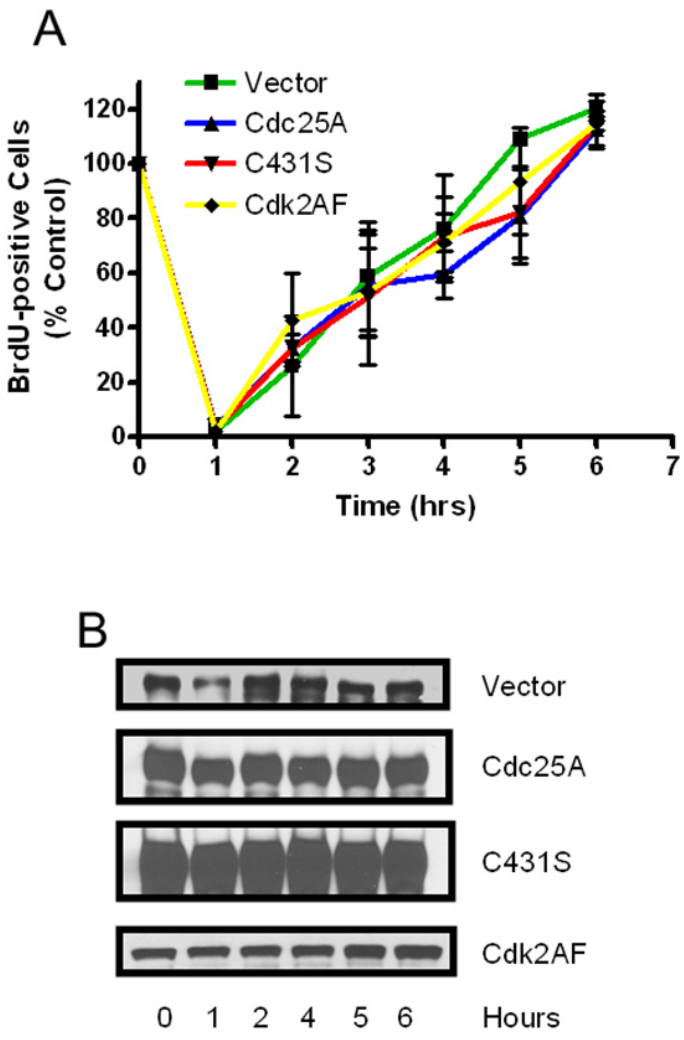

Figure 35. Expression of Cdc25A, C431S-Cdc25A, or Cdk2AF failed to alter the kinetics of SNCEE-mediated inhibition of DNA synthesis.

A, HCT116 cells were transfected with vectors encoding the indicated proteins (or empty vector). After 24 hours, cells were treated with 100 μM SNCEE, and labeled with 10 μM BrdU for 30 minutes before harvesting at the indicated times post-SNCEE treatment. Error bars = SEM, N=3. *B*, Duplicate plates were transfected and treated with SNCEE as in *A*, and harvested for Western blotting at the indicated times. Vector, Cdc25A, and C431S display blots for Cdc25A protein, whereas Cdk2AF displays a blot for Cdk2 protein.

activity) may be required for recovery from S-phase checkpoint, they are not sufficient to restore DNA synthesis in nitrosatively-stressed cells.

5.2.4 Cdk2 was not directly inhibited by SNCEE

An alternative explanation for the inability of Cdk2AF to restore DNA synthesis would be that SNCEE may directly inhibit Cdk2 activity. I determined whether SNCEE inhibited Cdk2/cyclin A kinase activity *in vitro*. I treated Cdk2 with the Cdk inhibitor roscovitine or with increasing concentrations of SNCEE, and measured the ability of Cdk2 to incorporate ^{33}P from ATP into recombinant human Histone H1.2 (Figure 36). In the absence of Cdk2, no significant incorporation of ^{33}P into Histone H1.2 was observed. Cdk2 in the presence of CEE resulted in rapid incorporation of ^{33}P into Histone H1.2, which could be inhibited nearly completely with 100 μM roscovitine. However, increasing concentrations of SNCEE had no significant effect on Cdk2 kinase activity ($p > 0.10$). This indicated that SNCEE did not interfere with Cdk2 kinase activity.

Collectively, these data indicate that iNOS-derived •NO or nitrosative stress induced by SNCEE inhibited DNA synthesis in a transient fashion. Although Cdc25A levels were decreased with kinetics consistent with a role for Cdc25A in S-phase inhibition and recovery, increasing Cdc25A levels/activity via Cdc25A overexpression or Cdk2AF expression was not sufficient to bypass DNA synthesis inhibition nor to change the kinetics or recovery from DNA synthesis inhibition in response to •NO/RNS.

5.2.5 SNCEE decoupled Cdc25A from ASK-1 and activated the downstream target of ASK-1 signaling p38

Because Cdc25A did not appear limiting for cell cycle progression following nitrosative insult, I investigated other potential effects of Cdc25A suppression following nitrosative stress. I and others have found that Cdc25A interacts with ASK-1 (Figure 37) (103). Cdc25A inhibits

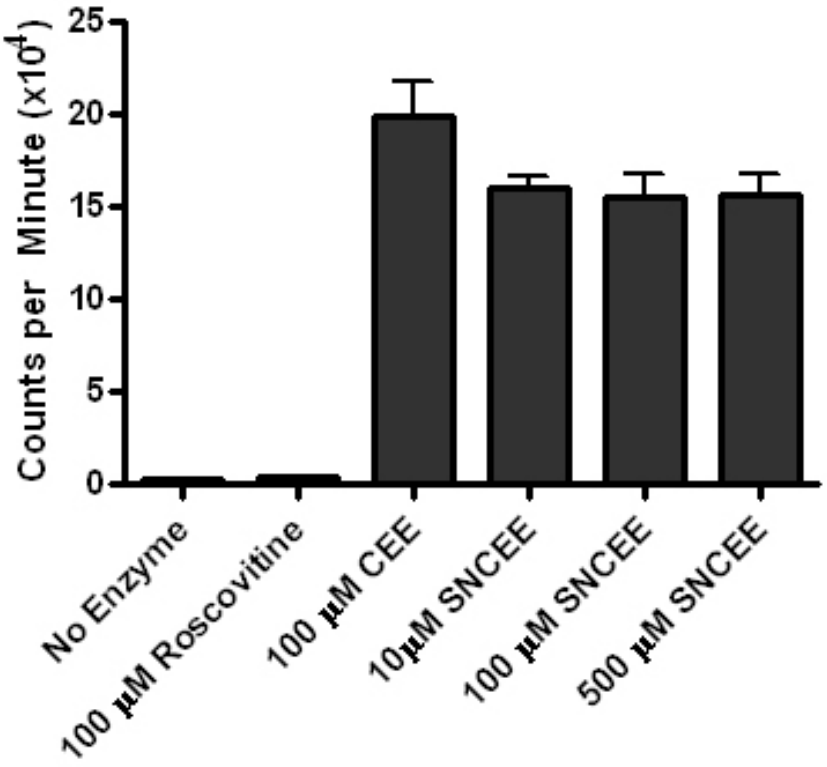

Figure 36. SNCEE did not significantly inhibit Cdk2 activity *in vitro*.

Cdk2/cyclin A was treated with the indicated compounds before its ability to incorporate ^{33}P from [^{33}P]-ATP into Histone H1.2 was evaluated. Error bars = SEM, N = 4.

ASK-1, and overexpression of Cdc25A protects cells from oxidiative stress-induced apoptosis by preventing the activation of kinases downstream from ASK-1, such as p38 (103). Thus, I hypothesized that Cdc25A protein modification (Figure 16) or suppression (Figure 21) by

nitrosative stress would sensitize cells to apoptotic stimuli by decreasing its association with ASK-1. I expressed Cdc25A and HA-tagged ASK-1 (HA-ASK-1) in HCT116 cells and measured the effect of SNCEE-induced nitrosative stress on Cdc25A-ASK-1 interaction by co-immunoprecipitation (Figure 37). SNCEE decreased the amount of Cdc25A associated with ASK-1 at two hours, consistent with Cdc25A loss following SNCEE (Figure 21*B*). As dissociation of Cdc25A would be anticipated to promote ASK-1 activation, I asked whether the ASK-1 pathway was activated in response to SNCEE. I treated HCT116 cells with 100 μM SNCEE, and measured the activation of the ASK-1-downstream kinase p38 using phosphospecific antibodies (Figure 38). SNCEE induced a time-dependent activation of p38 that trailed accumulation of RSNOs (Figure 19*A*) and roughly coincided with loss of Cdc25A protein (Figure 21*B*).

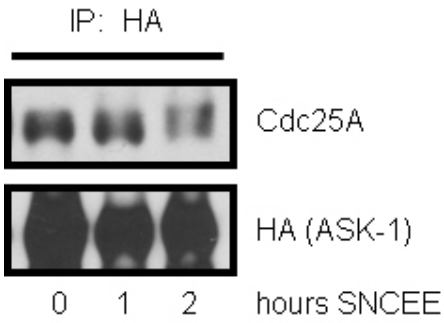

Figure 37. SNCEE decreased the Cdc25A-associated fraction of ASK-1.

HCT116 cells were transfected with vectors encoding untagged Cdc25A and HA-tagged ASK-1. Twenty-four hours later, cells were treated with 100 μM SNCEE. At the indicated times, ASK-1-associated proteins were coimmunoprecipitated as described in *Experimental Methods* section 2.5 and subjected to Western blotting with the for Cdc25A and HA-ASK-1. N=3.

5.2.6 SNCEE sensitized cells to ASK-1-dependent apoptosis

cis-Diaminedichloroplatinum(II) (CDDP) induces apoptosis through the ASK-1 pathway (104). We treated cells with 10 μM CDDP after pretreatment with 100 μM of either decomposed SNCEE or fresh SNCEE and measured apoptosis after 48 hours (Figure 39*A*). SNCEE alone did not affect basal nuclear fragmentation frequency compared to decomposed SNCEE (2.08% ± 0.51 vs. 1.58% ± 0.31, Figure 39*A*), and pretreatment of cells with SNCEE increased apoptosis two-fold (13.83% ± 1.37) following CDDP compared to decomposed SNCEE-pretreated cells (7.00% ± 0.87). Similarly, SNCEE pretreatment before 10 μM CDDP induced cleavage of PARP and procaspase-3 as evidenced by accumulation of cleaved PARP and p17/p20 caspase-3 subunits (Figure 39*B*) whereas decomposed SNCEE and CDDP cotreatment did not. Together, these results indicate that nitrosative stress sensitized cells to ASK-1-dependent apoptotic cell death, consistent with an inhibitory role for Cdc25A in ASK-1-mediated apoptosis.

5.3 DISCUSSION

A recurrent paradigm in Cdc25A biology has been that in response to cellular stress Cdc25A is rapidly targeted for proteasomal degradation, resulting in the inhibitory hyperphosphorylation of Cdk2, thus initiating cell cycle arrest. Although in response to •NO Cdk2 is inhibited and DNA synthesis is halted (226, 227), our findings herein draw into question the ubiquity of the established model of intra-S-phase checkpoint. Activation of origins of DNA replication is dependent upon the activity of Cdk2 and Cdc7 kinases, which are the targets of the ATM- and

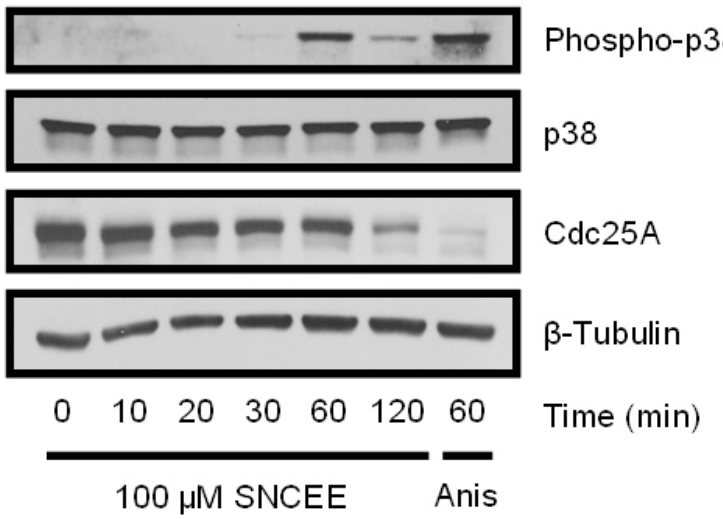

Figure 38. SNCEE activated p38 kinase.

HCT116 cells were treated with 100 μM SNCEE or with 200 ng/mL anisomycin (Anis) for the indicated times before harvesting and Western blotting for the indicated proteins.

ATR-dependent DNA replication checkpoints, respectively (105, 267). Numerous studies have reported that aberrant Cdk2 activation either by Cdc25A overexpression or Cdk2AF expression is sufficient to bypass the ATM-mediated intra-S-phase checkpoint in response to damaged DNA (71, 74, 105). Conversely, in the ATR-dependent replication checkpoint, Cdk2AF has no effect on DNA synthesis (267). The unaltered half-life of Cdc25A in response to SNCEE (Figure 23) and failure of caffeine (which inhibits both ATM and ATR kinases) to suppress Cdc25A loss (Figure 24) suggests that the canonical ATR/ATM-mediated intra-S-phase checkpoint pathway is not activated in response to •NO/nitrosative stress, and the failure of Cdc25A overexpression or Cdk2AF expression to reinitiate DNA synthesis (the so-called "RDS" phenotype) supports the hypothesis that •NO/nitrosative stress inhibits DNA synthesis via novel mechanism(s). Overexpression of Cdc25A did not accelerate recovery from DNA synthesis inhibition. This does not, however, mean that Cdc25A expression or activity is not required for recovery from

DNA synthesis inhibition. It is possible that a threshold concentration of Cdc25A is necessary for the reinitiation of DNA synthesis, and suprathreshold Cdc25A levels do not contribute additionally. This would be in contrast to that reported for Cdc25B, in which overexpression was able to accelerate recovery from the G_2 checkpoint after DNA damage (87).

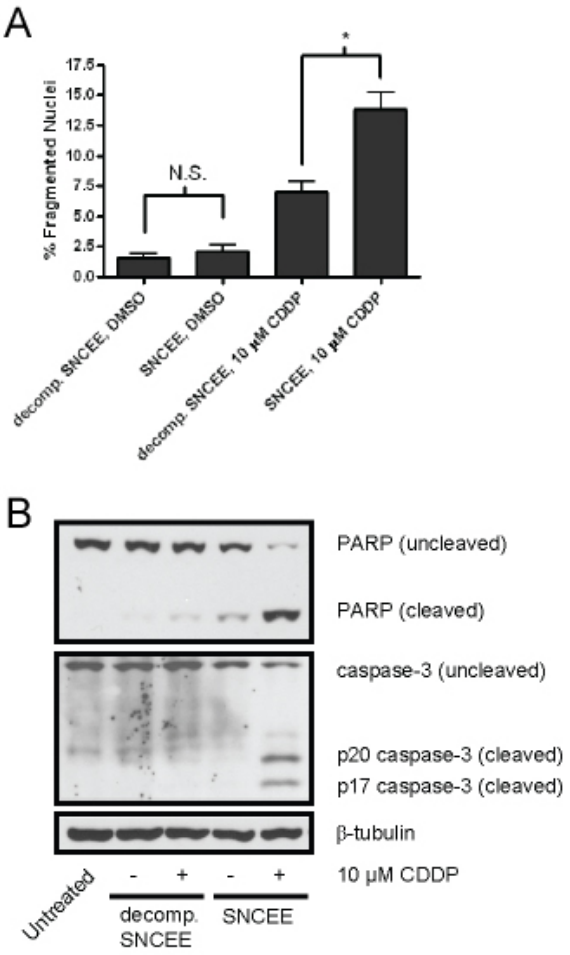

Figure 39. SNCEE sensitized cells to cisplatin.

A, HCT116 cells were treated with 100 μM of decomposed or fresh SNCEE. One hour later, cells were treated with DMSO or with 10 μM cisplatin (CDDP). Cells were fixed 48 hours later, and nuclei were stained with 1 μg/mL Hoechst 33342, and fragmented nuclei were counted by fluorescence microscopy at 20X magnification. Results are expressed as means ± SEM of four experiments in which three fields of view per sample were counted. N.S., not significant; *, $p < 0.001$. *B*, HCT116 cells were untreated or treated as described in *A*, and harvested for Western blotting with the indicated antibodies 24 hours later. N=2.

Whereas Cdc25A bypasses the intra-S-phase checkpoint in response to IR (71), it has previously been reported that Cdc25A$^{+/-}$ MEFs (which produce about half as much Cdc25A protein as wild-type MEFs) display difficulty recovering from IR-induced G_2 checkpoint, implying that Cdc25A protein levels are limiting (89).

It should be recognized that DNA replication was not totally inhibited in response to •NO/RNS, as evidenced by some BrdU incorporation in iNOS-expressing and SNCEE-treated S-phase cells compared to hydroxyurea-treated cells, which incorporated no BrdU (data not shown). This implies either that DNA is being synthesized from a reduced number of origins of replication within a cell (268), or that synthesis from existing origins is slowed. Further studies will be necessary to distinguish between these two possibilities. In support of the former hypothesis is precedent from viral replication systems of redox-sensitive replication factors (269). The bovine papillomavirus type 1 E2 protein contains a reactive cysteine that is sensitive to oxidation or chemical modification-induced inhibition of origin binding and is flanked by a basic lysine residue, reminiscent of the acid-base motif which is predictive of *S*-nitros(yl)ation sites (270). If a similar redox-sensitivity of the human replication complex exists, nitrosative stress could be expected to disrupt replication complex function. Whether mammalian replication complex proteins are sensitive to redox stimuli is not currently known.

In support of the "slowed synthesis" hypothesis are reports that •NO/RNS can inhibit RR (166, 167, 169). Depletion of intracellular ribonucleotide stores would slow DNA synthesis by depleting the raw materials. Although this is an attractive justification for decreased DNA synthesis in nitrosatively-challenged cells, multiple reports have demonstrated that repletion of cellular deoxyribonucleotides to bypass the requirement for RR activity results in a mediocre

restoration of DNA synthesis at best (166, 167, 221). Additionally, nucleotide depletion would be expected to activate ATR and accelerate Cdc25A degradation as is observed upon treatment of cells with hydroxyurea (79), which was not observed in response to SNCEE. Thus, RR inhibition may contribute to •NO/nitrosative inhibition of DNA synthesis, but is probably not the only culprit.

How does •NO/nitrosative stress inhibit DNA synthesis without activating ATM/ATR? Activation of ATM has been reported in response to RNS that act as nitrating agents (229), implying that the checkpoint pathway can respond to at least some types of RNS. Failure of •NO/nitrosative stress to activate the ATM/ATR pathways suggests either that aberrant replication structures are not being formed, are not being recognized, or are not transmitting these signals to the cell cycle machinery (ie, Cdc25A). The single-stranded DNA-binding protein replication protein A (RPA) is regulated by oxidation/reduction of a key cysteine residue that upon oxidation prevents RPA binding to ssDNA (271). Binding of ssDNA-associated RPA by the ATR/ATRIP complex (see Figure 6) appears to be required at least under some circumstances for ATR activation (272). Thus, post-translational modification of RPA may result in failed sensing of stalled or malformed replication forks generated by nitrosative stress, and result in subsequent failure to activate ATR. Our characterization of SNCEE-treated cells indicated that thiols were depleted, which means that intracellular oxidative stress was occurring to some degree. Intriguingly, it has been reported that pretreatment of cells with the LMM thiols *N*-acetylcysteine or GSH before exposure to •NO prevents DNA synthesis inhibition, suggesting a potential redox sensitive component of the DNA replication machinery (273).

In some cases, high levels of •NO confer a growth advantage to tumors (231, 233). However, *in vitro* studies consistently suggest that •NO inhibits progression through the cell

cycle. The growth advantage conveyed to some tumors by •NO may not necessarily be mediated by enhanced cell division; •NO has been reported to increase the vascularity (and thus presumably the blood supply and nutrient delivery) of tumors (228, 231). This may result in a greater average cell division rate in the •NO-exposed tumor because it is "well-fed" when compared to the undervascularized tumor. Also, the size of a tumor is determined by the equilibrium struck between cell division and cell death. As •NO inhibits apoptosis in some models (211, 212) the spontaneous death rate may be decreased in •NO-exposed tumors sufficiently to result in larger net tumors. Regardless, Cdc25A overexpression did not appear to convey a selective growth advantage to nitrosatively-challenged tumor cells, indicating that other mechanisms are involved.

We found that pretreatment of cells with SNCEE decreased Cdc25A protein levels (Figure 21) and sensitized cells to cisplatin (Figure 39), which causes apoptosis via ASK-1 activation (104). We also observed activation of the ASK-1 target kinase p38 following SNCEE coincident with Cdc25A loss, and found that SNCEE decreased Cdc25A association with cellular ASK-1. Together, these data implicate nitrosative stress-induced loss of Cdc25A as a potential chemosensitizer by promoting activation of ASK-1. Previous studies have shown that Cdc25A overexpression can protect against insults to the redox status of the cell via inhibition of ASK-1 (103); therefore it is logical to consider that loss of Cdc25A expression due to nitrosative insult may sensitize cells to stimuli that perturb either the cellular redox state or to agents that induce apoptosis through ASK-1 activation. Further studies will address this hypothesis.

In summary, iNOS-derived •NO or SNCEE decreased DNA synthesis in HCT116 cells, but did not abrogate it entirely. Although Cdc25A expression was reduced in nitrosatively-challenged cells, neither Cdc25A protein levels nor Cdk2 activity was limiting for DNA

synthesis following nitrosative stress. Additionally, we found that Cdc25A is decreased in nitrosatively-stressed cells, and that activation of the p38 kinase coincides with Cdc25A loss. Also, Cdc25A interacted with ASK-1, and SNCEE treatment decoupled Cdc25A from ASK-1 sensitized cells to apoptosis in response to cisplatin. Thus loss of Cdc25A in response to nitrosative stimuli may lower the apoptotic threshold for cells. Together, these data distinguish DNA synthesis inhibition in response to nitrosative insult with that triggered by the intra-S-phase checkpoint, and indicate that nitrosative stress-induced suppression of Cdc25A may alter the cellular survival balance in response to genotoxic stimuli.

6.0 CONCLUSION

Nitrosative insult rapidly inhibited Cdc25A enzymatic activity in a fashion that was reversible by reductants. In cells, induction of nitrosative stress either by iNOS-mediated •NO overproduction or by the chemical nitrosant SNCEE decreased Cdc25A protein levels in multiple human tumor cell lines. Suppression of Cdc25A following nitrosative stress was mediated by hyper-phosphorylation and inhibition of eIF2α, resulting in translational suppression of Cdc25A. Suppression of Cdc25A was accompanied by inhibition of DNA synthesis in nitrosatively-challenged cells. Although Cdc25A is required for progression through S-phase, reintroduction of Cdc25A expression or activity (via Cdk2AF) was not sufficient to restore DNA synthesis or change the kinetics of the onset or recovery of inhibition, thus distinguishing inhibition of DNA synthesis by nitrosative stress from the intra-S-phase checkpoint. Activation of ASK-1 target kinase p38 was observed in response to SNCEE with kinetics consistent with loss of Cdc25A, and ASK-1 interacted with Cdc25A under basal conditions. SNCEE decoupled ASK-1 from Cdc25A, and pretreatment of cells with SNCEE doubled apoptosis in response to CDDP, providing evidence that suppression of Cdc25A in response to nitrosative stress lowers the apoptotic threshold of cells for genotoxic stimuli. Nitrosative insult of differing intensities or durations therefore may provide the cell with the opportunity to selectively regulate phosphatase-dependent vs. independent Cdc25A activities, and thus the Cdc25A-dependent cellular consequences.

APPENDIX A

ANTIBODIES FOR WESTERN BLOTTING

Antigen	Antibody species	Dilution	Vendor
Caspase-3	rabbit	1:1000	Assay Designs
Cdc25A (F-6)	mouse	1:100	Santa Cruz Biotechnology
Cdc25B	mouse	1:2500	BD Pharmingen
Cdc25C	rabbit	1:1000	Santa Cruz Biotechnology
Cdk1	mouse	1:500	Santa Cruz Biotechnology
Phospho-Cdk1^{Tyr15}	rabbit	1:1000	Cell Signaling Technology
Cdk2	rabbit	1:5000	Santa Cruz Biotechnology
Chk2	mouse	1:200	Santa Cruz Biotechnology
Cyclin D_1	mouse	1:500	BD Pharmingen
eIF2α	rabbit	1:1000	Cell Signaling Technology
Phospho-eIF2α^{Ser51}	rabbit	1:1000	Cell Signaling Technology
GAPDH	rabbit	1:1000	Cell Signaling Technology
HA	mouse	1:1000	Covance Research Products, Inc.
iNOS	mouse	1:2500	BD Pharmingen
c-Myc	mouse	1:100	Santa Cruz Biotechnology
Nitrotyrosine	rabbit	1:100	Cayman Chemical
p21	rabbit	1:500	Calbiochem
p53	rabbit	1:1000	Cell Signaling Technology
PARP	rabbit	1:1000	Cell Signaling Technology
β-Tubulin	mouse	1:20,000	Cedarlane Laboratories

BIBLIOGRAPHY

1. Sherr CJ, Roberts JM. CDK inhibitors: positive and negative regulators of G1-phase progression. Genes Dev 1999;13:1501-12.
2. Chu IM, Hengst L, Slingerland JM. The Cdk inhibitor p27 in human cancer: prognostic potential and relevance to anticancer therapy. Nat Rev Cancer 2008;8:253-67.
3. Parker LL, Atherton-Fessler S, Lee MS, *et al.* Cyclin promotes the tyrosine phosphorylation of p34cdc2 in a wee1+ dependent manner. EMBO J 1991;10:1255-63.
4. McGowan CH, Russell P. Human Wee1 kinase inhibits cell division by phosphorylating p34cdc2 exclusively on Tyr15. EMBO J 1993;12:75-85.
5. Parker LL, Atherton-Fessler S, Piwnica-Worms H. p107wee1 is a dual-specificity kinase that phosphorylates p34cdc2 on tyrosine 15. Proc Natl Acad Sci U S A 1992;89:2917-21.
6. Liu F, Stanton JJ, Wu Z, Piwnica-Worms H. The human Myt1 kinase preferentially phosphorylates Cdc2 on threonine 14 and localizes to the endoplasmic reticulum and Golgi complex. Mol Cell Biol 1997;17:571-83.
7. Fesquet D, Labbe JC, Derancourt J, *et al.* The MO15 gene encodes the catalytic subunit of a protein kinase that activates cdc2 and other cyclin-dependent kinases (CDKs) through phosphorylation of Thr161 and its homologues. EMBO J 1993;12:3111-21.

8. Aprelikova O, Xiong Y, Liu ET. Both p16 and p21 families of cyclin-dependent kinase (CDK) inhibitors block the phosphorylation of cyclin-dependent kinases by the CDK-activating kinase. J Biol Chem 1995;270:18195-7.

9. Fantes P. Epistatic gene interactions in the control of division in fission yeast. Nature 1979;279:428-30.

10. Russell P, Nurse P. cdc25+ functions as an inducer in the mitotic control of fission yeast. Cell 1986;45:145-53.

11. Nurse P. Genetic control of cell size at cell division in yeast. Nature 1975;256:547-51.

12. Nurse P, Thuriaux P. Regulatory genes controlling mitosis in the fission yeast Schizosaccharomyces pombe. Genetics 1980;96:627-37.

13. Russell P, Nurse P. Negative regulation of mitosis by wee1+, a gene encoding a protein kinase homolog. Cell 1987;49:559-67.

14. Fantes PA. Isolation of cell size mutants of a fission yeast by a new selective method: characterization of mutants and implications for division control mechanisms. J Bacteriol 1981;146:746-54.

15. Moreno S, Nurse P, Russell P. Regulation of mitosis by cyclic accumulation of p80cdc25 mitotic inducer in fission yeast. Nature 1990;344:549-52.

16. Moreno S, Hayles J, Nurse P. Regulation of p34cdc2 protein kinase during mitosis. Cell 1989;58:361-72.

17. Gould KL, Nurse P. Tyrosine phosphorylation of the fission yeast cdc2+ protein kinase regulates entry into mitosis. Nature 1989;342:39-45.

18. Gould KL, Moreno S, Tonks NK, Nurse P. Complementation of the mitotic activator, p80cdc25, by a human protein-tyrosine phosphatase. Science 1990;250:1573-6.

19. Strausfeld U, Labbe JC, Fesquet D*, et al.* Dephosphorylation and activation of a p34cdc2/cyclin B complex in vitro by human CDC25 protein. Nature 1991;351:242-5.

20. Dunphy WG, Kumagai A. The cdc25 protein contains an intrinsic phosphatase activity. Cell 1991;67:189-96.

21. Gautier J, Solomon MJ, Booher RN, Bazan JF, Kirschner MW. cdc25 is a specific tyrosine phosphatase that directly activates p34cdc2. Cell 1991;67:197-211.

22. Kumagai A, Dunphy WG. The cdc25 protein controls tyrosine dephosphorylation of the cdc2 protein in a cell-free system. Cell 1991;64:903-14.

23. Sadhu K, Reed SI, Richardson H, Russell P. Human homolog of fission yeast cdc25 mitotic inducer is predominantly expressed in G2. Proc Natl Acad Sci U S A 1990;87:5139-43.

24. Galaktionov K, Beach D. Specific activation of cdc25 tyrosine phosphatases by B-type cyclins: evidence for multiple roles of mitotic cyclins. Cell 1991;67:1181-94.

25. Demetrick DJ, Beach DH. Chromosome mapping of human CDC25A and CDC25B phosphatases. Genomics 1993;18:144-7.

26. Lane SA, Baker E, Sutherland GR, Tonks I, Hayward N, Ellem K. The human cell cycle gene CDC25B is located at 20p13. Genomics 1993;15:693-4.

27. Taviaux SA, Demaille JG. Localization of human cell cycle regulatory genes CDC25C to 5q31 and WEE1 to 11p15.3-11p15.1 by fluorescence in situ hybridization. Genomics 1993;15:194-6.

28. Wegener S, Hampe W, Herrmann D, Schaller HC. Alternative splicing in the regulatory region of the human phosphatases CDC25A and CDC25C. Eur J Cell Biol 2000;79:810-5.

29. Baldin V, Cans C, Superti-Furga G, Ducommun B. Alternative splicing of the human CDC25B tyrosine phosphatase. Possible implications for growth control? Oncogene 1997;14:2485-95.

30. Lyon MA, Ducruet AP, Wipf P, Lazo JS. Dual-specificity phosphatases as targets for antineoplastic agents. Nat Rev Drug Discov 2002;1:961-76.

31. Kallstrom H, Lindqvist A, Pospisil V, Lundgren A, Rosenthal CK. Cdc25A localisation and shuttling: characterisation of sequences mediating nuclear export and import. Exp Cell Res 2005;303:89-100.

32. Davezac N, Baldin V, Gabrielli B*, et al.* Regulation of CDC25B phosphatases subcellular localization. Oncogene 2000;19:2179-85.

33. Uchida S, Ohtsubo M, Shimura M*, et al.* Nuclear export signal in CDC25B. Biochem Biophys Res Commun 2004;316:226-32.

34. Graves PR, Lovly CM, Uy GL, Piwnica-Worms H. Localization of human Cdc25C is regulated both by nuclear export and 14-3-3 protein binding. Oncogene 2001;20:1839-51.

35. Peng CY, Graves PR, Thoma RS, Wu Z, Shaw AS, Piwnica-Worms H. Mitotic and G2 checkpoint control: regulation of 14-3-3 protein binding by phosphorylation of Cdc25C on serine-216. Science 1997;277:1501-5.

36. Aitken A. 14-3-3 proteins: a historic overview. Semin Cancer Biol 2006;16:162-72.

37. Chen MS, Ryan CE, Piwnica-Worms H. Chk1 kinase negatively regulates mitotic function of Cdc25A phosphatase through 14-3-3 binding. Mol Cell Biol 2003;23:7488-97.

38. Mils V, Baldin V, Goubin F*, et al.* Specific interaction between 14-3-3 isoforms and the human CDC25B phosphatase. Oncogene 2000;19:1257-65.

39. Bulavin DV, Higashimoto Y, Popoff IJ, *et al.* Initiation of a G2/M checkpoint after ultraviolet radiation requires p38 kinase. Nature 2001;411:102-7.

40. Reynolds RA, Yem AW, Wolfe CL, Deibel MR, Jr., Chidester CG, Watenpaugh KD. Crystal structure of the catalytic subunit of Cdc25B required for G2/M phase transition of the cell cycle. J Mol Biol 1999;293:559-68.

41. Buhrman G, Parker B, Sohn J, Rudolph J, Mattos C. Structural mechanism of oxidative regulation of the phosphatase Cdc25B via an intramolecular disulfide bond. Biochemistry 2005;44:5307-16.

42. Fauman EB, Cogswell JP, Lovejoy B, *et al.* Crystal structure of the catalytic domain of the human cell cycle control phosphatase, Cdc25A. Cell 1998;93:617-25.

43. Rudolph J. Catalytic mechanism of Cdc25. Biochemistry 2002;41:14613-23.

44. Chen W, Wilborn M, Rudolph J. Dual-specific Cdc25B phosphatase: in search of the catalytic acid. Biochemistry 2000;39:10781-9.

45. Terada Y, Tatsuka M, Jinno S, Okayama H. Requirement for tyrosine phosphorylation of Cdk4 in G1 arrest induced by ultraviolet irradiation. Nature 1995;376:358-62.

46. Blomberg I, Hoffmann I. Ectopic expression of Cdc25A accelerates the G(1)/S transition and leads to premature activation of cyclin E- and cyclin A-dependent kinases. Mol Cell Biol 1999;19:6183-94.

47. Sexl V, Diehl JA, Sherr CJ, Ashmun R, Beach D, Roussel MF. A rate limiting function of cdc25A for S phase entry inversely correlates with tyrosine dephosphorylation of Cdk2. Oncogene 1999;18:573-82.

48. Hoffmann I, Draetta G, Karsenti E. Activation of the phosphatase activity of human cdc25A by a cdk2-cyclin E dependent phosphorylation at the G1/S transition. EMBO J 1994;13:4302-10.

49. Jinno S, Suto K, Nagata A*, et al.* Cdc25A is a novel phosphatase functioning early in the cell cycle. EMBO J 1994;13:1549-56.

50. Sebastian B, Kakizuka A, Hunter T. Cdc25M2 activation of cyclin-dependent kinases by dephosphorylation of threonine-14 and tyrosine-15. Proc Natl Acad Sci U S A 1993;90:3521-4.

51. Lammer C, Wagerer S, Saffrich R, Mertens D, Ansorge W, Hoffmann I. The cdc25B phosphatase is essential for the G2/M phase transition in human cells. J Cell Sci 1998;111:2445-53.

52. Garner-Hamrick PA, Fisher C. Antisense phosphorothioate oligonucleotides specifically down-regulate cdc25B causing S-phase delay and persistent antiproliferative effects. Int J Cancer 1998;76:720-8.

53. Turowski P, Franckhauser C, Morris MC, Vaglio P, Fernandez A, Lamb NJ. Functional cdc25C dual-specificity phosphatase is required for S-phase entry in human cells. Mol Biol Cell 2003;14:2984-98.

54. Chen MS, Hurov J, White LS, Woodford-Thomas T, Piwnica-Worms H. Absence of apparent phenotype in mice lacking Cdc25C protein phosphatase. Mol Cell Biol 2001;21:3853-61.

55. Ferguson AM, White LS, Donovan PJ, Piwnica-Worms H. Normal cell cycle and checkpoint responses in mice and cells lacking Cdc25B and Cdc25C protein phosphatases. Mol Cell Biol 2005;25:2853-60.

56. Lincoln AJ, Wickramasinghe D, Stein P*, et al.* Cdc25b phosphatase is required for resumption of meiosis during oocyte maturation. Nat Genet 2002;30:446-9.

57. Mailand N, Podtelejnikov AV, Groth A, Mann M, Bartek J, Lukas J. Regulation of G(2)/M events by Cdc25A through phosphorylation-dependent modulation of its stability. EMBO J 2002;21:5911-20.

58. Karlsson C, Katich S, Hagting A, Hoffmann I, Pines J. Cdc25B and Cdc25C differ markedly in their properties as initiators of mitosis. J Cell Biol 1999;146:573-84.

59. Lindqvist A, Kallstrom H, Lundgren A, Barsoum E, Rosenthal CK. Cdc25B cooperates with Cdc25A to induce mitosis but has a unique role in activating cyclin B1-Cdk1 at the centrosome. J Cell Biol 2005;171:35-45.

60. Bailly E, Doree M, Nurse P, Bornens M. p34cdc2 is located in both nucleus and cytoplasm; part is centrosomally associated at G2/M and enters vesicles at anaphase. EMBO J 1989;8:3985-95.

61. Bailly E, Pines J, Hunter T, Bornens M. Cytoplasmic accumulation of cyclin B1 in human cells: association with a detergent-resistant compartment and with the centrosome. J Cell Sci 1992;101:529-45.

62. Jackman M, Lindon C, Nigg EA, Pines J. Active cyclin B1-Cdk1 first appears on centrosomes in prophase. Nat Cell Biol 2003;5:143-8.

63. Hoffmann I, Clarke PR, Marcote MJ, Karsenti E, Draetta G. Phosphorylation and activation of human cdc25-C by cdc2--cyclin B and its involvement in the self-amplification of MPF at mitosis. EMBO J 1993;12:53-63.

64. Gabrielli BG, De Souza CP, Tonks ID, Clark JM, Hayward NK, Ellem KA. Cytoplasmic accumulation of cdc25B phosphatase in mitosis triggers centrosomal microtubule nucleation in HeLa cells. J Cell Sci 1996;109:1081-93.

65. Millar JB, Blevitt J, Gerace L, Sadhu K, Featherstone C, Russell P. p55CDC25 is a nuclear protein required for the initiation of mitosis in human cells. Proc Natl Acad Sci U S A 1991;88:10500-4.

66. Boutros R, Lobjois V, Ducommun B. CDC25B involvement in the centrosome duplication cycle and in microtubule nucleation. Cancer Res 2007;67:11557-64.

67. Cazales M, Boutros R, Brezak MC, Chaumeron S, Prevost G, Ducommun B. Pharmacologic inhibition of CDC25 phosphatases impairs interphase microtubule dynamics and mitotic spindle assembly. Mol Cancer Ther 2007;6:318-25.

68. Noll A, Ruppenthal SL, Montenarh M. The mitotic phosphatase cdc25C at the Golgi apparatus. Biochem Biophys Res Commun 2006;351:825-30.

69. Busch C, Barton O, Morgenstern E*, et al.* The G2/M checkpoint phosphatase cdc25C is located within centrosomes. Int J Biochem Cell Biol 2007;39:1707-13.

70. Errol C. Friedberg GCW, Wolfram Siede, Richard D. Wood, Roger A. Schultz, Tom Ellenberger. DNA Repair and Mutagenesis. 2 ed. Washington, D.C.: ASM Press; 2006.

71. Falck J, Mailand N, Syljuasen RG, Bartek J, Lukas J. The ATM-Chk2-Cdc25A checkpoint pathway guards against radioresistant DNA synthesis. Nature 2001;410:842-7.

72. Mailand N, Falck J, Lukas C*, et al.* Rapid destruction of human Cdc25A in response to DNA damage. Science 2000;288:1425-9.

73. Reinhardt HC, Aslanian AS, Lees JA, Yaffe MB. p53-deficient cells rely on ATM- and ATR-mediated checkpoint signaling through the p38MAPK/MK2 pathway for survival after DNA damage. Cancer Cell 2007;11:175-89.

74. Sorensen CS, Syljuasen RG, Falck J*, et al.* Chk1 regulates the S phase checkpoint by coupling the physiological turnover and ionizing radiation-induced accelerated proteolysis of Cdc25A. Cancer Cell 2003;3:247-58.

75. Manke IA, Nguyen A, Lim D, Stewart MQ, Elia AE, Yaffe MB. MAPKAP kinase-2 is a cell cycle checkpoint kinase that regulates the G2/M transition and S phase progression in response to UV irradiation. Mol Cell 2005;17:37-48.

76. Kang T, Wei Y, Honaker Y*, et al.* GSK-3 beta targets Cdc25A for ubiquitin-mediated proteolysis, and GSK-3 beta inactivation correlates with Cdc25A overproduction in human cancers. Cancer Cell 2008;13:36-47.

77. Jin J, Shirogane T, Xu L*, et al.* SCFbeta-TRCP links Chk1 signaling to degradation of the Cdc25A protein phosphatase. Genes Dev 2003;17:3062-74.

78. Busino L, Donzelli M, Chiesa M*, et al.* Degradation of Cdc25A by beta-TrCP during S phase and in response to DNA damage. Nature 2003;426:87-91.

79. Molinari M, Mercurio C, Dominguez J, Goubin F, Draetta GF. Human Cdc25 A inactivation in response to S phase inhibition and its role in preventing premature mitosis. EMBO Rep 2000;1:71-9.

80. Chow JP, Siu WY, Fung TK*, et al.* DNA damage during the spindle-assembly checkpoint degrades CDC25A, inhibits cyclin-CDC2 complexes, and reverses cells to interphase. Mol Biol Cell 2003;14:3989-4002.

81. Xiao D, Johnson CS, Trump DL, Singh SV. Proteasome-mediated degradation of cell division cycle 25C and cyclin-dependent kinase 1 in phenethyl isothiocyanate-induced G2-M-phase cell cycle arrest in PC-3 human prostate cancer cells. Mol Cancer Ther 2004;3:567-75.

82. Chen F, Zhang Z, Bower J*, et al.* Arsenite-induced Cdc25C degradation is through the KEN-box and ubiquitin-proteasome pathway. Proc Natl Acad Sci U S A 2002;99:1990-5.

83. Sancar A, Lindsey-Boltz LA, Unsal-Kacmaz K, Linn S. Molecular mechanisms of mammalian DNA repair and the DNA damage checkpoints. Annu Rev Biochem 2004;73:39-85.

84. Vigneron A, Cherier J, Barre B, Gamelin E, Coqueret O. The cell cycle inhibitor p21waf1 binds to the myc and cdc25A promoters upon DNA damage and induces transcriptional repression. J Biol Chem 2006;281:34742-50.

85. Hammer S, To KK, Yoo YG, Koshiji M, Huang LE. Hypoxic suppression of the cell cycle gene CDC25A in tumor cells. Cell Cycle 2007;6:1919-26.

86. St Clair S, Giono L, Varmeh-Ziaie S*, et al.* DNA damage-induced downregulation of Cdc25C is mediated by p53 via two independent mechanisms: one involves direct binding to the cdc25C promoter. Mol Cell 2004;16:725-36.

87. Bansal P, Lazo JS. Induction of Cdc25B regulates cell cycle resumption after genotoxic stress. Cancer Res 2007;67:3356-63.

88. van Vugt MA, Bras A, Medema RH. Polo-like kinase-1 controls recovery from a G2 DNA damage-induced arrest in mammalian cells. Mol Cell 2004;15:799-811.

89. Ray D, Terao Y, Nimbalkar D*, et al.* Hemizygous disruption of Cdc25A inhibits cellular transformation and mammary tumorigenesis in mice. Cancer Res 2007;67:6605-11.

90. Hanahan D, Weinberg RA. The hallmarks of cancer. Cell 2000;100:57-70.

91. Boutros R, Lobjois V, Ducommun B. CDC25 phosphatases in cancer cells: key players? Good targets? Nat Rev Cancer 2007;7:495-507.

92. Loffler H, Syljuasen RG, Bartkova J, Worm J, Lukas J, Bartek J. Distinct modes of deregulation of the proto-oncogenic Cdc25A phosphatase in human breast cancer cell lines. Oncogene 2003;22:8063-71.

93. Galaktionov K, Lee AK, Eckstein J, *et al.* CDC25 phosphatases as potential human oncogenes. Science 1995;269:1575-7.

94. Ray D, Terao Y, Fuhrken PG, *et al.* Deregulated CDC25A expression promotes mammary tumorigenesis with genomic instability. Cancer Res 2007;67:984-91.

95. Bartkova J, Horejsi Z, Koed K, *et al.* DNA damage response as a candidate anti-cancer barrier in early human tumorigenesis. Nature 2005;434:864-70.

96. Fuhrmann G, Leisser C, Rosenberger G, *et al.* Cdc25A phosphatase suppresses apoptosis induced by serum deprivation. Oncogene 2001;20:4542-53.

97. Galaktionov K, Chen X, Beach D. Cdc25 cell-cycle phosphatase as a target of c-myc. Nature 1996;382:511-7.

98. Macdonald K, Bennett MR. cdc25A is necessary but not sufficient for optimal c-myc-induced apoptosis and cell proliferation of vascular smooth muscle cells. Circ Res 1999;84:820-30.

99. Huang TS, Shu CH, Yang WK, Whang-Peng J. Activation of CDC 25 phosphatase and CDC 2 kinase involved in GL331-induced apoptosis. Cancer Res 1997;57:2974-8.

100. Mochizuki T, Kitanaka C, Noguchi K, Muramatsu T, Asai A, Kuchino Y. Physical and functional interactions between Pim-1 kinase and Cdc25A phosphatase. Implications for

the Pim-1-mediated activation of the c-Myc signaling pathway. J Biol Chem 1999;274:18659-66.

101. Leisser C, Rosenberger G, Maier S*, et al.* Subcellular localisation of Cdc25A determines cell fate. Cell Death Differ 2004;11:80-9.

102. Krupitza G, Grusch M, Braun K*, et al.* TNFalpha-mediated cell death is independent of cdc25A. Cell Death Differ 1998;5:758-64.

103. Zou X, Tsutsui T, Ray D*, et al.* The cell cycle-regulatory CDC25A phosphatase inhibits apoptosis signal-regulating kinase 1. Mol Cell Biol 2001;21:4818-28.

104. Chen Z, Seimiya H, Naito M*, et al.* ASK1 mediates apoptotic cell death induced by genotoxic stress. Oncogene 1999;18:173-80.

105. Costanzo V, Robertson K, Ying CY*, et al.* Reconstitution of an ATM-dependent checkpoint that inhibits chromosomal DNA replication following DNA damage. Mol Cell 2000;6:649-59.

106. Vigo E, Muller H, Prosperini E*, et al.* CDC25A phosphatase is a target of E2F and is required for efficient E2F-induced S phase. Mol Cell Biol 1999;19:6379-95.

107. Chen X, Prywes R. Serum-induced expression of the cdc25A gene by relief of E2F-mediated repression. Mol Cell Biol 1999;19:4695-702.

108. Barre B, Vigneron A, Coqueret O. The STAT3 transcription factor is a target for the Myc and riboblastoma proteins on the Cdc25A promoter. J Biol Chem 2005;280:15673-81.

109. Rother K, Kirschner R, Sanger K, Bohlig L, Mossner J, Engeland K. p53 downregulates expression of the G1/S cell cycle phosphatase Cdc25A. Oncogene 2007;26:1949-53.

110. Ducruet AP, Lazo JS. Regulation of Cdc25A half-life in interphase by cyclin-dependent kinase 2 activity. J Biol Chem 2003;278:31838-42.

111. Donzelli M, Squatrito M, Ganoth D, Hershko A, Pagano M, Draetta GF. Dual mode of degradation of Cdc25 A phosphatase. EMBO J 2002;21:4875-84.

112. Zhao H, Watkins JL, Piwnica-Worms H. Disruption of the checkpoint kinase 1/cell division cycle 25A pathway abrogates ionizing radiation-induced S and G2 checkpoints. Proc Natl Acad Sci U S A 2002;99:14795-800.

113. Nakayama KI, Nakayama K. Ubiquitin ligases: cell-cycle control and cancer. Nat Rev Cancer 2006;6:369-81.

114. Busino L, Chiesa M, Draetta GF, Donzelli M. Cdc25A phosphatase: combinatorial phosphorylation, ubiquitylation and proteolysis. Oncogene 2004;23:2050-6.

115. Esteban V, Vazquez-Novelle MD, Calvo E, Bueno A, Sacristan MP. Human Cdc14A reverses CDK1 phosphorylation of Cdc25A on serines 115 and 320. Cell Cycle 2006;5:2894-8.

116. Forman HJ, Fukuto JM, Torres M. Redox signaling: thiol chemistry defines which reactive oxygen and nitrogen species can act as second messengers. Am J Physiol Cell Physiol 2004;287:C246-56.

117. Sohn J, Rudolph J. Catalytic and chemical competence of regulation of cdc25 phosphatase by oxidation/reduction. Biochemistry 2003;42:10060-70.

118. Stefankova P, Kollarova M, Barak I. Thioredoxin - structural and functional complexity. Gen Physiol Biophys 2005;24:3-11.

119. Cleland WW. Dithiothreitol, a New Protective Reagent for Sh Groups. Biochemistry 1964;3:480-2.

120. Savitsky PA, Finkel T. Redox regulation of Cdc25C. J Biol Chem 2002;277:20535-40.

121. Brisson M, Foster C, Wipf P, *et al.* Independent mechanistic inhibition of cdc25 phosphatases by a natural product caulibugulone. Mol Pharmacol 2007;71:184-92.

122. Goodwin EC, DiMaio D. Repression of human papillomavirus oncogenes in HeLa cervical carcinoma cells causes the orderly reactivation of dormant tumor suppressor pathways. Proc Natl Acad Sci U S A 2000;97:12513-8.

123. Scheffner M, Munger K, Byrne JC, Howley PM. The state of the p53 and retinoblastoma genes in human cervical carcinoma cell lines. Proc Natl Acad Sci U S A 1991;88:5523-7.

124. Ignarro LJ, Byrns RE, Buga GM, Wood KS. Endothelium-derived relaxing factor from pulmonary artery and vein possesses pharmacologic and chemical properties identical to those of nitric oxide radical. Circ Res 1987;61:866-79.

125. Palmer RM, Ferrige AG, Moncada S. Nitric oxide release accounts for the biological activity of endothelium-derived relaxing factor. Nature 1987;327:524-6.

126. Alderton WK, Cooper CE, Knowles RG. Nitric oxide synthases: structure, function and inhibition. Biochem J 2001;357:593-615.

127. Schmidt HH, Hofmann H, Schindler U, Shutenko ZS, Cunningham DD, Feelisch M. No .NO from NO synthase. Proc Natl Acad Sci U S A 1996;93:14492-7.

128. Heinzel B, John M, Klatt P, Bohme E, Mayer B. Ca2+/calmodulin-dependent formation of hydrogen peroxide by brain nitric oxide synthase. Biochem J 1992;281:627-30.

129. Pou S, Pou WS, Bredt DS, Snyder SH, Rosen GM. Generation of superoxide by purified brain nitric oxide synthase. J Biol Chem 1992;267:24173-6.

130. Xia Y, Roman LJ, Masters BS, Zweier JL. Inducible nitric-oxide synthase generates superoxide from the reductase domain. J Biol Chem 1998;273:22635-9.

131. Xia Y, Zweier JL. Superoxide and peroxynitrite generation from inducible nitric oxide synthase in macrophages. Proc Natl Acad Sci U S A 1997;94:6954-8.

132. Gaston B, Singel D, Doctor A, Stamler JS. S-nitrosothiol signaling in respiratory biology. Am J Respir Crit Care Med 2006;173:1186-93.

133. Millar TM, Stevens CR, Benjamin N, Eisenthal R, Harrison R, Blake DR. Xanthine oxidoreductase catalyses the reduction of nitrates and nitrite to nitric oxide under hypoxic conditions. FEBS Lett 1998;427:225-8.

134. Cosby K, Partovi KS, Crawford JH, *et al.* Nitrite reduction to nitric oxide by deoxyhemoglobin vasodilates the human circulation. Nat Med 2003;9:1498-505.

135. Vanin AF, Bevers LM, Slama-Schwok A, van Faassen EE. Nitric oxide synthase reduces nitrite to NO under anoxia. Cell Mol Life Sci 2007;64:96-103.

136. Schopfer FJ, Baker PR, Giles G, *et al.* Fatty acid transduction of nitric oxide signaling. Nitrolinoleic acid is a hydrophobically stabilized nitric oxide donor. J Biol Chem 2005;280:19289-97.

137. Lima ES, Bonini MG, Augusto O, Barbeiro HV, Souza HP, Abdalla DS. Nitrated lipids decompose to nitric oxide and lipid radicals and cause vasorelaxation. Free Radic Biol Med 2005;39:532-9.

138. Lancaster JR, Jr. A tutorial on the diffusibility and reactivity of free nitric oxide. Nitric Oxide 1997;1:18-30.

139. Stamler JS, Singel DJ, Loscalzo J. Biochemistry of nitric oxide and its redox-activated forms. Science 1992;258:1898-902.

140. Augusto O, Bonini MG, Amanso AM, Linares E, Santos CC, De Menezes SL. Nitrogen dioxide and carbonate radical anion: two emerging radicals in biology. Free Radic Biol Med 2002;32:841-59.

141. Ford E, Hughes MN, Wardman P. Kinetics of the reactions of nitrogen dioxide with glutathione, cysteine, and uric acid at physiological pH. Free Radic Biol Med 2002;32:1314-23.

142. Moller MN, Li Q, Lancaster JR, Jr., Denicola A. Acceleration of nitric oxide autoxidation and nitrosation by membranes. IUBMB Life 2007;59:243-8.

143. Liu X, Miller MJ, Joshi MS, Thomas DD, Lancaster JR, Jr. Accelerated reaction of nitric oxide with O2 within the hydrophobic interior of biological membranes. Proc Natl Acad Sci U S A 1998;95:2175-9.

144. Doyle MP, Hoekstra JW. Oxidation of nitrogen oxides by bound dioxygen in hemoproteins. J Inorg Biochem 1981;14:351-8.

145. Ridnour LA, Thomas DD, Mancardi D*, et al.* The chemistry of nitrosative stress induced by nitric oxide and reactive nitrogen oxide species. Putting perspective on stressful biological situations. Biol Chem 2004;385:1-10.

146. Espey MG, Thomas DD, Miranda KM, Wink DA. Focusing of nitric oxide mediated nitrosation and oxidative nitrosylation as a consequence of reaction with superoxide. Proc Natl Acad Sci U S A 2002;99:11127-32.

147. Kissner R, Nauser T, Bugnon P, Lye PG, Koppenol WH. Formation and properties of peroxynitrite as studied by laser flash photolysis, high-pressure stopped-flow technique, and pulse radiolysis. Chem Res Toxicol 1997;10:1285-92.

148. Beckman JS, Beckman TW, Chen J, Marshall PA, Freeman BA. Apparent hydroxyl radical production by peroxynitrite: implications for endothelial injury from nitric oxide and superoxide. Proc Natl Acad Sci U S A 1990;87:1620-4.

149. Schopfer FJ, Baker PR, Freeman BA. NO-dependent protein nitration: a cell signaling event or an oxidative inflammatory response? Trends Biochem Sci 2003;28:646-54.

150. Koppenol WH, Moreno JJ, Pryor WA, Ischiropoulos H, Beckman JS. Peroxynitrite, a cloaked oxidant formed by nitric oxide and superoxide. Chem Res Toxicol 1992;5:834-42.

151. Radi R, Beckman JS, Bush KM, Freeman BA. Peroxynitrite oxidation of sulfhydryls. The cytotoxic potential of superoxide and nitric oxide. J Biol Chem 1991;266:4244-50.

152. Radi R, Beckman JS, Bush KM, Freeman BA. Peroxynitrite-induced membrane lipid peroxidation: the cytotoxic potential of superoxide and nitric oxide. Arch Biochem Biophys 1991;288:481-7.

153. Bonini MG, Radi R, Ferrer-Sueta G, Ferreira AM, Augusto O. Direct EPR detection of the carbonate radical anion produced from peroxynitrite and carbon dioxide. J Biol Chem 1999;274:10802-6.

154. Bonini MG, Augusto O. Carbon dioxide stimulates the production of thiyl, sulfinyl, and disulfide radical anion from thiol oxidation by peroxynitrite. J Biol Chem 2001;276:9749-54.

155. McCleverty JA. Chemistry of nitric oxide relevant to biology. Chem Rev 2004;104:403-18.

156. Thomas DD, Miranda KM, Colton CA, Citrin D, Espey MG, Wink DA. Heme proteins and nitric oxide (NO): the neglected, eloquent chemistry in NO redox signaling and regulation. Antioxid Redox Signal 2003;5:307-17.

157. Evgenov OV, Pacher P, Schmidt PM, Hasko G, Schmidt HH, Stasch JP. NO-independent stimulators and activators of soluble guanylate cyclase: discovery and therapeutic potential. Nat Rev Drug Discov 2006;5:755-68.

158. Gorbunov NV, Osipov AN, Day BW, Zayas-Rivera B, Kagan VE, Elsayed NM. Reduction of ferrylmyoglobin and ferrylhemoglobin by nitric oxide: a protective mechanism against ferryl hemoprotein-induced oxidations. Biochemistry 1995;34:6689-99.

159. Wink DA, Mitchell JB. Chemical biology of nitric oxide: Insights into regulatory, cytotoxic, and cytoprotective mechanisms of nitric oxide. Free Radic Biol Med 1998;25:434-56.

160. Thomas DD, Ridnour LA, Espey MG, *et al.* Superoxide fluxes limit nitric oxide-induced signaling. J Biol Chem 2006;281:25984-93.

161. Burley DS, Ferdinandy P, Baxter GF. Cyclic GMP and protein kinase-G in myocardial ischaemia-reperfusion: opportunities and obstacles for survival signaling. Br J Pharmacol 2007;152:855-69.

162. Ignarro LJ, Wood KS, Wolin MS. Activation of purified soluble guanylate cyclase by protoporphyrin IX. Proc Natl Acad Sci U S A 1982;79:2870-3.

163. Condorelli P, George SC. In vivo control of soluble guanylate cyclase activation by nitric oxide: a kinetic analysis. Biophys J 2001;80:2110-9.

164. Stubbe J. Ribonucleotide reductases: amazing and confusing. J Biol Chem 1990;265:5329-32.

165. Nordlund P, Reichard P. Ribonucleotide reductases. Annu Rev Biochem 2006;75:681-706.

166. Kwon NS, Stuehr DJ, Nathan CF. Inhibition of tumor cell ribonucleotide reductase by macrophage-derived nitric oxide. J Exp Med 1991;174:761-7.

167. Lepoivre M, Flaman JM, Bobe P, Lemaire G, Henry Y. Quenching of the tyrosyl free radical of ribonucleotide reductase by nitric oxide. Relationship to cytostasis induced in tumor cells by cytotoxic macrophages. J Biol Chem 1994;269:21891-7.

168. Roy B, Lepoivre M, Henry Y, Fontecave M. Inhibition of ribonucleotide reductase by nitric oxide derived from thionitrites: reversible modifications of both subunits. Biochemistry 1995;34:5411-8.

169. Haskin CJ, Ravi N, Lynch JB, Munck E, Que L, Jr. Reaction of NO with the reduced R2 protein of ribonucleotide reductase from Escherichia coli. Biochemistry 1995;34:11090-8.

170. Matsumoto A, Comatas KE, Liu L, Stamler JS. Screening for nitric oxide-dependent protein-protein interactions. Science 2003;301:657-61.

171. Hess DT, Matsumoto A, Kim SO, Marshall HE, Stamler JS. Protein S-nitrosylation: purview and parameters. Nat Rev Mol Cell Biol 2005;6:150-66.

172. Yamakura F, Taka H, Fujimura T, Murayama K. Inactivation of human manganese-superoxide dismutase by peroxynitrite is caused by exclusive nitration of tyrosine 34 to 3-nitrotyrosine. J Biol Chem 1998;273:14085-9.

173. Townsend DM, Findlay VJ, Fazilev F*, et al.* A glutathione S-transferase pi-activated prodrug causes kinase activation concurrent with S-glutathionylation of proteins. Mol Pharmacol 2006;69:501-8.

174. Prutz WA, Monig H, Butler J, Land EJ. Reactions of nitrogen dioxide in aqueous model systems: oxidation of tyrosine units in peptides and proteins. Arch Biochem Biophys 1985;243:125-34.

175. Baldus S, Eiserich JP, Mani A*, et al.* Endothelial transcytosis of myeloperoxidase confers specificity to vascular ECM proteins as targets of tyrosine nitration. J Clin Invest 2001;108:1759-70.

176. Kamisaki Y, Wada K, Bian K*, et al.* An activity in rat tissues that modifies nitrotyrosine-containing proteins. Proc Natl Acad Sci U S A 1998;95:11584-9.

177. Koeck T, Fu X, Hazen SL, Crabb JW, Stuehr DJ, Aulak KS. Rapid and selective oxygen-regulated protein tyrosine denitration and nitration in mitochondria. J Biol Chem 2004;279:27257-62.

178. Souza JM, Choi I, Chen Q*, et al.* Proteolytic degradation of tyrosine nitrated proteins. Arch Biochem Biophys 2000;380:360-6.

179. Ji Y, Akerboom TP, Sies H, Thomas JA. S-nitrosylation and S-glutathiolation of protein sulfhydryls by S-nitroso glutathione. Arch Biochem Biophys 1999;362:67-78.

180. Konorev EA, Hogg N, Kalyanaraman B. Rapid and irreversible inhibition of creatine kinase by peroxynitrite. FEBS Lett 1998;427:171-4.

181. Andersen JF, Sanders DA, Gasdaska JR, Weichsel A, Powis G, Montfort WR. Human thioredoxin homodimers: regulation by pH, role of aspartate 60, and crystal structure of the aspartate 60 --> asparagine mutant. Biochemistry 1997;36:13979-88.

182. Rudolph J. Redox regulation of the Cdc25 phosphatases. Antioxid Redox Signal 2005;7:761-7.

183. van Montfort RL, Congreve M, Tisi D, Carr R, Jhoti H. Oxidation state of the active-site cysteine in protein tyrosine phosphatase 1B. Nature 2003;423:773-7.

184. Salmeen A, Andersen JN, Myers MP*, et al.* Redox regulation of protein tyrosine phosphatase 1B involves a sulphenyl-amide intermediate. Nature 2003;423:769-73.

185. Rinna A, Torres M, Forman HJ. Stimulation of the alveolar macrophage respiratory burst by ADP causes selective glutathionylation of protein tyrosine phosphatase 1B. Free Radic Biol Med 2006;41:86-91.

186. Barrett WC, DeGnore JP, Konig S*, et al.* Regulation of PTP1B via glutathionylation of the active site cysteine 215. Biochemistry 1999;38:6699-705.

187. Sengupta R, Ryter SW, Zuckerbraun BS, Tzeng E, Billiar TR, Stoyanovsky DA. Thioredoxin catalyzes the denitrosation of low-molecular mass and protein S-nitrosothiols. Biochemistry 2007;46:8472-83.

188. Mitchell DA, Marletta MA. Thioredoxin catalyzes the S-nitrosation of the caspase-3 active site cysteine. Nat Chem Biol 2005;1:154-8.

189. Barrett DM, Black SM, Todor H, Schmidt-Ullrich RK, Dawson KS, Mikkelsen RB. Inhibition of protein-tyrosine phosphatases by mild oxidative stresses is dependent on S-nitrosylation. J Biol Chem 2005;280:14453-61.

190. Choi YB, Tenneti L, Le DA*, et al.* Molecular basis of NMDA receptor-coupled ion channel modulation by S-nitrosylation. Nat Neurosci 2000;3:15-21.

191. Lander HM, Ogiste JS, Pearce SF, Levi R, Novogrodsky A. Nitric oxide-stimulated guanine nucleotide exchange on p21ras. J Biol Chem 1995;270:7017-20.

192. Kim SF, Huri DA, Snyder SH. Inducible nitric oxide synthase binds, S-nitrosylates, and activates cyclooxygenase-2. Science 2005;310:1966-70.

193. Li F, Sonveaux P, Rabbani ZN*, et al.* Regulation of HIF-1alpha stability through S-nitrosylation. Mol Cell 2007;26:63-74.

194. Singh RJ, Hogg N, Joseph J, Kalyanaraman B. Mechanism of nitric oxide release from S-nitrosothiols. J Biol Chem 1996;271:18596-603.

195. Perez-Mato I, Castro C, Ruiz FA, Corrales FJ, Mato JM. Methionine adenosyltransferase S-nitrosylation is regulated by the basic and acidic amino acids surrounding the target thiol. J Biol Chem 1999;274:17075-9.

196. Greco TM, Hodara R, Parastatidis I*, et al.* Identification of S-nitrosylation motifs by site-specific mapping of the S-nitrosocysteine proteome in human vascular smooth muscle cells. Proc Natl Acad Sci U S A 2006;103:7420-5.

197. Lancaster JR, Jr., Gaston B. NO and nitrosothiols: spatial confinement and free diffusion. Am J Physiol Lung Cell Mol Physiol 2004;287:L465-6.

198. Dicks AP, Swift HR, Williams DLH, Butler AR, AlSadoni HH, Cox BG. Identification of Cu+ as the effective reagent in nitric oxide formation from S-nitrosothiols (RSNO). Journal of the Chemical Society-Perkin Transactions 2 1996:481-7.

199. Cook JA, Kim SY, Teague D*, et al.* Convenient colorimetric and fluorometric assays for S-nitrosothiols. Anal Biochem 1996;238:150-8.

200. Dicks AP, Beloso PH, Williams DLH. Decomposition of S-nitrosothiols: The effects of added thiols. Journal of the Chemical Society-Perkin Transactions 2 1997:1429-34.

201. Hausladen A, Rafikov R, Angelo M, Singel DJ, Nudler E, Stamler JS. Assessment of nitric oxide signals by triiodide chemiluminescence. Proc Natl Acad Sci U S A 2007;104:2157-62.

202. Stoyanovsky DA, Tyurina YY, Tyurin VA*, et al.* Thioredoxin and lipoic acid catalyze the denitrosation of low molecular weight and protein S-nitrosothiols. J Am Chem Soc 2005;127:15815-23.

203. Nikitovic D, Holmgren A. S-nitrosoglutathione is cleaved by the thioredoxin system with liberation of glutathione and redox regulating nitric oxide. J Biol Chem 1996;271:19180-5.

204. Liu L, Hausladen A, Zeng M, Que L, Heitman J, Stamler JS. A metabolic enzyme for S-nitrosothiol conserved from bacteria to humans. Nature 2001;410:490-4.

205. Jourd'heuil D, Laroux FS, Miles AM, Wink DA, Grisham MB. Effect of superoxide dismutase on the stability of S-nitrosothiols. Arch Biochem Biophys 1999;361:323-30.

206. Ramachandran N, Root P, Jiang XM, Hogg PJ, Mutus B. Mechanism of transfer of NO from extracellular S-nitrosothiols into the cytosol by cell-surface protein disulfide isomerase. Proc Natl Acad Sci U S A 2001;98:9539-44.

207. Kluge I, Gutteck-Amsler U, Zollinger M, Do KQ. S-nitrosoglutathione in rat cerebellum: identification and quantification by liquid chromatography-mass spectrometry. J Neurochem 1997;69:2599-607.

208. Espey MG, Miranda KM, Pluta RM, Wink DA. Nitrosative capacity of macrophages is dependent on nitric-oxide synthase induction signals. J Biol Chem 2000;275:11341-7.

209. Eu JP, Liu L, Zeng M, Stamler JS. An apoptotic model for nitrosative stress. Biochemistry 2000;39:1040-7.

210. Tyurina YY, Basova LV, Konduru NV*, et al.* Nitrosative stress inhibits the aminophospholipid translocase resulting in phosphatidylserine externalization and macrophage engulfment: implications for the resolution of inflammation. J Biol Chem 2007;282:8498-509.

211. Kim YM, Talanian RV, Billiar TR. Nitric oxide inhibits apoptosis by preventing increases in caspase-3-like activity via two distinct mechanisms. J Biol Chem 1997;272:31138-48.

212. Kim YM, Kim TH, Chung HT, Talanian RV, Yin XM, Billiar TR. Nitric oxide prevents tumor necrosis factor alpha-induced rat hepatocyte apoptosis by the interruption of mitochondrial apoptotic signaling through S-nitrosylation of caspase-8. Hepatology 2000;32:770-8.

213. Uehara T, Nakamura T, Yao D*, et al.* S-nitrosylated protein-disulphide isomerase links protein misfolding to neurodegeneration. Nature 2006;441:513-7.

214. Uehara T. Accumulation of misfolded protein through nitrosative stress linked to neurodegenerative disorders. Antioxid Redox Signal 2007;9:597-601.

215. Yilmaz G, Surer H, Inan LE, Coskun O, Yucel D. Increased nitrosative and oxidative stress in platelets of migraine patients. Tohoku J Exp Med 2007;211:23-30.

216. Kaneki M, Shimizu N, Yamada D, Chang K. Nitrosative stress and pathogenesis of insulin resistance. Antioxid Redox Signal 2007;9:319-29.

217. Fukumura D, Kashiwagi S, Jain RK. The role of nitric oxide in tumour progression. Nat Rev Cancer 2006;6:521-34.

218. Beevi SS, Rasheed MH, Geetha A. Evidence of oxidative and nitrosative stress in patients with cervical squamous cell carcinoma. Clin Chim Acta 2007;375:119-23.

219. Forrester K, Ambs S, Lupold SE*, et al.* Nitric oxide-induced p53 accumulation and regulation of inducible nitric oxide synthase expression by wild-type p53. Proc Natl Acad Sci U S A 1996;93:2442-7.

220. Mirvish SS. Role of N-nitroso compounds (NOC) and N-nitrosation in etiology of gastric, esophageal, nasopharyngeal and bladder cancer and contribution to cancer of known exposures to NOC. Cancer Lett 1995;93:17-48.

221. Sarkar R, Gordon D, Stanley JC, Webb RC. Dual cell cycle-specific mechanisms mediate the antimitogenic effects of nitric oxide in vascular smooth muscle cells. J Hypertens 1997;15:275-83.

222. Nunokawa Y, Tanaka S. Interferon-gamma inhibits proliferation of rat vascular smooth muscle cells by nitric oxide generation. Biochem Biophys Res Commun 1992;188:409-15.

223. Sarkar R, Gordon D, Stanley JC, Webb RC. Cell cycle effects of nitric oxide on vascular smooth muscle cells. Am J Physiol 1997;272:H1810-8.

224. Ziche M, Morbidelli L, Masini E, Granger H, Geppetti P, Ledda F. Nitric oxide promotes DNA synthesis and cyclic GMP formation in endothelial cells from postcapillary venules. Biochem Biophys Res Commun 1993;192:1198-203.

225. Guo K, Andres V, Walsh K. Nitric oxide-induced downregulation of Cdk2 activity and cyclin A gene transcription in vascular smooth muscle cells. Circulation 1998;97:2066-72.

226. Sharma RV, Tan E, Fang S, Gurjar MV, Bhalla RC. NOS gene transfer inhibits expression of cell cycle regulatory molecules in vascular smooth muscle cells. Am J Physiol 1999;276:H1450-9.

227. Tanner FC, Meier P, Greutert H, Champion C, Nabel EG, Luscher TF. Nitric oxide modulates expression of cell cycle regulatory proteins: a cytostatic strategy for inhibition of human vascular smooth muscle cell proliferation. Circulation 2000;101:1982-9.

228. Jenkins DC, Charles IG, Thomsen LL*, et al.* Roles of nitric oxide in tumor growth. Proc Natl Acad Sci U S A 1995;92:4392-6.

229. Ranjan P, Heintz NH. S-phase arrest by reactive nitrogen species is bypassed by okadaic acid, an inhibitor of protein phosphatases PP1/PP2A. Free Radic Biol Med 2006;40:247-59.

230. Hussain SP, Trivers GE, Hofseth LJ, *et al.* Nitric oxide, a mediator of inflammation, suppresses tumorigenesis. Cancer Res 2004;64:6849-53.

231. Konopka TE, Barker JE, Bamford TL, Guida E, Anderson RL, Stewart AG. Nitric oxide synthase II gene disruption: implications for tumor growth and vascular endothelial growth factor production. Cancer Res 2001;61:3182-7.

232. Scott DJ, Hull MA, Cartwright EJ, *et al.* Lack of inducible nitric oxide synthase promotes intestinal tumorigenesis in the Apc(Min/+) mouse. Gastroenterology 2001;121:889-99.

233. Nishikawa M, Chang B, Inoue M. Inducible NO synthase inhibits the growth of free tumor cells, but enhances the growth of solid tumors. Carcinogenesis 2004;25:2101-5.

234. Shi Q, Xiong Q, Wang B, Le X, Khan NA, Xie K. Influence of nitric oxide synthase II gene disruption on tumor growth and metastasis. Cancer Res 2000;60:2579-83.

235. Wei D, Richardson EL, Zhu K, *et al.* Direct demonstration of negative regulation of tumor growth and metastasis by host-inducible nitric oxide synthase. Cancer Res 2003;63:3855-9.

236. Seth D, Rudolph J. Redox control of cell cycle progression via Cdc25 phosphatase (Mih1p) in S. cerevisiae. Cell Cycle 2006;5:2172-3.

237. Clancy R, Cederbaum AI, Stoyanovsky DA. Preparation and properties of S-nitroso-L-cysteine ethyl ester, an intracellular nitrosating agent. J Med Chem 2001;44:2035-8.

238. Xia K, Lee RS, Narsimhan RP, Mukhopadhyay NK, Neel BG, Roberts TM. Tyrosine phosphorylation of the proto-oncoprotein Raf-1 is regulated by Raf-1 itself and the phosphatase Cdc25A. Mol Cell Biol 1999;19:4819-24.

239. Gu Y, Rosenblatt J, Morgan DO. Cell cycle regulation of CDK2 activity by phosphorylation of Thr160 and Tyr15. EMBO J 1992;11:3995-4005.

240. Ichijo H, Nishida E, Irie K*, et al.* Induction of apoptosis by ASK1, a mammalian MAPKKK that activates SAPK/JNK and p38 signaling pathways. Science 1997;275:90-4.

241. Tzeng E, Billiar TR, Robbins PD, Loftus M, Stuehr DJ. Expression of human inducible nitric oxide synthase in a tetrahydrobiopterin (H4B)-deficient cell line: H4B promotes assembly of enzyme subunits into an active dimer. Proc Natl Acad Sci U S A 1995;92:11771-5.

242. Lazo JS, Aslan DC, Southwick EC*, et al.* Discovery and biological evaluation of a new family of potent inhibitors of the dual specificity protein phosphatase Cdc25. J Med Chem 2001;44:4042-9.

243. Jaffrey SR, Snyder SH. The biotin switch method for the detection of S-nitrosylated proteins. Sci STKE 2001;2001:PL1.

244. Li S, Whorton AR. Regulation of protein tyrosine phosphatase 1B in intact cells by S-nitrosothiols. Arch Biochem Biophys 2003;410:269-79.

245. Kwiecien I, Sokolowska M, Luchter-Wasylewska E, Wlodek L. Inhibition of the catalytic activity of rhodanese by S-nitrosylation using nitric oxide donors. Int J Biochem Cell Biol 2003;35:1645-57.

246. Weichsel A, Brailey JL, Montfort WR. Buried S-nitrosocysteine revealed in crystal structures of human thioredoxin. Biochemistry 2007;46:1219-27.

247. Galaktionov K, Jessus C, Beach D. Raf1 interaction with Cdc25 phosphatase ties mitogenic signal transduction to cell cycle activation. Genes Dev 1995;9:1046-58.

248. Forrester MT, Foster MW, Stamler JS. Assessment and application of the biotin switch technique for examining protein S-nitrosylation under conditions of pharmacologically induced oxidative stress. J Biol Chem 2007;282:13977-83.

249. Xian M, Wang K, Chen X*, et al.* Inhibition of protein tyrosine phosphatases by low-molecular-weight S-nitrosothiols and S-nitrosylated human serum albumin. Biochem Biophys Res Commun 2000;268:310-4.

250. Yu CX, Li S, Whorton AR. Redox regulation of PTEN by S-nitrosothiols. Mol Pharmacol 2005;68:847-54.

251. Wang X, Kettenhofen NJ, Shiva S, Hogg N, Gladwin MT. Copper dependence of the biotin switch assay: Modified assay for measuring cellular and blood nitrosated proteins. Free Radic Biol Med 2008;4:4.

252. Katti SK, LeMaster DM, Eklund H. Crystal structure of thioredoxin from Escherichia coli at 1.68 A resolution. J Mol Biol 1990;212:167-84.

253. Peluffo G, Radi R. Biochemistry of protein tyrosine nitration in cardiovascular pathology. Cardiovasc Res 2007;75:291-302.

254. Sandau KB, Faus HG, Brune B. Induction of hypoxia-inducible-factor 1 by nitric oxide is mediated via the PI 3K pathway. Biochem Biophys Res Commun 2000;278:263-7.

255. Ho YS, Wang YJ, Lin JK. Induction of p53 and p21/WAF1/CIP1 expression by nitric oxide and their association with apoptosis in human cancer cells. Mol Carcinog 1996;16:20-31.

256. Holcik M, Sonenberg N. Translational control in stress and apoptosis. Nat Rev Mol Cell Biol 2005;6:318-27.

257. Wek RC, Jiang HY, Anthony TG. Coping with stress: eIF2 kinases and translational control. Biochem Soc Trans 2006;34:7-11.

258. Boyce M, Bryant KF, Jousse C*, et al.* A selective inhibitor of eIF2alpha dephosphorylation protects cells from ER stress. Science 2005;307:935-9.

259. Ali A, Zhang J, Bao S*, et al.* Requirement of protein phosphatase 5 in DNA-damage-induced ATM activation. Genes Dev 2004;18:249-54.

260. Chen MX, McPartlin AE, Brown L, Chen YH, Barker HM, Cohen PT. A novel human protein serine/threonine phosphatase, which possesses four tetratricopeptide repeat motifs and localizes to the nucleus. EMBO J 1994;13:4278-90.

261. Brush MH, Weiser DC, Shenolikar S. Growth arrest and DNA damage-inducible protein GADD34 targets protein phosphatase 1 alpha to the endoplasmic reticulum and promotes dephosphorylation of the alpha subunit of eukaryotic translation initiation factor 2. Mol Cell Biol 2003;23:1292-303.

262. O'Loghlen A, Perez-Morgado MI, Salinas M, Martin ME. Reversible inhibition of the protein phosphatase 1 by hydrogen peroxide. Potential regulation of eIF2 alpha phosphorylation in differentiated PC12 cells. Arch Biochem Biophys 2003;417:194-202.

263. Harding HP, Zhang Y, Bertolotti A, Zeng H, Ron D. Perk is essential for translational regulation and cell survival during the unfolded protein response. Mol Cell 2000;5:897-904.

264. Dickhout JG, Hossain GS, Pozza LM, Zhou J, Lhotak S, Austin RC. Peroxynitrite causes endoplasmic reticulum stress and apoptosis in human vascular endothelium: implications in atherogenesis. Arterioscler Thromb Vasc Biol 2005;25:2623-9.

265. Chen JJ, London IM. Regulation of protein synthesis by heme-regulated eIF-2 alpha kinase. Trends Biochem Sci 1995;20:105-8.

266. Cangi MG, Cukor B, Soung P*, et al.* Role of the Cdc25A phosphatase in human breast cancer. J Clin Invest 2000;106:753-61.

267. Costanzo V, Shechter D, Lupardus PJ, Cimprich KA, Gottesman M, Gautier J. An ATR- and Cdc7-dependent DNA damage checkpoint that inhibits initiation of DNA replication. Mol Cell 2003;11:203-13.

268. Bousset K, Diffley JF. The Cdc7 protein kinase is required for origin firing during S phase. Genes Dev 1998;12:480-90.

269. Sanders CM, Sizov D, Seavers PR, Ortiz-Lombardia M, Antson AA. Transcription activator structure reveals redox control of a replication initiation reaction. Nucleic Acids Res 2007;35:3504-15.

270. McBride AA, Klausner RD, Howley PM. Conserved cysteine residue in the DNA-binding domain of the bovine papillomavirus type 1 E2 protein confers redox regulation of the DNA-binding activity in vitro. Proc Natl Acad Sci U S A 1992;89:7531-5.

271. Park JS, Wang M, Park SJ, Lee SH. Zinc finger of replication protein A, a non-DNA binding element, regulates its DNA binding activity through redox. J Biol Chem 1999;274:29075-80.

272. Zou L, Elledge SJ. Sensing DNA damage through ATRIP recognition of RPA-ssDNA complexes. Science 2003;300:1542-8.

273. Bundy RE, Marczin N, Chester AH, Yacoub M. A redox-based mechanism for nitric oxide-induced inhibition of DNA synthesis in human vascular smooth muscle cells. Br J Pharmacol 2000;129:1513-21.